ADRIANA ROSAURA GONZALEZ ALCIVAR

EFFECT OF COMPOSTING ON BIODEGRADATION OF COMPOSTABLE AND CONVENTIONAL MICROPLASTIC BY BACTERIAL COMMUNITIES FROM SEWAGE SLUDGE

UNIVERSIDADE DO ALGARVE

Faculdade de Ciências e Tecnologia

2023

ADRIANA ROSAURA GONZALEZ ALCIVAR

EFFECT OF COMPOSTING ON BIODEGRADATION OF COMPOSTABLE AND CONVENTIONAL MICROPLASTIC BY BACTERIAL COMMUNITIES FROM SEWAGE SLUDGE

Mestrado em Inovação Química e Regulamentação / Erasmus Mundus MSc in Chemical Innovation and Regulation
Trabalho efetuado sob a orientação de:
Dr. Isabel Marín Beltrán
Prof. Maria Clara Costa

UNIVERSIDADE DO ALGARVE

Faculdade de Ciências e Tecnologia
2023

EFFECT OF COMPOSTING ON BIODEGRADATION OF COMPOSTABLE AND CONVENTIONAL MICROPLASTIC BY BACTERIAL COMMUNITIES FROM SEWAGE SLUDGE

Declaration of Authorship

I hereby declare that I am the author of this work, which is original and unpublished. Authors and works consulted are properly cited in the text and listed in the list of references included.

_____

Adriana Rosaura Gonzalez Alcivar

Acknowledgements

I would like to take this opportunity to express my gratitude to the European Commission and the Erasmus Mundus Program, for their financial backing for this Erasmus Mundus MSc in Chemical Innovation and Regulation (ChIR) through grant agreement nr 619824-EMJMD. Without their financial support, this chance would have never existed.

I would like to thank Professor Isabel Cavaco for always giving me the best advice at the right time. To Alessandra Tolomelli, who helped me when I was having trouble, and to Professor Emilio Tagliavini, who is always willing to share his knowledge. I will always be thankful that you believed in me.

I would like to express my sincere gratitude to my supervisor. Dr. Isabel Marín Beltrán, her intellectual advice, expert guidance, and material support has been instrumental towards the completion of this research. To professor Clara Costa for giving me motivation and efficient feedback.

I want to express my gratitude to my family, Marina, Wilfrido, Isabel and Irene, because they encouraged me to follow my dreams no matter what. Even when I am thousands of miles away from Ecuador, I carry them with me in my heart. No matter the distance "La familia siempre unida".

I would like to thank my partner Tobie. He has been my rock every time I feel like giving up. Thanks for supporting me in my goals even if that implies distance and a different schedule. I could not make it without you. We did it!

I would like to express my sincere thanks to Matt, Hector, Ricardo, Carlos, Gisela, Esther, Serena, and Thet, who have become like family to me throughout this time that I've been living in the Algarve. Without them, Faro will be completely incomprehensible. Without them Faro would make no sense.

This work was financed by Portuguese national funds through FCT – Fundação para a Ciências e Tecnologia, I.P., within the scope of the project PTDC/CTA-AMB/7782/2020, and through projects UIDB/04326/2020, UIDP/04326/2020 and LA/P/0101/2020. Isabel Marín Beltrán was awarded with a fellowship from the Stimulus of Scientific Employment, Individual Support 2017 Call (CEECIND/03072/2017).

Resumo

Os plásticos tornaram-se parte integrante das nossas vidas diárias devido às suas características particulares, nomeadamente resistência, durabilidade, flexibilidade, rigidez e baixo custo. No entanto, quando os plásticos se fragmentam e se tornam microplásticos (MP), eles representam uma ameaça global para os ecossistemas aquáticos e terrestres. Vários estudos relataram que as Estações de Tratamento de Águas Residuais (ETARs) são uma das principais fontes de MP para o oceano. Atualmente, as ETARs relatam que podem remover até 98% do MPs do afluente (Carr et al., 2016; Murphy et al., 2016; Simon et al., 2018; Talvitie et al., 2017). No entanto, a maioria desses MP não são realmente eliminados, mas acabam nas lamas resultantes do processo de tratamento. A atual regulamentação das lamas, criada em 1986, não contempla os MPs como poluente. Esta lama é normalmente utilizada como fertilizante em solos agrícolas na Europa após um processo de compostagem. Estudos efetuados relataram que os MPs podem afetar a taxa de germinação, diminuir o comprimento e a biomassa da raiz das plantas, bem como alterar a atividade microbiana e a transferência de nutrientes entre a planta e o solo.

Para abordar a problemática dos MPs nas lamas das ETARs este trabalho teve como foco avaliar a biodegradação de microplásticos compostáveis e convencionais em processos simulados de compostagem (antes da aplicação no solo) num período de 30 e 60 dias. A biodegradação de MPs durante o processo de compostagem teve em conta o tipo de plástico, considerando a comunidade bacteriana inicialmente presente na lama desidratada, e a mesma comunidade bio-aumentada com um isolado do género *Bacillus*. Além disso, avaliou as mudanças na concentração de MPs da lama desidratada no tempo inicial e após 60 dias de compostagem para determinar se após esse período o número de partículas de MP diminui ou aumenta em quantidade e em tamanho.

Para o efeito, adicionamos lama de uma ETAR europeia com filmes MP (2-2 mm) de uma garrafa de tereftalato de polietileno (PET) e de um saco compostável (de acordo com informação do vendedor) de polietileno de baixa densidade (CPE). A configuração experimental consistiu em: 25g de lama enriquecida com 40 partículas de PET, 25g de lama enriquecida com 40 partículas CPE. Estes dois tratamentos foram repetidos, mas inoculando um isolado bacteriano do género *Bacillus* que tinha sido usado previamente e que mostrou potencial para degradar polímeros de PET (Fernández de Villalobos et al., 2022; Ngonyani, 2022). A lama sem adição de MPs ou inóculo bacteriano foi usada como controlo. As amostras foram mantidas a 50ºC por 60 dias, sendo monitorizado mensalmente (após 30 e 60 dias) o teor de matéria orgânica, o pH, a razão C:N, a mudança nos grupos funcionais dos MPs e as

mudanças na comunidade bacteriana. Além disso, alterações morfológicas na superfície do MP foram inspecionadas usando microscopia eletrónica de varrimento (SEM) no final da prova. Os MPs contidos na fase inicial e final do ensaio na lama foram extraídos seguindo um procedimento de separação por densidade, seguido de digestão com peróxido de hidrogénio. As partículas suspeitas de MP foram submetidas a análise de FTIR para verificação de sua composição química.

Todos os parâmetros monitorizados indicaram diferenças estatisticamente significativas ao longo do tempo (pH, matéria orgânica (OM%) e razão C:N) as quais são inerente ao próprio processo de compostagem. PET revelou valores maiores que PET+B (ensaio com bioaumentação de *Bacillus*), enquanto para o mesmo parâmetro, o controlo teve mais OM do que CPE (polietileno compostável). A razão C:N mostrou diminuir significativamente com o tempo. 40 MP, que equivale a 0,06 % no ensaio CPE e 0,09 % no ensaio PET, não teve efeito sobre os parâmetros pH, OM % e razão C:N nas amostras de compostagem. Esta quantidade de MPs não teve efeito percetível em 25 gramas de compostagem. Esses resultados abrem uma porta para a legislação e os limites permitidos de microplásticos nas lamas de esgoto. No entanto, isso não indica que o 40 MP não possa afetar o desempenho de plantas ou microorganismos. Outras ensaios e testes toxicológicos devem ser explorados em estudos futuros.

Após compostagem as partículas de CPE evidenciaram mudanças significantes na região entre ~1710-16 cm^{-1} e ~1541-49 cm^{-1}, bem como a ~1046-10 cm^{-1} e ~870-76 cm^{-1}. Após 30 dias, o pico observado a ~1641-53 cm^{-1} apresentou uma diferença relativamente aos observados nos MPs dos ensaios CPE+B (ensaio com polietileno compostável e bioaumentação de *Bacillus*) e CPE (ensaio com polietileno compostável sem bioaumentação). Este aumento do pico pode estar ligado à produção de grupos carboxílicos e à biodegradação de polímeros. Para o ensaio de compostagem com PET, a alteração mais notável foi na regiãode ~1630-52 cm^{-1} para ~1530-42 cm^{-1} , onde o tratamento PET+B mostrou uma absorção maior do que o que se observou com PET. O pico ~1630-52 cm^{-1} pode ser interpretado como resultando da oxidação do polímero. Ospicos observados a ~2916-2 cm^{-1}, ~2849-56 cm^{-1}, ~1709-17 cm^{-1} e ~1234-48 cm^{-1}, que são atribuídos a ligações típicas do PET, mudam após 60 dias de compostagem, sendo o pico do tratamento PET+B maior que o do PET e o do controlo. Além disso, o pico observado a 1709-17 cm^{-1} da compostagem do PET foi maior do que o observado no controlo. O pico de ~1234-48 cm^{-1} foi maior para no ensaio de controlo (K) do que nos ensaios PET+B e com PET. A adição ou ausência de picos tem sido associada à atividade microbiana.

Os MPs resultantes dos ensaios PET, BPET+B, CPE e CPE+B apresentaram biofilmes bacterianos após 60 dias, porém não foram observadas alterações morfológicas entre os tratamentos PET e BPET+B. Partículas de MP submetidas à comunidade bacteriana inicial (CPE) diferiram daquelas tratadas com bactérias bioaumentadas (CPE+B). Interessantemente, no ensaio CPE+B os MPs apresentaram cavidades e superfícies rugosas, provavelmente ligadas a atividades enzimáticas bacterianas que terão utilizado o polímero plástico como fonte de carbono (Ojha et al., 2017).

A concentração de MPs na lama desidratada após 60 dias foi de 27 MP por g, comparada a 4 MP por g no início (antes de iniciar o ensaio de compostagem). Poliéster (28%) e polivinil (20%) foram os polímeros mais abundantes. A forma mais comum foi fibras (84%) e o preto (50%) foi a cor mais comum. O grupo de tamanho mais prevalente para o tempo inicial é de 1000 a 2000 μm, representando 26% das partículas, seguido pelo grupo de 400-600 μm (23%). No tempo final o tamanho mais prevalente é 200-400 com 29%, seguido de 400-600 com 19%. Após 60 dias, o número de MPs na amostra aumenta, mas também o tamanho, portanto, não se pode assumir que eles foram fragmentados ao longo do tempo, aumentando em número, mas diminuindo em tamanho.

Em resumo, após 60 dias, 40 MPs não tiveram efeito no processo de compostagem. Houve uma diferença considerável entre os picos indicando alterações químicas para os MP PET e CPE; sendo, portanto, compatível com a ocorrência de biodegradação. O saco biodegradável não quebrou conforme o esperado, apesar de estar listado como compostável. Estes resultados sugerem uma necessidade urgente de atualizar a legislação atual referente às lamas produzidas em ETARs, comtemplando a presença de poluentes emergentes como os MPs.

Palavras chave: composto, biodegradação, microplásticos, lamas de ETAR

Abstract

Microplastics (MP) threaten the aquatic and terrestrial ecosystems. Several studies have reported that wastewater treatment plants (WWTPs) are one of the main sources of MP to the ocean, even though they remove up to 98% of MPs from the influent (Carr et al., 2016; Murphy et al., 2016; Simon et al., 2018; Talvitie et al., 2017). Most of these MPs are not really eliminated but end up in the sewage sludge. This sludge is normally used as fertilizer in agricultural soils, after a composting process. However, current regulation does not consider the concentration of MP in sludge before their application on natural soils. This work focused on evaluating the effect of composting on MP particles. For this, we spiked sewage sludge from a European WWTP with MP films (2 mm^{-2}) from a polyethylene terephthalate (PET) bottle and a compostable (according to the seller) bag of polyethylene (CPE). The experimental set-up consisted of: sludge spiked with 40 PET MP, sludge spiked with 40 CPE MP. These two treatments were repeated but inoculating a bacterial isolate from the genus *Bacillus*. Sludge with no added MP or bacterial inoculum was used as control. Samples were kept at 50ºC for 60 days, and organic matter content, pH, C:N ratio, the change in the functional groups of MP, and changes in the bacterial community were monitored monthly. Results showed that 40 MP had no effect on the composting process. There were differences among peaks indicating chemical changes and biodegradation for PET and CPE MP. After 60 days, scanning electron microscopy revealed adhering biofilms and a hole for CPE MP submitted to bioaugmentation treatment but did not decompose as expected. The concentration of MPs in the sludge after 60 days was 27 MP by g^{-1}, compared to 4 MP by g^{-1} at the beginning. Polyester (28%) was the most abundant polymer and fibers (84%) the most common shape.

Keywords: compost, biodegradation, microplastics, sewage sludge

Subject Index

Figure Index

Table Index

Abbreviations and Acronyms

ATR: Attenuated Total Reflectance

BA: bulking agent

CCMAR: Centre for Marine Sciences

CPE: compostable polyethylene

CPE+B: compostable polyethylene with bioaugmented *Bacillus*

DNA: Deoxyribonucleic acid

dw: dry weight

FTIR: Fourier-Transform Infrared spectroscopy

MPs: microplastics

MSM: mineral salt medium

PA: polyamide

PE: polyethylene

PES: polyethersulfone

PET: polyethylene terephthalate

PET+B: polyethylene terephthalate with bioaugmented *Bacillus*

PLA: polylactic acid

PP: polypropylene

PS: polystyrene

SDS: Sodium dodecyl sulfate

SEM: Scanning electron microscopy

SS: sewage sludge

UV - Ultraviolet

WWTP: Wastewater Treatment Plant

1. Introduction

1.1.What is plastic and why they constitute an environmental problem?

Plastics are nowadays part of our daily lives, due to their strength and durability, rigidity, toughness, and low cost, which have allowed them to replace materials such as wood, glass, or metal. Plastics are widely used in packaging, automobiles, infrastructure, technology, textiles, etc. Under the term plastics is included a wide-range of polymers, that can originate from petroleum-based or bio-based components. These polymers are generated by monomers ordered in various ways; the configuration of the monomers having a direct impact on the plastic's unique properties and degradability (Crawford & Quinn, 2017). The same qualities that make plastics so appealing to the market become in terms of pollution, bioaccumulation, and biodegradability a well-known issue for the environment (ECHA, 2021; Eerkes-Medrano & Thompson, 2018; Lebreton et al., 2017; SAPEA, 2020).

It was determined that around 268,940 tons of plastic debris were floating in the ocean by the year 2013 (Eriksen et al., 2014). Furthermore, recent studies have shown that, of the 6300 million tons of plastic waste produced by humanity until 2015 just 9% has been properly recycled, 12% was incinerated, and the majority (79%) has been accumulated in landfills or the natural environment (Geyer et al., 2017). Between 307 and 925 million items of litter are released annually into the ocean, 626 million items flow into European seas every year and 82 % of that debris is plastic that comes from land (EEA, 2022). If the present pace of plastic manufacturing and waste management is maintained in the coming years, over 12,000 million tons of plastic trash will be in landfills or the natural environment by 2050 (SAPEA, 2020).

From the point of view of the circular economy, there are ways to deal with plastic pollution before it breaks down into small pieces, such as reusing, reducing, and recycling. Also, bioplastics that can be biodegradable can be a great option (Ashter, 2016).

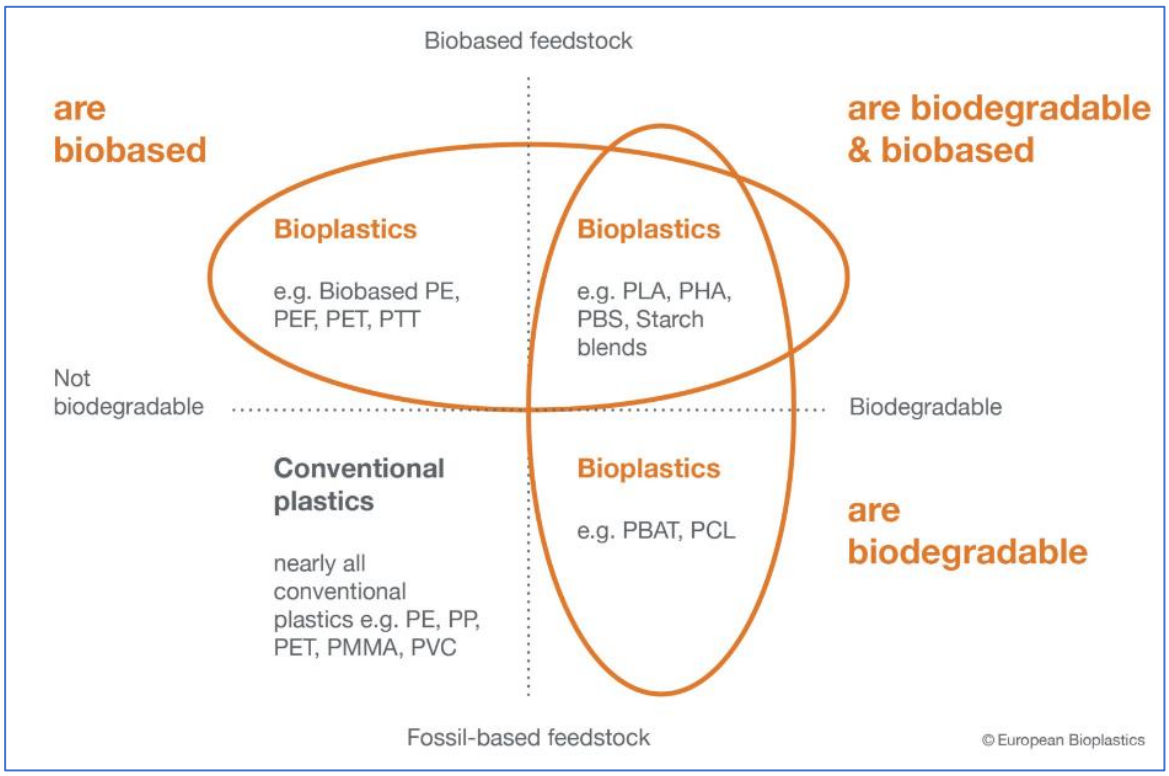

Figure 1.1. Classification of bioplastics to the feedstock according to the feedstock according EUBIO, (2022a)

There is much confusion nowadays with the terminology bioplastic but to make it simple (Figure 1.1), bioplastic can be biodegradable or nonbiodegradable and can be biobased (polylactic acid (PLA), polyhydroxyalkanoates, starch) or petroleum based (Carvalheira et al., 2022). Bioplastic can be biobased feedstock but not necessarily biodegradable, it can be biobased feedstock and biodegradable and lastly it can be petroleum-based feedstock and biodegradable (EUBIO, 2022a). Therefore, bioplastic or biobased does not equate to biodegradable, as the biodegradability does not depend on the resource base of a material, but rather its chemical structure (EUBIO, 2022a).

In 2018, biodegradable bioplastic accounts for 43% bioplastic output, but by 2022, this percentage will have climbed to 52% (EUBIO, 2022b, 2018). However, bioplastics still account for less than 1% of the more than 390 million tons of plastic generated annually (EUBIO, 2022b).

1.2. Microplastics

Microplastics (MPs) are plastic debris between 1µm and 5mm (Cole et al., 2011) with two distinct origins (primary source and secondary source). Primary MPs are produced in such small size on purpose, to be added to items such as cosmetics or cleaning products like a tooth paste (Du et al., 2021). The secondary MPs are the product of fragmented macro and mesoplastic by photodegradation, wind, waves and other forms of natural weathering, they can also be formed from washing or wearing of synthetic textiles (Amobonye et al., 2021; Boucher & Friot, 2017).

The European Chemicals Agency (ECHA) calculated that 176,000 tons of microplastics produced accidently are released into European surface waterways annually and that 145,000 tons of microplastics produced purposely are utilized annually in Europe (Eriksen et al., 2014). To prevent irreversible pollution, it is necessary to identify the sources where these MPs are released to control them or create effective mechanisms to contain them in order to avoid their arrival to open environments (rivers, oceans, soil, etc.), since it is almost impossible to remove them due to their small size.

One of the greatest concerns about MPs is their capacity to absorb other pollutants such as persistent organic pollutants, heavy metals or pathogens (Barus et al., 2021; SAPEA, 2020). Since MPs can be ingested by several organisms and be transferred through the trophic chain (Browne et al., 2013) the absorbed contaminants can be also transferred and eventually released to the tissues and organs of animals through ingestion. The detrimental effects caused by MP ingestion such as toxicity, inflammatory reactions, gastrointestinal blockages, reduction in energy reserves (among others) in aquatic environments are well-studied in primary consumers of the trophic chain (Browne et al., 2013; Farrell & Nelson, 2013; Pannetier et al., 2019; Rochman et al., 2013; Wright et al., 2013) but the effects and consequences in terrestrial environment just recently started to be a subject of study due to the use of sewage sludge as a fertilizer, compost that accumulate the MPs in the soil over time with successive sludge applications (Corradini et al., 2019; Helmberger et al., 2020). In order to understand why it is crucial to implement MP policies and plans for MPs in sewage sludge some studies about the effects of MPs on plants were reviewed.

The findings of a study on the impact of nano and MPs on a vascular plant with a concentration ranging from 10^3 to 10^7particles mL^{-1} showed short-term negative consequences in the first 8 hours of germination (Bosker et al., 2019). The germination rate of seeds exposed to 4.8 µm MPs decreased from 78% in the control group to 17% in the highest exposure group. After 24 hours, significant differences in root growth were also noted. In

another investigation, six different microplastics (PES fibers, PA beads, and four fragment types: PE, PET, PP, and PS) were introduced to determine how they affect soil and spring onion (*Allium fistulosum*) performance, where PES fibers and PA beads showed the most pronounced effects in plant biomass, tissue elemental composition, root traits, and soil microbial activities, affecting the plant traits and function (de Souza Machado et al., 2019). In a mesocosm experiment, different types of MPs such as PLA, high density polyethylene, and clothing fibers in a concentration of 0.1% w/w, 0.1% w/w and 0.001% w/w, respectively, were introduced to soil as well as to the rosy-tipped earthworm (*Aporrectodea rosea*) and the perennial ryegrass *Lolium perenne* to determine the biophysical soil response. The results demonstrated modifications of water-stable soil aggregates, a decrease in shoot height and seed germination due to the presence of fibers or PLA, and a decrease in *A. rosea* biomass and soil pH due to the presence of HDPE (Boots et al., 2019). In addition, polyester microfibers have shown the capacity to change the dominance of plant species. For example, *Calamagrostis* and *Allelophatic hieracium*invasive species in Europe) became more common when microfibers were present, while the biomass of species that could help other plant species grow (e.g. *Holcus*) declined (Lozano & Rillig, 2020).

All these studies indicate that the effects of MPs can vary according to the characteristics of the MP used: chemical characteristics, shape and size. The most frequent effects are a reduction in germination rate and a change in soil stability. In any case, all the studies found that MPs had a negative impact not only on plants but also on the soil, even in the case of MPs considered biodegradable like PLA. MPs can affect plant biomass, tissue elemental composition, root properties, soil microbial activity, and nutrient cycling. None of the changes reported on the papers showed any advantage, but detrimental effects to soil ecosystem services and terrestrial biodiversity (Boots et al., 2019; Bosker et al., 2019; de Souza Machado et al., 2019; Iqbal et al., 2020; Lozano & Rillig, 2020).The circular economy concept (reuse, reduce and recycling) cannot be applied to solve the problem of MPs due to the small size of particles. Therefore, degradation is the most feasible option to address the MPs pollution. Since all MPs are polymers, made of large chains of molecules, degradation is any process that breaks these chains into shorter chains of lower molecular weight and fewer monomers (oligomers), or the constituent monomers (Crawford & Quinn, 2017). There are two ways in which this can occur; biotic and abiotic (Crawford & Quinn, 2017). There are many microorganisms capable of breaking down the long chains of molecules of polymers since they can use the carbon present in the plastic as an energy source (Oliveira et al., 2020; Sheik et al., 2015).

1.3. Wastewater treatment processes and the accumulation of MPs in sewage sludge

Wastewater treatment plants (WWTP) have been pointed as an important source of MPs to the aquatic environment. This can be expected, since they are not designed to remove MPs (Boucher & Friot, 2017; Reddy & Nair, 2022). Still, WWTPs have a high percentage (70%-99%) of MP removal through the water line/effluent (Carr et al., 2016; Murphy et al., 2016; Simon et al., 2018; Talvitie et al., 2017). However, these "removed" MPs are not really eliminated, they end up in the sewage sludge. This means that up to 99 % of the MPs that were not released into the effluent, which is clean water, are now in the sewage sludge (Magnusson & Norén, 2014).

Europe produces 8.67 million tons of sewage sludge; direct application in agriculture is the most popular option, followed by composting. Europe utilized 23% of sewage sludge in agriculture in 2014 and 47.5% in agriculture in 2018 (EurEau, 2021; Hudcová et al., 2019). Norway, Luxembourg, Spain, and the United Kingdom applied more than 70% of sewage sludge on agriculture, while Portugal applied more than 90% (EurEau, 2021). The information shows that the amount of sewage sludge (SS) is increasing and also the application of this byproduct on agricultural land to address the overproduction (Eriksson et al., 2008; Li et al., 2011; Seleiman et al., 2020).

Globally, the safe disposal of SS is a significant environmental concern due to risk for humans, animals, effects on soil and vegetation (Hudcová et al., 2019). A research conducted in China analyzed 28 WWTPs and found an average of (22.7 ± 12.1) x 10^3 particles of MPs per kg of SS (Li et al., 2018). The majority were fibers (63%). On the basis of China's total sludge production, the average number of sludge-based MPs entering the environment was predicted to be 1.56x10^{14} each year (Li et al., 2018). A study in Chile found that MP content in sludge ranged from 18 to 41 particles g^{-1}, 90% of them having a fiber-shape (Corradini et al., 2019). In England, other research has identified MPs through the entire sludge treatment stream with concentrations ranging from 37.7 to 97.2 particles g^{-1} of treated sewage sludge (dw) in all samples (Harley-Nyang et al., 2022). A study conducted in Ireland characterized MPs in sludge samples from 7 WWTPs and found that abundances ranged from 4.20 to 15.39 particles g^{-1} (dw) (Mahon et al., 2017).

1.4. Use of sludge as fertilizer of soils

SS is a solid or semi-solid by-product of domestic, industrial, and storm wastewaters treated through aerobic or anaerobic digestion processes in WWTPs (Seleiman et al., 2020). This by-product is a sustainable option for the soil from an agricultural and circular economy perspective (reuse and recovery), not only due to its low cost, but also due to its beneficial properties such as organic carbon content, nitrogen, phosphorus, and micronutrients and reduces the synthetic inorganic fertilizers (Domini et al., 2022; Seleiman et al., 2020) that is the reason why it has been used as fertilizer for agricultural land for a long time (Eriksson et al., 2008).

However, despite the advantages of using sewage sludge on agricultural lands, one of the issues is the microplastics content, which is not degraded by pre-treatment because it is persistent and will accumulate in the soil and biomagnifies into the terrestrial environment, posing a threat to species' equilibrium and ecosystem services (Corradini et al., 2019; Kumar et al., 2021).

The largest sludge producers in 2020 in Europe are Poland, Netherlands, Turkey, Romania and Austria. Portugal has not declared the amount of SS used in the agriculture. However, this data is not complete since for some countries like Portugal, Italy, France and Switzerland it was not possible to find updated information about the sewage sludge (Erostat, 2023).

The most common method of final sludge disposal in the EU-15 in 2014 and 2015 was incineration (47.3% and 61.5%, respectively), followed by sludge reuse including direct agricultural application and composting (48.2%, 38.2%) (Hudcová et al., 2019). Currently, EU studies showed that 53% of produced SS is used for final disposal, used in agriculture/composting, while only 20% is used for incineration (Zaharioiu et al., 2021).

To be able to utilize the SS in the soil, prior treatment is required. Current management techniques include biological treatment (anaerobic digestion or co-digestion with other organic waste), chemical oxidation (ozonation and wet oxidation), lime stabilization, and the production of compost. For energy generation, thermal treatment by pyrolysis or gasification can also be applied (Bianchini et al., 2016; Cydzik-Kwiatkowska et al., 2022; Ma et al., 2022; Mahon et al., 2017). The techniques mentioned to pre-treat SS have varying benefits, including the removal of pathogens. However, information about the effectivity of degradation of MP during compost or other pre-treatments is very limited. Only the hyperthermophilic composting technology (composting method created at temperatures above 90 °C, in the presence of

hyperthermophilic bacteria) has been shown to effectively depolymerize the long chain structure of polystyrene (Chen et al., 2020).

One option to address the problem of generation of SS in WWTP is to replace the conventional "activated sludge system" with new technologies like aerobic granular sludge reactors. It has been demonstrated that the amount of SS produced by aerobic granular sludge reactors is significantly less when compared to the conventional system (Bengtsson et al., 2019). Therefore, one could guess that the amount of MPs could be substantially reduced from the sludge as well. MP concentrations in sludge may also be impacted by other factors related to the WWTP characteristics such as servicing area, fraction of industrial wastewater, secondary treatment, and sludge dewatering (Li et al., 2018).

Composting is one of the options to address the problem of sludge production from WWTPs (Hudcová et al., 2019). Compost containing sludge consists of one to two-thirds of SS; the remaining consisting on a bulking agent that can be green waste and biowaste (Hudcová et al., 2019). It is a biological process that uses naturally occurring microorganisms to convert biodegradable organic matter into a humus-like product (Uçaroğlu & Alkan, 2016). Composting can eliminate pathogens, transforms nitrogen from unstable ammonia to stable organic forms of nitrogen, and reduces waste volume. In addition, composting contributes to the activity of thermophilic bacteria by creating a high-temperature environment, and it is one of the most important sludge treatment technologies (Chen et al., 2020). Some methods, such as hyperthermophilic composting, have been shown to be effective at degrading MPs; nonetheless, a greater knowledge of the action of composting and its thermophilic bacteria on MPs is essential for the development of highly efficient approaches for MPs removal in SS (Chen et al., 2020).

Current legislation in Europe for SS dates to 12 June 1986 and only considers maximum levels of heavy metal concentration (Cd, Cu, Hg, Ni, Pb and Zn) and pathogens before the application of sludge on agricultural soils. The law has not been updated to include MP therefore there is no current law or rule restricting their presence in SS to this day (Council Directive 86/278/EEC, 1986). Some countries like Germany or Austria, have introduced more stringent requirements about SS and the use over agricultural lands to reduce pollutant inputs into the soil. However, regulation about MPs remains unknow (Hudcová et al., 2019).

Composting was chosen as the method to examine the biodegradability of MPs in SS obtained from an aerobic granular system, since it is one of the most cost-effective and straightforward strategies to give it a second life or address the issue of sewage sludge production.

1.5. Objective:

To evaluate the biodegradation of compostable and conventional microplastics in sewage sludge, simulating a compost process (before land application).

A. Determine the biodegradability of compostable and conventional microplastics spiked in the dehydrated sewage sludge by composting, after a period of 30 and 60 days.

B. Compare the biodegradation of MPs during the composting process by type of plastic, considering the bacterial community initially present in the dehydrated sludge, and the same community bio-augmented with an isolate from the genus *Bacillus*

C. Evaluate changes in the concentration, size and type of MPs from the dehydrated/dewatered sludge after 60 days of composting.

1.6. Hypothesis

A. Compostable low-density polyethylene (CPE) is expected to biodegrade during the process, while slight changes are expected to occur in conventional polyethylene terephthalate (PET) (bio-deterioration/bio-fragmentation)

B. The bioaugmented community will enhance the biodegradation of MPs.

C. The presence of MPs is expected to alter the remineralization of organic matter (OM)

D. MPs initially present in the sludge are expected to break during the compost process, resulting in a higher number of MPs after 60 days.

2. Material and Methods

2.1. Sampling site/ Collection of sewage sludge

The samples of sewage sludge were collected from a WWTP located in Europe, which includes an aerobic granular system. The granules have a range size between 3– 4 mm of diameter with a smooth, irregular, elongated, and round shape. This obtained SS had been dehydrated before.

Figure 2.1. Dehydrated sewage sludge obtained from a WWTP in Europe with a granular bioreactor.

2.2. Polymers of study

Commercially available plastic products were manually cut into MP films (~2 mm^{-1}) and used to assess their biodegradation, simulating a compost process. For this purpose, polyethylene (PE) and polyethylene terephthalate (PET) were selected, as they are two of the most popular plastics demanded in Europe (6.3 Mt and 4 Mt, respectively) (Plastic Europe, 2022). PE MP films were obtained from a commercially plastic bag from a local shop in the United Kingdom, labeled as “Compostable bag” (hereafter referred as CPE) and PET MPs were obtained from a conventional plastic water bottle, acquired from a supermarket in Portugal.

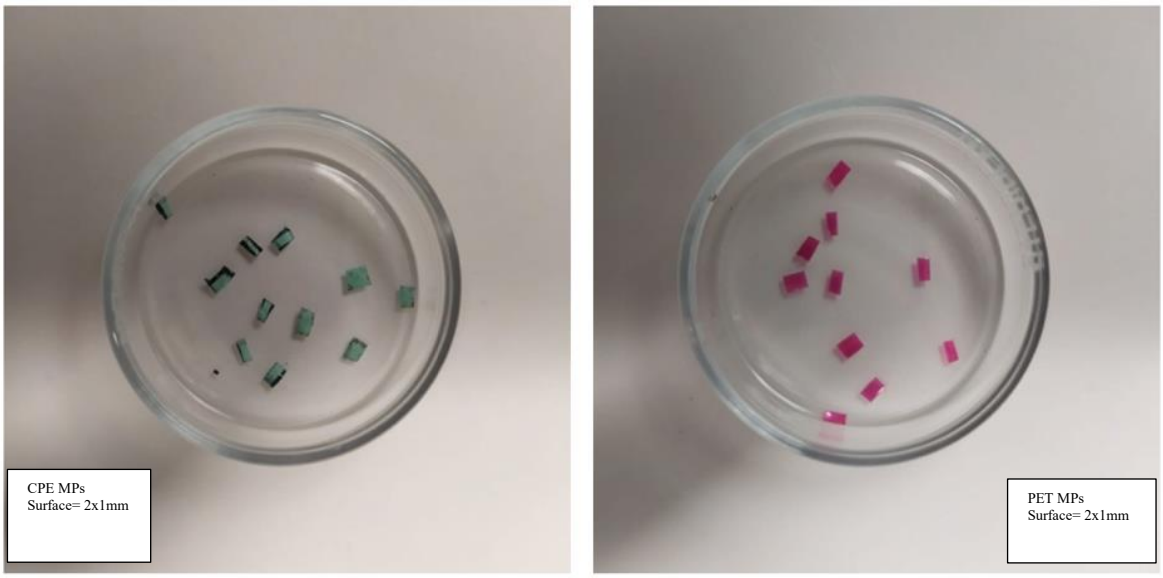

Figure 2.2. Target polymers to study. To the left Compostable low-density polyethylene (CPE) MP and to the right polyethylene terephthalate (PET) tinted with Nile red.

960 MP particles (480 PET and 480 CPE) in form of films were manually manufactured under sterile conditions with the help of metal scissors and tweezers; with an approximate length of 2 mm, and an approximate width of 1mm. The approximate weight for each particle of CPE was 0.36 mg and for PET 0.56 mg (Fig. 3). Both types of MP particles were sterilized using ultraviolet radiation (253.7 nm) for 30 minutes before their use in the experiments. This sterilization method was proven the best to avoid the growth of microorganisms (Fernández de Villalobos et al., 2022).

Additionally, the PET particles were colored with Nile Red (10 µg/ml) (Technical grade, Sigma Aldrich) to be able to recover them more easily. This method is used by some researchers to analyze MPs from environmental samples in the absence of more sophisticated instruments (e.g. FTIR), since it allows for a cheap and quick identification of plastic particles (e.g. Shim et al., 2016).

Error! Reference source not found. summarizes the main characteristics of both polymers. P ET is used in the manufacture of a wide range of products, like food and drink containers, electronic components and as fibers in clothing, because it possesses features such as excellent resistance to aging, flexibility, wear, and heat, as well as being lightweight, impact- and shatter-resistant (Crawford & Quinn, 2017; Szczurek et al., 2023). PET is a thermoplastic polyester with the chemical formulation $C_{10}H_8O_4$ (Crawford & Quinn, 2017; Szczurek et al., 2023) (Figure 2.3). It is composed by terephthalic acid and ethylene glycol monomers (Bardoquillo et al., 2023). Its molecular orientation in solid phase is semicrystalline (Crawford & Quinn, 2017).

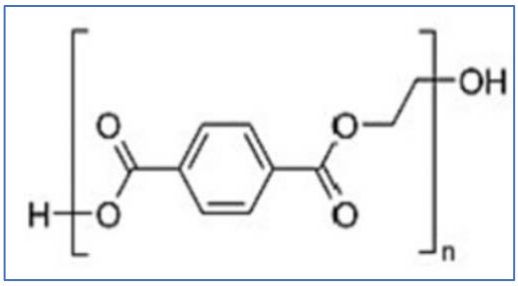

Figure 2.3. Chemical structure of PET polymer

As shown in Figure 2.3., the PET monomer consists of an aromatic ring coupled with a short aliphatic chain (Reese, 2003; Fotopoulou & Karapanagioti, 2017). PET is also characterized by a high ratio of aromatic terephthalate units and it is also semicrystalline, consisting of both crystalline and amorphous domains (Taniguchi, et al., 2019). Knowing the molecular structure of the target polymers is essential for the study, since the degradation process of polymers depends, among other environmental factors, on its molecular weight, the reactive functional groups in the backbone, chain mobility/flexibility, degree of crystallinity, and surface hydrophobicity (Zheng, et al., 2005; Fotopoulou & Karapanagioti, 2017; Tiwari, et al., 2018;Taniguchi, et al., 2019; Ahmaditabatabaei, et al., 2021).

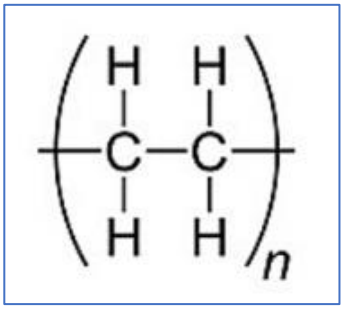

Figure 2.4. Chemical structure of low-density polyethylene polymer

Low density polyethylene is a synthetic resin with good flexibility pliable, soft and readily flexed, that's why it is widely used in retail packing applications, trash bags, film products, injection molded products, medical appliances, and pharmaceutical and food packaging materials (Ding et al., 2022; Peacock, 2000). LDPE is thermoplastic polymer with the chemical formulation C_2H_4 (Crawford & Quinn, 2017). It is composed of long chains of ethylene monomers (Figure 2.4.) (Bardoquillo et al., 2023) and its molecular orientation in solid phase is semicrystalline (Crawford & Quinn, 2017). LDPE has a density lower than water, as well as good water repellent characteristics, therefore, it tends to float on surface waters (Crawford & Quinn, 2017).

Table 1.1. Principal properties of target polymers, also environmental weakness, temperature, and UV light resistance. Autor Crawford & Quinn, (2017) modified

Plastic	General properties	Environmental weakness	Maximum temperature (°C)	Resistance to UV light
PET 	Transparency to visible light and microwaves. Very good resistance to ageing, wear and heat. Lightweight, impact and shatter resistant. Good gas and moisture barrier properties	Can hydrolyze in water, wet or humid conditions at high temperatures (>73–78°C)	80–140	Fair
LDPE 	Depending on the degree of crystallinity, PE can be flexible (low-density). When stabilized, PE exhibits good weathering resistance and good chemical resistance. Water repellent	Prone to cracking under stress. Photo-oxidizes	80–100	Fair

2.3. Experimental set-up

For this, 1.2 kg from the dehydrated sludge were collected and mixed with 300 g of dry leaves, collected at the university campus, and used as bulking agents (80% sludge and 20% bulking agent (BA), as in previous work (Ma et al., 2022; Uçaroğlu & Alkan, 2016)) (Figure 2.5). This mixture was well homogenized and then divided into 33 glass flasks, each containing 25 g of the mixture – explain here the different treatments used.

Composting conditions were settled at 50 °C, during 60 days (Chen et al., 2020; Ma et al., 2022; Xing et al., 2022). Following similar specifications (Ma et al., 2022; Xing et al., 2022) the experimental sample consisted of 25 g composting material composed by 80% (w/w) of dehydrated sludge and 20% (w/w) of dry leaves.

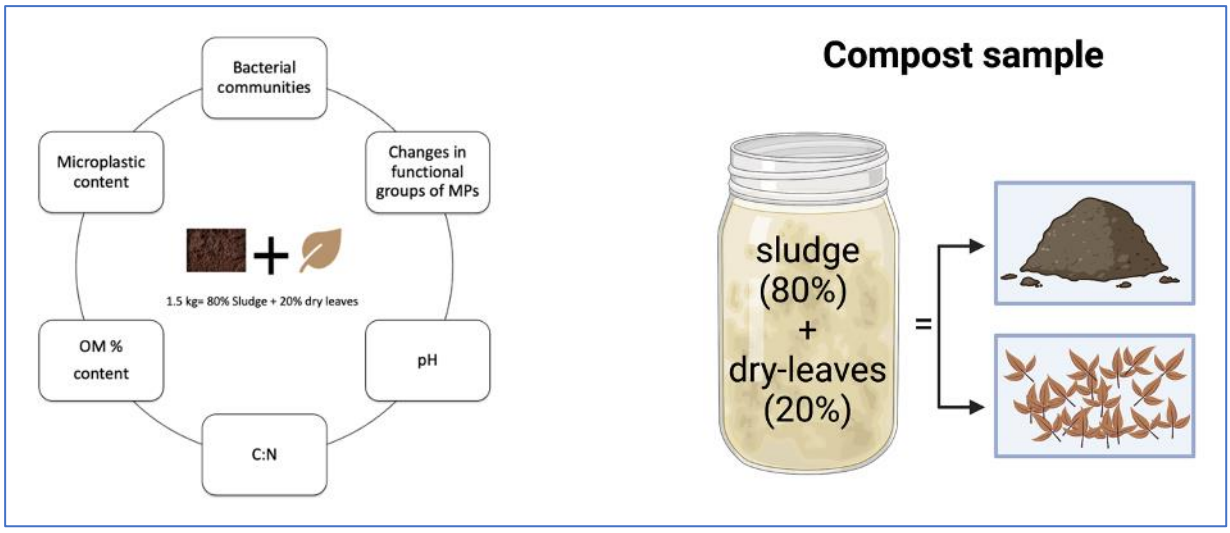

Figure 2.5. Variables that were controlled at the initial time (T0), after 30 days (T1) and after 60 days (T2): bacterial communities; changes in the functional group of MP, organic matter content (OM%), carbon/nitrogen ratio (C:N) and pH. Created with BioRender.com

The experiment consisted of simulating composting conditions to see whether, in a controlled environment, the *Bacillus* bacterium is capable of degrading PET and CPE, as well as the initial bacterial community from the SS (Figure 2.5.). The initial conditions of the experiment were 50 ºC, organic matter 85% ± 2; pH 5.79 ± 0.01, C:N ratio 12 ± 1.

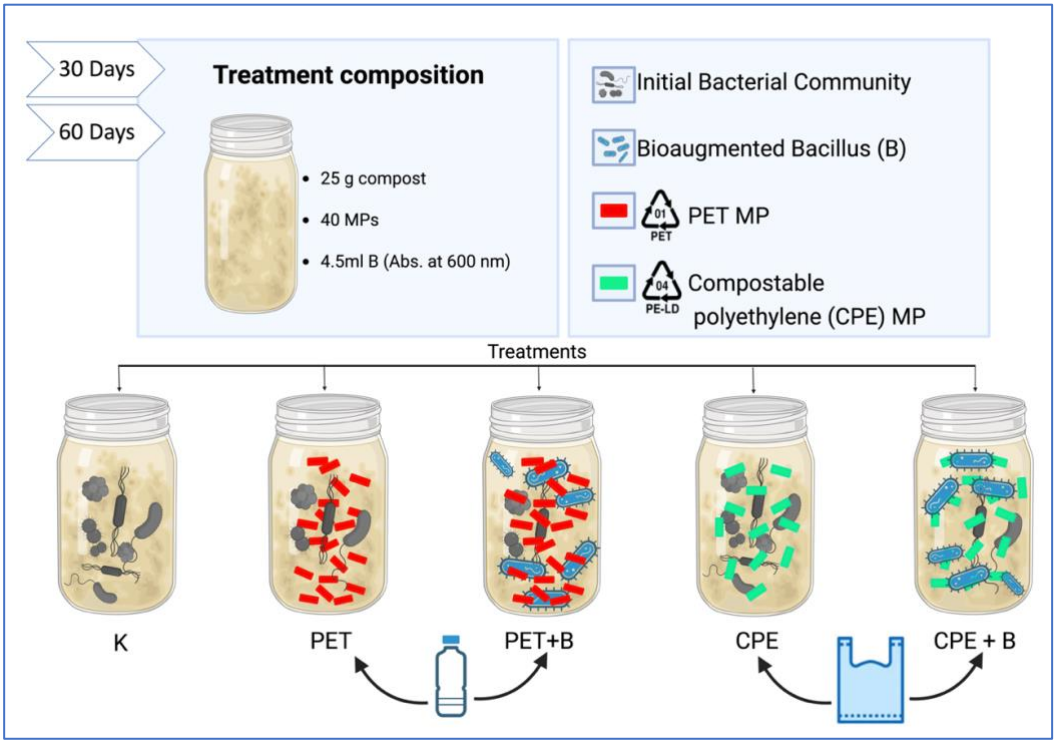

Figure 2.6. Scheme of the biodegradation experiment with the bioaugmented isolates, consisting of 4 treatments. Negative control (K), treatment with the initial bacterial community (PET/CPE), treatment with bioaugmented *Bacillus* (PET+B / CPE+B). Created with BioRender.com

The analysis of samples was performed in 2 batches (after 30 and 60 days), each batch containing 15 samples (5 samples with 3 replicates each) (see Table 2.1. and Figure 2.6). The blank or negative control, consisting of 80% of SS + 20% bulk agent without added MPs was settled in triplicate for each batch (Table 2.1). The biodegradation rate of CPE and PET will be measured by FTIR in 30 days and 60 days. Some of the composting sample was submitted to bioaugmentation by adding bacteria of the genus *Bacillus*. Each container included ~25 grams of composting sample (SS + BA) and 40 particles of PET/CPE except the negative control. 4.5 ml of a bacterium inoculum of the genus *Bacillus* was added to the treatments CPE+B and PET+B and 4.5 ml of mineral salt medium (MSM) was added to the other treatments CPE, PET, and the negative control containers that were without bioaugmented bacteria in order to standardize all the samples.

Table 2.1. Experimental design with 3 replicates for each treatment. (T0) means the initial time, (T1) 30 days and (T2) 60 days. "K" means negative control

SAMPLING TIME	TREATMENT	Medium	REPLICATES
T0	–		3
T1 (after ~30 days)	K (SLUDGE WITHOUT MPs)	~ 25 g of compost sample + 4.5 ml of MSM	3
	PET + sludge		3
	CPE + sludge		3
	PET + sludge + bioaugmented *Bacillus*	~ 25 g of compost sample + 4.5 ml of bioaugmented *Bacillus*	3
	CPE + sludge + bioaugmented *Bacillus*		3
T2 (after ~60 days)	K (SLUDGE WITHOUT MPs)	~ 25 g of compost sample + 4.5 ml of MSM	3
	PET + sludge		3
	CPE + sludge		3
	PET + sludge + bioaugmented *Bacillus*	~ 25 g of compost sample + 4.5 of bioaugmented *Bacillus*	3
	CPE + sludge + bioaugmented *Bacillus*		3

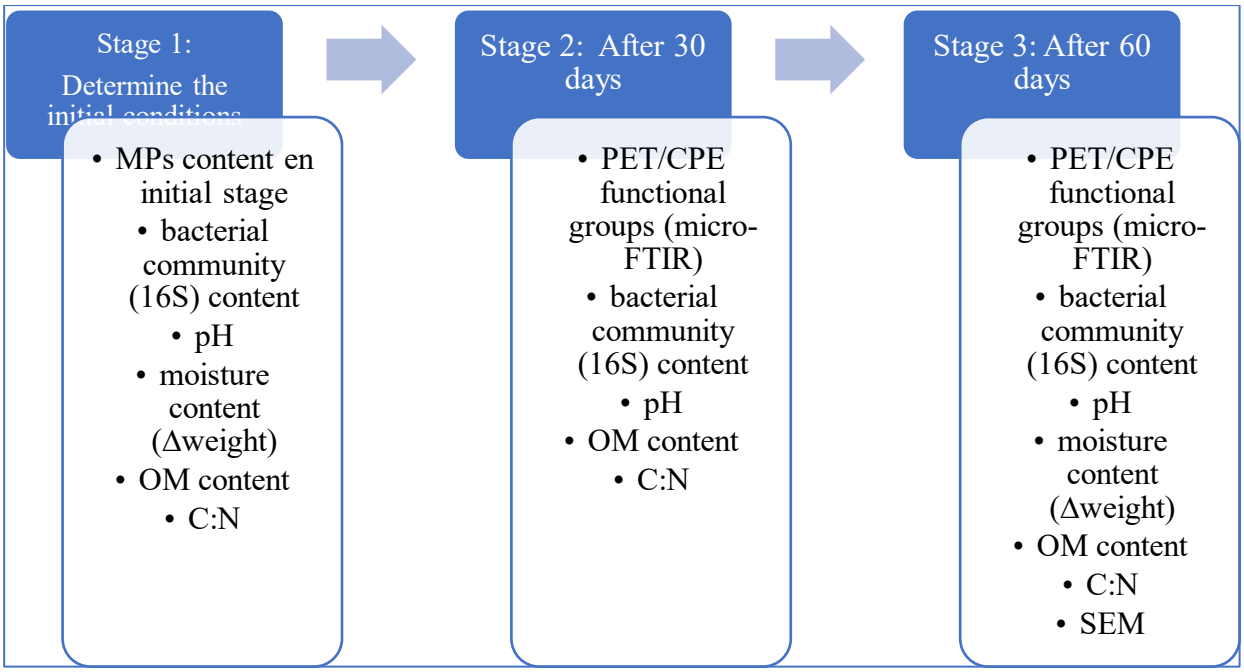

Figure 2.7. Stages of the experiment split in three stages where the first one is the initial time; Stage 2 was after 30 days and stage 3 after 60 days

2.4. Preparation of inoculum

The inoculum added to samples (PET+B and CPE+B) was an isolate of a bacteria that showed ability to grow on a minimum salt medium, using PET films as a sole C source (Ngonyani, 2022). The bacteria was isolated from a community of bacteria recovered from the tunicate *Didemnum sp* in a previous work (Fernández de Villalobos et al., 2022). This bacterium was bioaugmented to assess its potential to biodegrade PET and CPE with a composting technique.

Since the bacteria had been stored at -20 °C for 12 months approx. a PCR and sequencing to identify the genera was performed. Quality control of the sequence reads were done using the Geneious software 2022.2.2. Both forward and reverse sequences from each sample were trimmed to remove unclear nucleotides, and clean sequences were used for pairwise alignment. The determination of taxonomic identity was carried by Blast search of Gene Bank database of NCBI (https://blast.ncbi.nlm.nih.gov/). The alignments were based on the nucleotide sequences. The sequences from the GenBank that showed the highest query cover and percentage of identity with ours, were considered as the genus our species belonged to. Although species level could not be determined, because of the highest matches found with several of the reported species at the GenBank, it can be said with high confidence that our isolate belonged to the *Bacillus* group, as determined in a previous work (Ngonyani, 2022).

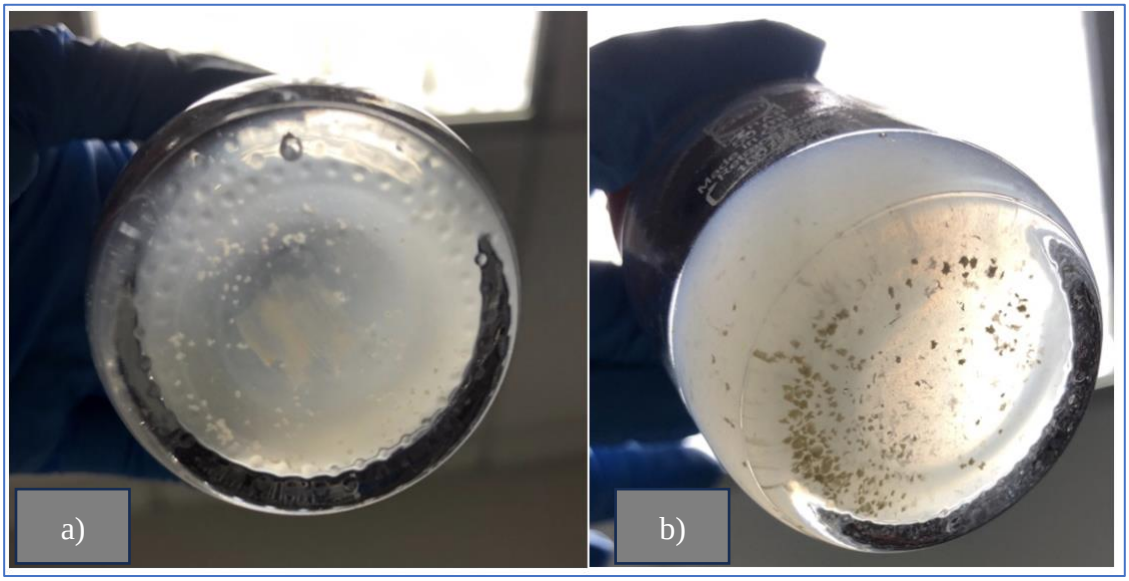

Figure 2.8. Bioaugmented bacteria from genus *Bacillus* suspended in MSM after 24 (a) hours and after 48 hours (b)

Based on previous works (Fernández de Villalobos et al., 2022) the bacterial inoculum was prepared by adding one aliquot of these samples to a flask containing MSM) (1:10 dilution). The samples were left in the dark, at 25 ± 1◦C under orbital agitation (150 rpm) for 24 h (Figure 2.9). The samples were then incubated under the same conditions as described previously. After 48 h of incubation, bacteria samples were centrifuged (4000 rpm; 10 min), the supernatant discarded, and the pellet washed and resuspended in new MSM. This washing procedure was repeated two times, and the final pellet was resuspended in the sterile MSM and used as inoculum in the experiment (Fernández de Villalobos et al., 2022).

2.5. Analytical and Chemical methods

2.5.1. Changes in functional groups of spiked MP through FTIR-ATR

For this experiment FTIR (Nicolet iN10MX, Thermo Scientific, Italy) was used to measure the chemical degradation of CPE/PET MP. After measuring the sample's weight 3 particles were recovered from each container. The coated MPs were washed with sodium dodecyl sulfate SDS and left to settle for four hours before being rinsed with distillate water and ethanol to remove any leftover bacteria that may have adhered to the particle, as impurities can interfere with μ-FTIR analyst. The Setup of the FTIR were in the “Collection Mode” ATR mode, with high spectral resolution, combined with spectra format % Absorbance; in “Advance” category the signal filter was optimal (Blackman-Harris) and the containers were autoclave-sterilized to avoid contamination.

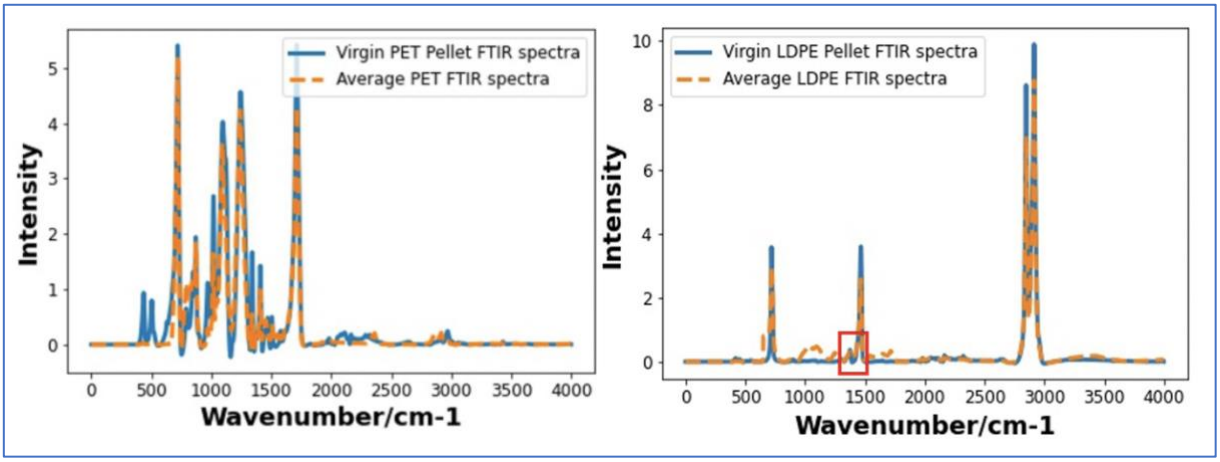

Figure 2.10. Example of PET/CPE peaks with FTIR-ATR spectra. Modified from Neo et al. (2023).

Table 2.2. Principal spectral absorption peak positions ($\boldsymbol{cm^{-1}}$) of the functional groups characterizing low-density PE (CPE/ polymers), according to the current literatures (modified after Fernández de Villalobos et al., 2022).

Peak band $\boldsymbol{cm^{-1}}$	Functional group	Reference
3728-3733	Hydroxyl or amino groups	(Coates, 2006) (Brandon et al., 2016)
2915-2917	CH_2 asymmetric C-H stretching	(Coates, 2006) (Jung et al., 2018)
2849-2851	CH_2 asymmetric C-H stretching	(Coates, 2006) (Jung et al., 2018)
1648-1650	C=C bond of the vinyl group/C=O bond of the carbonyl group	(Brandon et al., 2016) (Denaro et al., 2020)
1459-1470	Bending formation; CH_2 deformation split when PE is crystalline; attributed to C=C of an aromatic compound	(Auta et al., 2017)(Coates, 2006) (Jung et al., 2018)
1078-1081	Carbon-oxygen bonds	(Brandon et al., 2016)
870-871	Trans bending oxy-methylene group	(Mecozzi & Nisini, 2019)
730	CH_2 rocking deformation	(Coates, 2006) (Jung et al., 2018)
717-718	rocking deformation; CH_2 deformation slipt when PE is crystalline	(Coates, 2006) (Jung et al., 2018)

Table 2.3. Principal spectral absorption peak positions (cm^{-1}) of the functional groups characterizing PET/polymers, according to the current literature (modified after Fernández de Villalobos et al., 2022).

Peak band cm^{-1}	Functional group	Reference
3728–3733	Hydroxyl or amino groups	(Coates, 2006)
2921	CH_2 asymmetric stretch	(Coates, 2006) (Jung et al., 2018)
1715	C=O stretch (ketones)	(Coates, 2006) (Jung et al., 2018) (Mecozzi & Nisini, 2019)
1630–1655	C=C bond of the vinyl group/C=O bond of the carbonyl group	(Brandon et al., 2016; Denaro et al., 2020; Fotopoulou & Karapanagioti, 2015; Syranidou et al., 2019)21.07.2023 10:08:00
1458	Bending CH2	(Coates, 2006) (Jung et al., 2018) (Mecozzi & Nisini, 2019)
1410	In-plane vibrations of the benzene ring	(Denaro et al., 2020)
1335 - 1342	Trans wagging band -CH_2, Crystalline phase	(Denaro et al., 2020) (Mecozzi & Nisini, 2019)
1270	Stretching of the ester (O=C–O–) bond	(Coates, 2006) (Denaro et al., 2020) (Mecozzi & Nisini, 2019)
1234 - 1269	Asymmetric Stretch C-C-O group bonded to aromatic ring, C=O in-plane bending	(Denaro et al., 2020) (Jung et al., 2018) (Mecozzi & Nisini, 2019)
1100–1103	C–O–C stretch	(Coates, 2006) (Jung et al., 2018) (Mecozzi & Nisini, 2019)
1019–1020	Aromatic ring in-plane C–H bend	(Coates, 2006)
938 - 978	Gauche bending oxymethylene group, trans -C-O stretching	(Mecozzi & Nisini, 2019)
871–874	Trans bending oxymethylene group,	(Mecozzi & Nisini, 2019)
728–730	deformation of the aromatic ring	(Denaro et al., 2020)

2.5.2. Composting parameters

- **pH**

This analysis was measured using a pH-meter (CRISON, GLP21, Spain). The pH of the samples was obtained by shaking/mixing 2-3 grams of sample with distilled water at 1:10 (w/v) and 1 ml of potassium chloride to increase the conductivity of the solution without affecting the pH (Uçaroğlu & Alkan, 2016).

- **Moisture content**

After taking subsamples for the analysis of pH and recovery of MP (PET or CPE) particles, the remaining samples were left to dry at 100 ºC overnight. Then, the weight was determined,

and the moisture content was determined by subtracting the dry weight from the wet weight, according to the formula:

$Humidity$ (%) = ($Wet\ weight - Dry\ weigth$)/Wet weight x 100

Afterwards, samples were homogenized, and sub-samples were taken for the following analysis: Organic matter, C and N, and MP content (only at the beginning and at the end of the experiment).

- **Organic matter**

After drying the samples at 100ºC, around 2.5 to 3 g of each sample were taken and summited to pyrolysis. Samples were subjected to 450 ºC for 4 hours. The ashes weight minus the weight of the subsample gave it the organic matter content, in grams. For a better comparison with other studies, results were transformed in grams, according to the formula:

OM (g) = weight (subsample) – weight of remaining ashes (after subjecting the sample to 450 ºC)

OM (%)= OM(g)/ sample *100

- **C:N**

Around 1 to 2 mg of sample were weighted in a microbalance (Sartorious; model: MSA36S-000-DH) to measure the content of Carbon and Nitrogen in the samples. The C:N ratio was measured using an elemental analyzer (Vario EL III Elemental Analyzer) (manufacter: Elementar; Model: Vario EL III).

2.5.3. DNA concentration

To identify the bacterial community initially present in the sludge and developed in the different treatments after 30 and 60 days under composting conditions, DNA was extracted from the samples. For this purpose, 0.31 ± 0.04 mg were taken from each sample for DNA determination. The DNA was extracted using the NZYTech® NZY Soil gDNA Isolation Kit, following the manufacturer's instructions. The quality and concentration of eluted DNA was then quantified using a NanoDrop spectrophotometer to measure DNA concentration and absorbance at 260 and 280 nm wavelengths (NanoDrop One C, Thermo Scientific, United States). Extracted DNA was subsequently sent to the Integrated Microbiome Resource laboratory (Halifax, Nova Scotia, Canada) for PCR amplification and sequencing of the full 16S gene (PacBio Sequel).

2.5.4. Scanning electron microscopy analysis

Scanning Electron Microscopy (SEM) is a tool that allowed us to examine the morphological change on the surface of the MPs. Previous to their observation and following previous experiments (Fernández de Villalobos et al., 2022; Ngonyani, 2022), microplastic particles from each treatment were washed with 2% (v/v) SDS during 4 h at room temperature, and then rinsed with distilled water and ethanol (70% v/v).

This analysis was performed at the end of the experiment, meaning after 60 days, to inspect if the particles' surface had undergone physical decomposition and if the bioaugmented bacteria enhanced this decomposition. One particle of each treatment (PET, PET+I, CPE, CPE+I) included a control for each type of plastic (KPET and KCPE) was analyzed by SEM (TESCAN Clara, Czech). Since MPs are non-conductive (Shi et al., 2022), particles were coated with gold nanoparticles before being mounted on the microscope following previous experiments (Fernández de Villalobos et al., 2022). Then the MPs were visualized under varying magnifications to observe their surface.

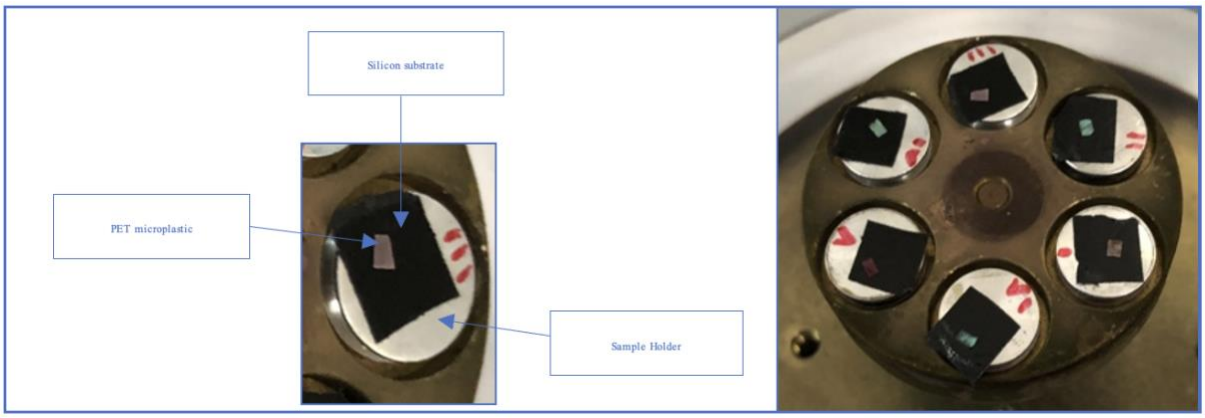

Figure 2.10. Sample preparation: (b) sample holder arranged on a SEM sample stand.

Morphology: Field Emission Scanning Electron Microscopy (TESCAN Clara, Czech), using 5kV accelerating voltage, ~10 pA current, 8-9 mm working distance and high vacuum. The micrographies were obtained with an Everhart-Thornley secondary electron detector.

The Energy Dispersive Spectroscopy experiments were performed with an X-ray spectrometer Bruker XFlash 6130 SDD detector with 126 eV spectral resolution at the FWHM/Mn Kα coupled to the FEG-SEM. The map and point analyses were acquired at 20kV

accelerating voltage, ~1 nA current, and 8-9 mm working distance and high vacuum. The data was collected and processed using the software Esprit 2.5.

2.5.5. Analysis of MPs from sewage sludge

Following the procedure performed in previous experiments (Van den Auwelant, 2022) the microplastics contained into the initial and final stage of the experiment in SS were extracted following a density separation protocol, followed by digestion with hydrogen peroxide. The density separation consisted of using a supersaturated NaCl solution (~1.2 g cm^{-3}) to keep the less dense particles (most plastic polymers) floating, while the denser particles will settle down. For this 100 ml of NaCl were added to 10 g (dry weight) of sample. The sample was stirred with a metallic spoon for ~ 4 min, and the sediment was left to settle for 12 h (Corradini et al., 2019). Afterwards, the solution was vacuum filtered through Whatman polyethersulfone (PES) filters (0.45 µm pore-size). To eliminate the organic matter from the samples, 20 ml of H_2O_2 (30%) were added to the filters, and they were kept at 50 ºC for 48-72 h. Due to the high organic matter content in the samples, it was necessary to repeat the step (adding more 20 ml of hydrogen peroxide) to obtain a filter clean enough to look in the microscope and mark the suspected MP particles to be analyzed by µFTIR. Once the organic matter was not visible anymore, the solution was filtered through 25 µm cellulose filters, and these filters were examined in the microscope. In the microscope, suspected MPs present in the filters were ¼ counted and classified according to the shape, color and size following the Guideline for the Monitoring and Assessment of Plastic Litter in the Ocean (GESAMP, 2019) and Van den Auwelant, (2022) from previous work. The suspected MPs were photographed with a Leica MC170 digital camera, measured, and characterized based on shape (fiber, fragment, or film). The chemical composition of the suspected MP particles was later verified in the µ-FTIR, under reflection mode (since often, the small size of the particles did not allow for ATR analysis) to characterize the type of polymer. Analysis were run with the following setting: In reflection mode, with high spectral resolution (16 scans run in 5 seconds), combined with spectra format % Absorbance; for the “Stage, Aperture and Display” the aperture varied depending of the size of suspected particle, example for fiber the aperture was around 25 µm and for fragments 50 µm or more depend of the size of the particle; in “Advance” category the signal filter was optimal (Blackman-Harris).

After the extraction by flotation the with NaCl solution Whatman No 25 µm cellulose filters were analyzed in a Leica S8 APO stereomicroscope (magnification 10X-80X). This procedure was performed just for the control (K) in the initial time and the end of the experiment (after 60 days). Since the samples were high in organic matter content the cellulose filters were abundant (approx. 8 filters by each replicate), then the filters were divided in 4 and analyzed ¼ of the filter. The particle concentration is given as number of particles by gram.

The quality control measures to avoid MP contamination were to cover the samples with aluminum through the whole procedure, avoiding plastic materials when possible; each material used was rinsed 3 times with filtered (0.22 µm) distilled water and 3 times with filtered (1 µm?) acetone and 3 times again with filtered (0.22 µm) and distilled water (Gewert et al., 2015). In addition, control blank samples were established, and the particles discovered in the control samples were subtracted from the overall amount of MP. Two particles were detected in the control.

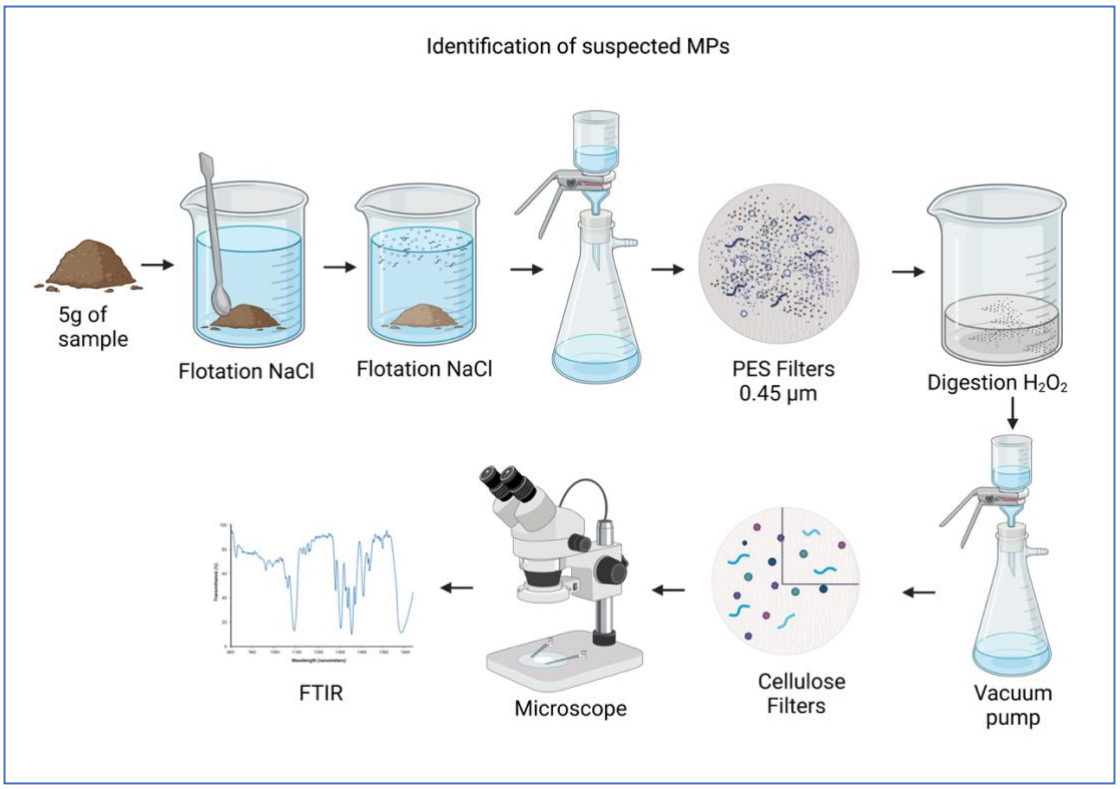

Figure 2.11. Protocol followed to analyze MPs from sewage sludge samples. Created with BioRender.com

Processes required to analyze MP by weighing the sample to determine the quantity of NaCl. To prevent contamination, the SS must be stirred with a spoon made of metal or glass. The pump must be equipped with PES filters, and only a minimal amount of supernatant should be introduced to prevent clogging. The digestion will rely on the organic matter content. The condition of the filters regarding digestion must be often monitored. After digestion, the liquid must be filtered again, but cellulose filters can be used since they will not be exposed to H_2O_2. To save time, a quarter of the filter can be examined under a microscope, and the suspected MP must be confirmed with an FTIR machine to determine its type.

Since the organic matter content was high, the cellulose filter obtained to analyze were abundant (around 8 filters per each replicate). Therefore, the filter was divided in four and one quarter of the filter was analyzed; and just 4 filters of each replicate were analyzed. The following criteria was used in the analysis of the suspected MPs founded in the filters:

>40% of match = Microplastic

<40%=unsure

Lost = Lost

The results were checked with the FTIR confirmation and were extrapolated to define the quantity of MPs by gram and were classified by type of polymer, shape (fiber, fragment, film or pellet) and color. Also, a comparison with the initial time and the final time was performed in order to determine if the quantity of MPs after 60 days decreased or not.

2.6. Statistical analysis

Shapiro-Wilk test was performed using the package dplyr (Wickham et al., 2023) of the R-studio (Version 1.0.143) software for the variables OM, C:N, pH, and FTIR peaks, to evaluate whether data came from a normal distribution. Since the results showed that this data did not came from a normal distribution ($p < 0.05$), the Wilcoxon non-parametric test was performed to assess for differences between treatments and incubation time. This test was performed using JMP Statistical Discovery software version 17.1 (SAS company NC, USA).

Similarly, to analyze differences in the absorbance intensity of the PET and CPE peaks measured by FTIR-ATR, the Wilcoxon signed-rank test was performed for each type of plastic, to assess for differences between samples containing the bioaugmented bacteria, and samples without inoculum.

3. Results and Discussion

3.1. Effects of MPs on composting parameters

Composting is an efficient bioremediation treatment for organic contaminants that are prevalent in soils and sediments due to its low cost and ease of operation (Lin et al., 2022). Composting offers various advantages over conventional single- and multistrain bio enhancement approaches, including a diverse microbial population, ease of operation, and the potential to manage higher concentrations (Lin et al., 2022). The main parameters measured for the compost experiment are expressed in the mean of 3 replicates and its standard deviation (±). The parameters of the compost experiment at the initial time (T0) were: pH (6 ± 1); OM% (85% ± 4); C:N (12 ± 1); and moisture content (42%) (Figure 3.1). Furthermore, the temperature settled at around 50 °C since high temperatures can enhance the degradation by making the contaminants less viscous and more bioavailable (Lin et al., 2022).

As can be seen in Figure 3.1a) the pH for the initial time was 6 ± 1. Due to the continued breakdown of organic acids, volatilization, and formation of NH_3 the pH did not remain within this range for very long (Lin et al., 2022). A study made by Uçaroğlu & Alkan, (2016) where they investigated the compostability of SS containing different bulking agents (BA) (Wheat straw, plane leaf, corncob, and sunflower stalk) to determine the most efficient bulking agent also showed similar pH (6.8 and 7.5) for the initial time even if the proportion of the bulking agent was different (40% BA and 60% SS).

As can be seen in Figure 3.1 b) the organic matter for the initial time was high (85 ± 4) %. The microbes utilize readily degradable organic matter as a nutrient source and microbial activity slows down as nutrient sources deplete (Lin et al., 2022). The observed OM content was higher compared with the study reported by Uçaroğlu & Alkan (2016), where a comparison of 4 types of bulking agents (wheat straw, plane leaf, corncob, and sunflower stalk) was made to identify the best one to compost SS. In the treatment with leaves, that would be equivalent to the one used in this experiment, they reported an OM content of 73% in initial time. This difference can be due to the percentage of bulking agents mixed with the SS since they applied 40% of BA and in this experiment just 20% was applied.

As can be seen in Figure 3.1c the C:N ratio in the initial time was 12 ± 1. Carbon and nitrogen are considered the key nutritional components of composting. Nitrogen supports cell growth, whereas carbon provides energy. Composting uses the C/N ratio to determine microbial nutrition (Lin et al., 2022). The measured parameter agreed with current literature where the range of C:N for compost material from SS is between 11.3–11.5 C:N ratio (Lin et al., 2022). The initial value (12 ± 1) of this experiment had similar values with Ma et al., (2022) study (C/N 10.1) where they explored the influence of polystyrene-microplastics (PS-MPs) on SS through composting by 30-day and added 0%, 0.5%, and 1% (w/w) PS-MPs. The author found variance between the treatments i.e. the pile C which contain 1% of PS showed a higher C:N ratio than the pile that did not contain PS MPs.

The moisture content in the initial time was 42%. Microorganisms need moisture to survive, therefore composting requires moisture. Waterlogs from composting with more than 70% moisture cause anaerobic conditions (Lin et al., 2022).

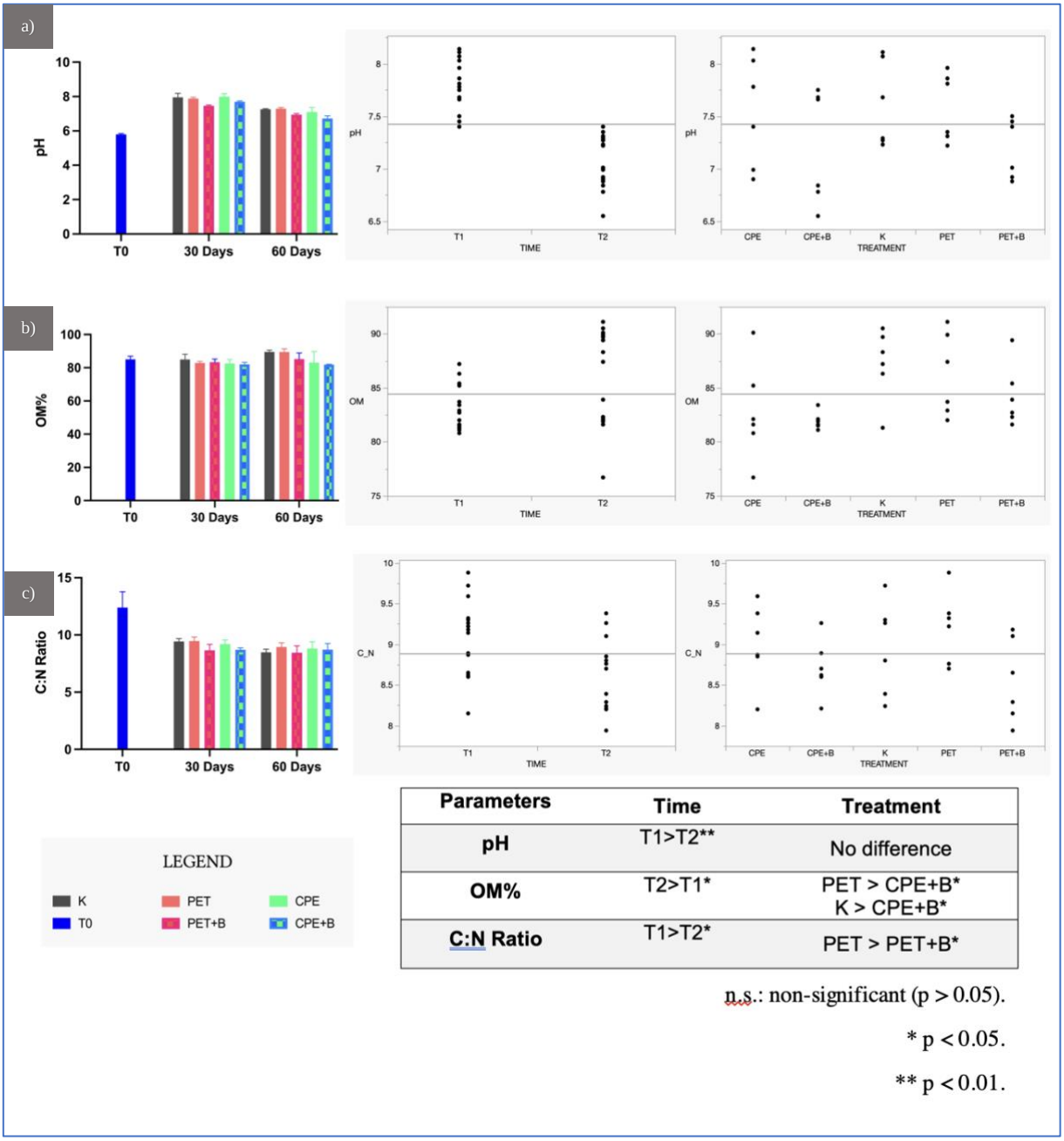

Parameters	Time	Treatment
pH	T1>T2**	No difference
OM%	T2>T1*	PET > CPE+B* K > CPE+B*
C:N Ratio	T1>T2*	PET > PET+B*

n.s.: non-significant ($p > 0.05$).

* $p < 0.05$.

** $p < 0.01$.

Figure 3.1. Principal parameters measured during the experiments. "X" axis shows the time for all the parameters. The Y axis shows a) pH; b) organic matter; c) C:N Ratio. Wilcoxson test graphics at the 95 % confidence level shows a comparison between time and treatments.

The pH values for K, CPE, CPE+B, PET and PET+B in 30 days were: 8.0 ± 0.2; 7.9 ±0.1; 8.0 ± 0.2; 7.5 ± 0.1; 7.7 ± 0.1, respectively. For 60 days in K, CPE, CPE+B, PET and PET+B was 7.3± 0.1; 7.3 ± 0.1; 7.1± 0.3; 6.9± 0.1 and 6.7 ± 0.2 respectively (Figure 3.1). The initial pH was lower and increased after 30 and 60 days. A considerable decrease was detected between 30 and 60 days of composting, but none between the different treatments (Figure 3.1). The increase in pH can be attributed to the ammonia created by the decomposition of nitrogen-containing organic matter, resulting in a neutral or slightly alkaline compost when it is ready

for use (Lin et al., 2022). It can be said 40 MPs from PET or CPE that represent 0.06% and 0.09% respectively in the sample did not have effect on pH levels (Table 5). In contrast, in a study by Ma et al. (2022) in which two distinct composting treatments were done with polystyrene MPs (addition of 0.5% and 1% of MP in terms of mass), the pH values were much lower when MPs were present. The quick breakdown of nitrogen-containing compounds and the formation of ammonia are predicted to cause the pH value to rise as the temperature rises (Ma et al., 2022) but his outcome is a consequence of the addition of MPs. MPs reduce the carbon microbial biomass, compost temperature, and consequently the pH. Another study showed that an addition of 10% MPs (g/g), significantly decreased soil pH and increased soil dissolved organic carbon (Wang et al., 2021). It can be inferred that the mass % of MPs (MPs/compost sample) used in this current experiment is not enough to affect the pH parameter.

The OM content K, CPE, CPE+B, PET and PET+B in 30 days were: 85±3; 83±1; 83±2; 83±2; 82±1, respectively. For 60 days in K, CPE, CPE+B, PET and PET+B was 90±1; 90±2; 83±7; 85±4; 82±0, respectively. When OM was compared amongst treatments (K, PET, PET+B, CPE, and CEP+B) using the Wilcoxon test, the control (K) was observed to be higher to CPE+B. Moreover, PET demonstrated greater values than CEP+B. This would mean that the inoculum is enhancing the remineralization of OM, lowering the OM content, while increasing the N content (and thus decreasing the C:N ratio). The OM content was higher after 60 days. Microplastics can inhibit the degradation of organic matter. These inhibitions can be related to the disruption of soluble proteins by MPs, which also reduced the capacity of microbes to degrade organic materials (Ma et al., 2022). Also, the use of dry leaves as bulking agents can interfere in the amount of OM mineralization due to the presence of lignin, making difficult to degrade (Uçaroğlu & Alkan, 2016). Contrarily, a report by Uçaroğlu & Alkan, (2016) showed a decrease from the initial value in OM (72.8% to 58.3%) in 21 days when applying leaves as a BA. Decreasing OM contents during composting are the result of OM mineralization by microorganisms (Uçaroğlu & Alkan, 2016), but this was not the case for this experiment where a slight increase was observed after 60 days.

The C:N ratio for K, CPE, CPE+B, PET and PET+B in 30 days were: 9 ± 0.25; 9 ± 0.36; 9 ± 0.36; 9 ± 0.52; 9 ± 0.16, respectively. For 60 days in K, CPE, CPE+B, PET and PET+B was 8 ± 0.29; 9 ± 0.38; 9 ± 0.59; 8 ± 0.60; 9 ± 0.53, respectively. Comparison between treatments with the Wilcoxon test allow to see a significant difference between PET and PET+B where PET is higher than PET+B. However, the C:N ratio decreased from 12 ± 1 to 9±0 after 30 days and was maintained after 60 days. This can mean that the C:N ratio reached a balance at 30 days. Furthermore, it was not affected by the type of treatment (CPE, CPE+B, PET and

PET+B). Similar results were shown in the study of Uçaroğlu & Alkan, (2016) where the initial C/N values decreased in 24% after 21 days and in the present study that decrease was 25%.

Table 3.1. Theoretical calculations for target polymers. The calculation was made considering the shape of the particle, to determine the volume, and then the density (according to plastic type PET or CPE)

POLYMER	MASS (mg) per particle	Total mass (40 MP particles)	% Mass (MP/compost sample)
CPE	0.36	14 mg	0.06
PET	0.56	22.5 mg	0.09

The presence of 40 particles of PE and PET accounted for a mass of ~14 mg and ~22.5 mg, respectively, as theoretically determined for this study, and empirically measured in previous similar experiments (Fernández de Villalobos et al., 2022; Ngonyani, 2022). 40 particles of CPE and PET accounted for 0.06% and 0.09%, respectively, of the total mass of the sample (Table 5), which may explain a small effect on the composting process. Others studies that present change on these parameters had the sample spiked with 0.5% to 10% (dry weight MP/ dry weight of sample). However, for the purposes of future legislation on the application of SS as soil fertilizer, toxicological tests should be performed to set a threshold on the number or percentage of mass of MP that can be considered safe to plants and terrestrial organisms before land application (Ma et al., 2022; Wang et al., 2021).

3.2. Changes in functional groups of spiked MPs

Fourier-Transform Infrared spectrometer (FTIR) is a useful technology that allows to identify the type of plastic polymers and MPs in environmental samples (Jung et al., 2018; Li et al., 2018). It is based on the identification of absorption bands at specific wavenumbers, that are attributed to specific functional groups. These bands can change in intensity, or even change their position, when polymers are degraded, allowing for the quantification of polymer degradation (Jung et al., 2018; Rajandas et al., 2012).

3.2.1. CPE/CPE+B

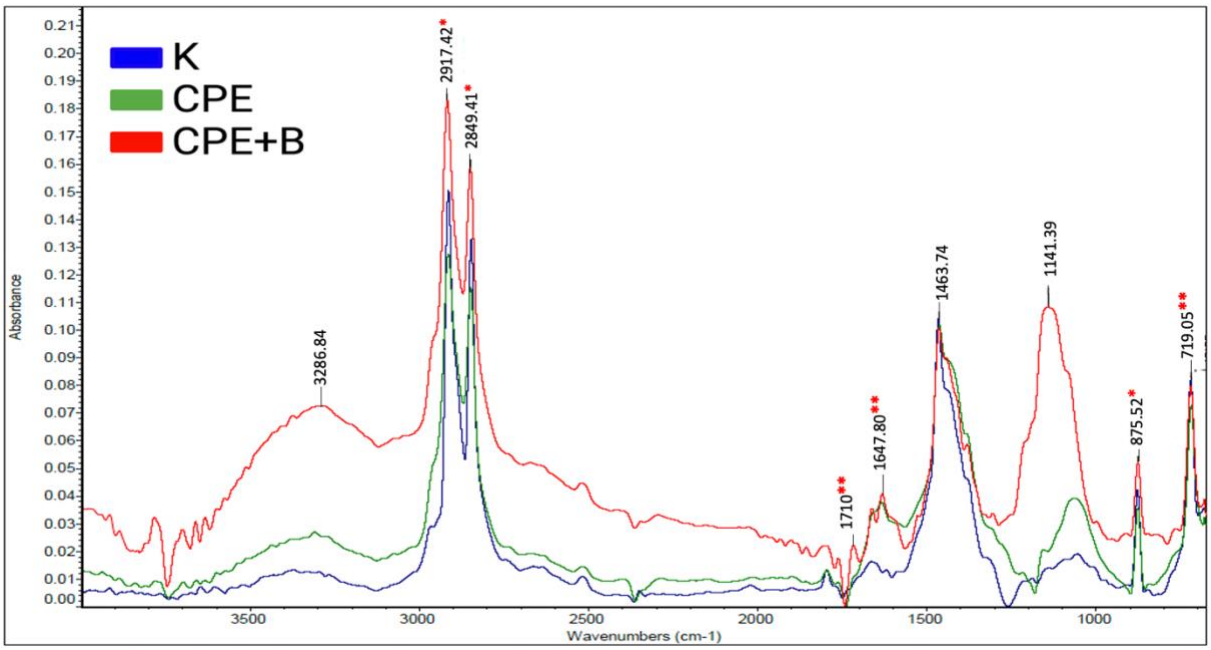

Figure 3.2. Spectra of CPE, CPE+B and control MP particles, as determined by FTIR-ATR after a composting period of 30 days. * $p < 0.05$. and ** $p < 0.01$. It was not possible to perform an "auto baseline" to keep the three spectra at the same level (and therefore it seems that, in general, peaks show a higher absorbance, but this does not always reflect reality, as determined by statistical analysis.

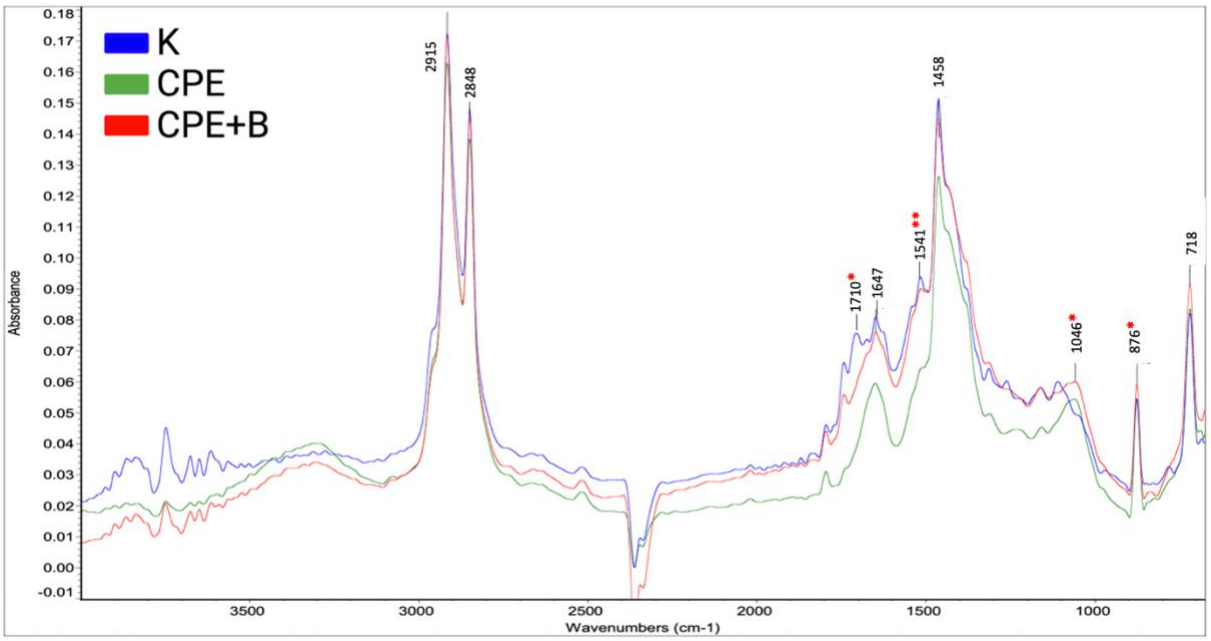

Figure 3.3. Spectra of CPE, CPE+B and control MP particles, as determined by FTIR-ATR after a composting period of 60 days. * $p < 0.05$. and ** $p < 0.01$. It was not possible to perform an "auto baseline" to keep the three spectra at the same level (and therefore it seems that, in general, peaks show a higher absorbance, but this does not always reflect reality, as determined by statistical analysis. The peak at about ~2300 $\boldsymbol{cm^{-1}}$ represents CO_2 that has collected in the analytical space; consequently, the statistical analyst has not taken it into account.

Figures 3.2 and 3.3 display the FTIR-ATR spectra of CPE and CPE+B MP after 30 and 60 days of composting process. As indicated in Table 3.2. below, nine significant absorption peaks were found and used to characterize CPE/CPE+B. These bands resemble those that have commonly been used in previous studies to characterize changes in the functional groups of the surface of PE MPs (Fernández de Villalobos et al., 2022)

Table 3.2. Statistical differences (Wilcoxon test) at the 95 % of confidence level on peak absorbance intensity for CPE MP subjected to a compost process for 30 days and 60 days. n.s.: non-significant ($p > 0.05$). * $p < 0.05$. and ** $p < 0.01$. Wilcoxon test compared the peaks in 30 days (T1) (T2), the increase or decrease of peaks between time (T1 vs T2) and between treatments (K vs CPE vs CPE+B)

Peaks	T1	T2	TIME	By treatment
2915-18	CPE+B > CPE *	n.s	T2>T1**	n.s
2848-51	CPE+B > CPE*	n.s	T2>T1**	n.s
1710-16	CPE+B > CPE**	CPE+B > CPE* K>CPE*	T2>T1*	CPE+B > CPE**
1641-53	CPE+B > CPE**	n.s	T2>T1**	n.s
1541-49	CPE+B > CPE**	CPE+B > CPE** K>CPE**	n.s	CPE+B > CPE** K>CPE*
1458-71	n.s	n.s	T2>T1**	n.s
1046-70	CPE+B >K* CPE+B > CPE*	CPE>K*	n.s	CPE>K*
870-76	CPE+B > CPE*	CPE> CPE+B*	T2>T1*	n.s
717-23	CPE+B >K*	n.s	T2>T1*	n.s

The peaks at ~2915 cm^{-1} and ~2848 cm^{-1} that belong to CH_2 asymmetric C-H stretching Table 2.2 showed higher absorbance from CPE+B compared to CPE after 30 days, but not after 60 days. After 60 days, the absorbance of the same peaks (2915-18 cm^{-1} and 2848-51cm^{-1}) increased in comparison to 30 days. Contrarily, in the study of Fernández de Villalobos et al., (2022) for the case of LDPE, there was a significant decrease in the characteristic methylene groups at ~2916 cm^{-1} and ~2851 cm^{-1} in the samples inoculated with marine bacteria. The peak ~2848 cm^{-1} is typical (native) bonds of C–H2 asymmetrical stretch and as a consequence of these changes, there is an increase in what is called the "vinyl: methylene index" over time (Fernández de Villalobos et al., 2022), which has been reported as indicative of biotic degradation (Fotopoulou & Karapanagioti, 2015).

The peak at ~1710-16 cm^{-1} corresponding to a ketone group (Coates, 2006; Fotopoulou & Karapanagioti, 2015; Jung et al., 2018; Mecozzi & Nisini, 2019) showed after 30 days of composting higher absorbance the CPE+B treatment compared to the CPE treatment; in 60 days, the difference was maintained (CPE+B was higher absorbance than CPE); and the control was also higher than CPE. The peak was greater after 60 days compared to 30 days, and a

comparison of treatments revealed that the CPE+B peak was greater than the CPE peak. This peak was attributed to C=O stretch by Jung et al., (2018) but for PET. This peak was not found in Fernández de Villalobos et al., (2022) investigation.

After 30 days, the peak at position ~1641 cm^{-1} that belongs to C=C bond of the vinyl group/C=O bond of the carbonyl group (Table 2.2) displayed a higher absorbance in CPE+B compared to CPE. Also, the peak showed higher absorbance after 60 days compared with 30 days. The increase in the absorbance of this peak can be linked to the production of carboxyl groups and, subsequently, polymer biodegradation (Fernández de Villalobos et al., 2022). The study of Fernández de Villalobos et al., (2022) also, reported higher absorbance of this peak when the MP was exposed to bacterial communities.

Peaks at ~1541 cm^{-1}, had higher absorbance from CPE+B compared with CPE treatment after 30 days and 60 days. The control (K) also showed higher absorbance than the CPE treatment, experiencing the greatest change in absorbance intensity. These differences were observed again between treatments (Table 2.2). This peak has not been reported before; therefore, it is essential to do more studies concerning the functional groups and the chemical changes associated when the MPs are exposed to bacteria.

The peak at 1458 cm^{-1} can be due to bending formation or CH_2 deformation split when PE is crystalline (Table 2.2) and did not show any statistical differences among treatments, but comparing experimental times, the peak showed a higher absorbance after 60 days, compared to 30 days. This peak could reflect the intrinsic constituents of Bacillus Cereus (Auta et al., 2017). Contrarily, the study by Auta et al. (2017) where bacterial isolates were screened for their potential to degrade UV-treated MPs from PE, PET, PP and PS, reported a decrease in the absorbance of this peak when MPs were exposed to bacterial isolates.

After 30 days, the peak at position ~1046 cm^{-1}, that belongs to C-O bond (Fotopoulou & Karapanagioti, 2015), was significantly higher in CPE+B than in CPE and control samples. This changed after 60 days, when that peak showed a higher absorbance in CPE than in the negative control. Fotopoulou & Karapanagioti (2015) reported that this ester linkage peak appeared on deteriorated plastics.

The peak at ~870 cm^{-1}, attributed to a trans-bending oxy-methylene group (Mecozzi & Nisini, 2019; Table 2.2 and 2.3) for CPE+B was higher in absorbance than in CPE after 30 days of treatment. Also, a higher absorbance after 60 days in comparison to 30 days was observed (Table 6). In the study conducted by Fernández de Villalobos et al. (2022), a higher absorbance of this peak was reported in samples inoculated with marine bacteria, and was attributed to a higher biodeterioration of the inoculated MP. The peak at ~717 cm^{-1} belongs to rocking

deformation; CH_2 deformation slipt when PE is crystalline (Table 2.2) showed a higher absorbance in CPE+B, compared to the control, after 30 days of composting, but no difference was observed after 60 days. When the time of treatment is compared, the peak after 60 days showed higher absorbance than after 30 days. These results agree with those of Auta et al., (2017) where this peak also increased after 40 days of incubation of PE films exposed to Bacillus cereus. (Coates, 2006; Jung et al., 2018)

3.2.2. PET/PET+B

Figures 3.4 and 3.5 display the FTIR-ATR spectra of PET and PET+B MP after 30 and 60 days of composting. As indicated in Table 7 below, fourteen peaks that represent functional groups were found and used to characterize PET/PET+B. These bands resemble those that have commonly been used to characterize the degradation or altering of the functional groups in the PET/PET+B chain, as shown in Table 2.3..

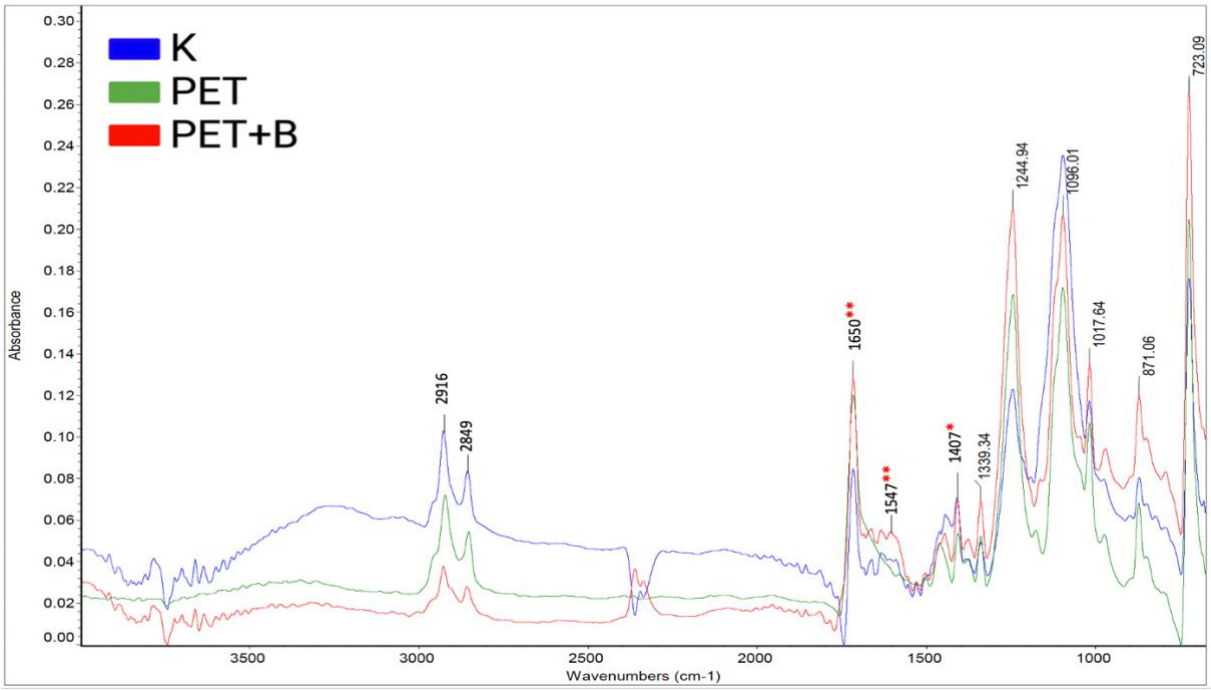

Figure 3.4. Spectra of PET, PET+B and control MP particles, as determined by FTIR-ATR after a composting period of 30 days. * $p < 0.05$. and ** $p < 0.01$. It was not possible to perform an "auto baseline" to keep the three spectra at the same level (and therefore it seems that, in general, peaks show a higher absorbance, but this does not always reflect reality, as determined by statistical analysis. The peak about ~2300 $\boldsymbol{cm^{-1}}$ represents CO_2 that has collected in the analytical space; consequently, the statistical analyst has not taken it into account.

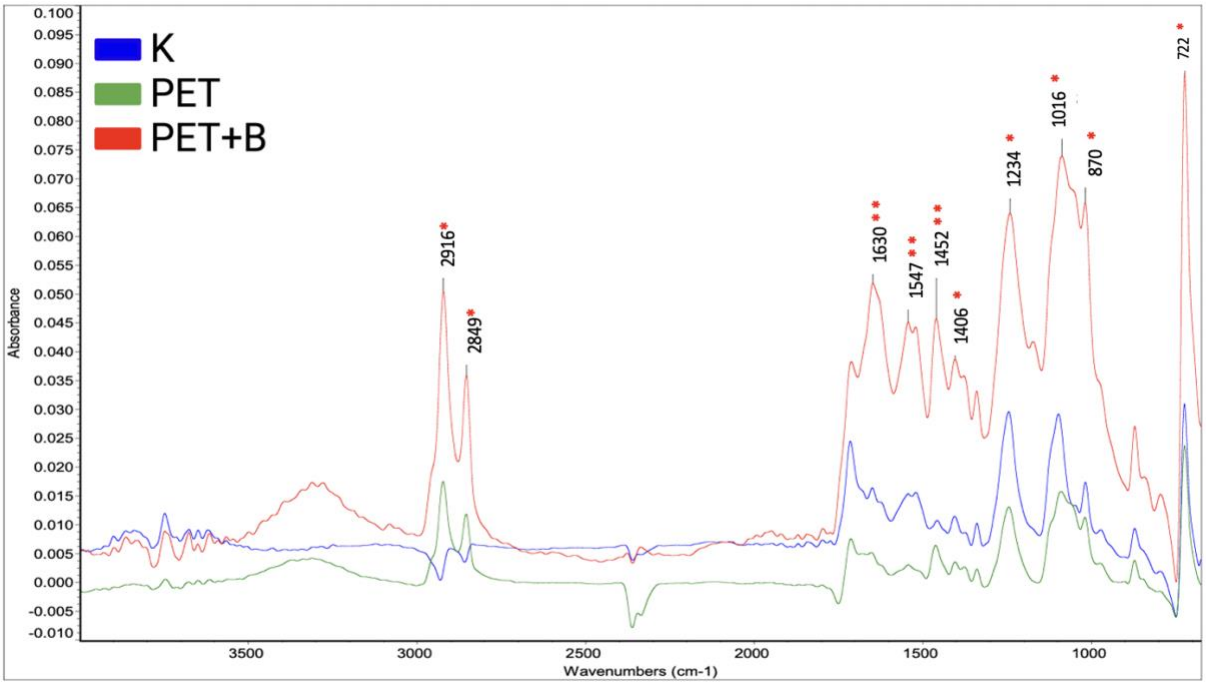

Figure 3.5. Spectra of PET, PET+B and control MP particles, as determined by FTIR-ATR after a composting period of 60 days. * $p < 0.05$. and ** $p < 0.01$. It was not possible to perform an "auto baseline" to keep the three spectra at the same level (and therefore it seems that, in general, peaks show a higher absorbance, but this does not always reflect reality, as determined by statistical analysis. The peak about ~2300 $\boldsymbol{cm^{-1}}$ represents CO_2 that has collected in the analytical space; consequently, the statistical analyst has not taken it into account.

Table 3.3. Statistical differences (Wilcoxon test) at the 95 % of confidence level on peak absorbance intensity for PET MP subjected to a compost process for 30 days and 60 days. n.s.: non-significant ($p>0.05$) *$p<0.05$ **$p<0.01$. Wilcoxon test compared the peaks in 30 days (T1), 60 days (T2), the increase or decrease of peaks between time (T1 vs T2) and between treatments (K vs PET vs PET+B)

Peaks	T1	T2	Time	Treatments
2916-27	n.s	PET+B>K*	n.s	n.s
2849-56	n.s	PET+B>K*	n.s	n.s
1709-17	n.s	PET+B>K* PET>K*	n.s	K>PET*
1630-52	PET+B>PET** K>PET**	PET+B>PET** K>PET*	n.s	PET+B>PET** K>PET*
1547-58	PET+B>PET** K>PET*	K>PET+B* K>PET**	n.s	PET+B>PET* K>PET**
1530-42	PET+B>PET** K>PET*	PET+B>PET** K>PET*	T2>T1*	PET+B>PET** K>PET*
1452-67	n.s	PET+B>PET**	T2>T1*	n.s
1406-09	PET+B>PET*	K>PET*	n.s	K>PET*

1335-42	n.s.	PET+B>PET** K>PET*	n.s	n.s
1234-48	n.s.	K>PET+B* K>PET*	n.s	n.s
1082-98	n.s.	K>PET+B* K>PET*	n.s	K>PET+B* K>PET*
1016-20	n.s.	K>PET*	n.s	n.s
870-874	n.s.	K>PET*	n.s	n.s
717-730	n.s.	K>PET+B*	n.s	n.s

Peaks at ~2916 cm^{-1} belong to CH2 asymmetric stretch; ~2849 cm^{-1} belong to CH2 asymmetric stretch, ~1709 cm^{-1} belong to C=O stretch (ketones), and ~1234 cm^{-1} belong to asymmetric Stretch C-C-O group bonded to aromatic ring, C=O in-plane bending (Table 2.3.), did not show statistical changes among treatments over the first 30 days, but did after 60 days. For these peaks at positions ~2916 cm^{-1}, ~2849 cm^{-1} and ~1709 cm^{-1}, the absorbance was greater in the PET+B treatment than in the control. Additionally, the peak at ~1709 cm^{-1} showed a greater absorbance intensity in the PET than in the control samples. The increase or decrease in the absorbance of certain peaks that reflected functional groups has been linked to microbial activity and its degradation. Similar results were observed in the work of Torena et al., (2021), in which bacterial communities (*Bacillus cereus* and *Agromyces mediolanus*) from activated sludge were screened for the ability to degrade PET, demonstrating an increase in the intensity of peaks at positions ~1712 cm^{-1} when the MPs were exposed to *Bacillus cereus* and *Agromyces mediolanus.*

The most remarkable alteration of peak absorbance, according to the statistics, was in the footprint region, from ~1630 cm^{-1} belonging to C=C bond of the vinyl group/C=O bond of the carbonyl group (Table 2.3.), to ~1530 cm^{-1}, where the PET+B treatment and control showed a higher absorbance than in the PET samples. The peak ~1630 cm^{-1} which has been either attributed to a vinyl bond or a carbonyl group (Table 2.3.) could be interpreted as the oxidation of the polymer and substitution of a C—C bond by a C—O bond (Brandon et al., 2016; Denaro et al., 2020; Fernández de Villalobos et al., 2022). The peaks at ~1016 cm^{-1} belonging to aromatic ring in-plane C–H bend and ~717 cm^{-1} belonging to the deformation of the aromatic ring (Table 2.3.) just showed the control has higher absorbance compared with PET for the peak ~1016 and ~870 and at 717 cm^{-1} the control also was higher in the PET+B.

The peak around ~1406 cm^{-1}, belonging to in-plane vibrations of the benzene ring (Denaro et al., 2020) after 30 days showed a higher absorbance in the PET+B treatment, as compared with PET treatment without inoculum. Also, after 60 days, the absorbance was higher for the control compared to PET treatment. In the study of Fernández de Villalobos et al.,(2022), where a biodegradability experiment was conducted with low-density polyethylene and biobased PET microplastic films by a consortium of marine bacteria during 45 days showed similarities with this study (after 30 days), since the treatment with PET MP inoculated with marine bacteria showed a higher absorbance of this peak, as compared to MP samples without bacteria. Contrarily, in the study of Auta et al. (2017) this peak was absent in PET MP samples inoculated with Bacillus cereus.

The peak at ~1335 cm^{-1} belonging to trans wagging band -CH_2, Crystalline phase (Table 2.3.) just showed differences among treatments after 60 days, where a higher absorbance was observed in PET+B and the negative control, as compared to the PET treatment. An increase of absorbance in this peak related to the crystalline polymer (Denaro et al., 2020) after a biological treatment is a sign that the plastic has broken down. This is because microbial hydrolytic activity in the amorphous parts of PET causes the polymer chains at the surface to re-crystallize, which is a sign of biodegradation (Torena et al., 2021). This peak had also been reported by Ngonyani (2022), who made an experiment to assess the potential of a marine bacteria community and two of its isolates to biodegrade PET plastic bottles and bio-based PET plastic bags for 90 and 45 days.

The peak at ~1234 cm^{-1} representing a stretching of the ester (O=C–O–) bond and also describing the crystalline and amorphous properties of PET (Mecozzi & Nisini, 2019) displayed a higher absorbance in the control compared to PET+B and PET samples just after 60 days. Contrarily, results observed in the work of Torena et al., (2021) mentioned previously, showed an increase in the absorbance of these peaks when exposed to the bacterial community. The high absorbance of this peak related to the crystallinity can be a sign of biodegradation (Torena et al., 2021).

Concerning the peak around ~1016 cm^{-1} , belonging to aromatic ring in-plane C–H bend (Table 2.3), there was no significant difference between the treatments after 30 days, but after 60 days the control showed a higher absorbance of this peak, compared to PET treatment. In the study of Fernández de Villalobos et al. (2022) a higher absorbance of this peak in the controls was also found, as compared to the samples inoculated with the bacterial community. A significant decrease in the peak at ~1020 cm^{-1} for PET treatment could be related to

degradation, since this peak is related to crystalline regions of the polymer, therefore a decrease in crystalline or increase in amorphous regions can trigger biodegradability (Mecozzi & Nisini, 2019).

It would be useful to compare different bacteria and polymers under composting conditions to see which one works better in soil environment, or set-up the optimum conditions to carry successfully the biodegradation. In Table 3.4. it is shown the target plastic and the organisms that have been tested to the biodegradation experiment.

Table 3.4. Biodegradation of target polymers by previous studies

Polymer	Degrading microorganism	References
PE	*Agromyces mediolanus*	(Torena et al., 2021)
	Aneurinibacillus sp	(Skariyachan et al., 2018)
	Bacillus cereus	(Auta et al., 2017) (Torena et al., 2021)
	Bacillus gottheilii	(Auta et al., 2017)
	Bacillus licheniformis	(Yao et al., 2022)
	Bacillus subtilis	(Vimala & Mathew, 2016) (Yao et al., 2022)
	Brevibacillus	(Gumbi et al., 2019)
	Brevibacillus borstelensis	(Hadad et al., 2005)
	Brevibacillus sps.	(Skariyachan et al., 2018)
	Penicillium simplicissimum	(Yamada-Onodera et al., 2001)
	Pseudomonas aeruginosa	(Gumbi et al., 2019) (Mouafo Tamnou et al., 2021)
	Rhodococcus ruber	(Sivan et al., 2006)
PET	*Agromyces mediolanus*	(Torena et al., 2021)
	Bacillus cereus	(Torena et al., 2021)
	Bacillus sp.	(Ngonyani, 2022)
	Cobetia, Marinobacter, Pseudoaltermonoas, Ruegeria	(Fernández de Villalobos et al., 2022)
	Halodesulfovibrio, Pseudoaltermonoas, Pseudomonas and Tepidibacter.	Fernández de Villalobos, Costa and Marín-Beltrán (2022); Marín-Beltrán et al. (unpublished)
	Ideonella sakaiensis;	Yoshida et al. 2016;

3.3. DNA concentration and quality for bacterial community identification

Currently, bacterial communities from initial time extracted from SS, bacterial communities after 30 days and after 60 days are still to be identified. The concentration of DNA extracted from the bacterial community in the initial time range vary from 56.91 ng/µL to 63.12 ng/µL. After 30 and 60 days, the concentration of DNA extracted from the bacterial community in samples range from 3.09 ng/µL to 48.04 ng/µL and 5.36 ng/µL to 14.74 ng/µL, respectively (Table 3.5.)

This results contrast with Fernández de Villalobos et al., (2022) and Ngonyani, (2022) where the concentration of extracted DNA was 1,69 to 5,85 ng/µL and 0.1 to 1.5 ng/µL respectively. These results can have a considerable difference because they were analyzing the bacterial community adhered to MP and the current experiment extracted the DNA from SS where the bacterial communities are expected to be in higher number and diversity.

The ratio of absorbance at 260 nm and 280 nm is used to assess the purity of DNA and RNA. The ratio of absorbance A260/A280 at the initial time, ranged from 1.23 to 1.93; at 30 days from 1.40 to 2.47; and at 60 days from 1.22 to 1.63. (Table 3.5.). A ratio of ~1.8 is generally accepted as “pure” for DNA; a ratio of ~2.0 is generally accepted as “pure” for RNA. The data indicated good-quality DNA.

The A260/A230 ratio is used as a secondary measure of nucleic acid purity. A260/A230 at the initial time ranged from 0.10 to 1.65; at 30 days from 0.08 to 1.62; and at 60 days 0.13 to 0.38. Good ratio values are in the range of 2.0-2.2. The values of the A260/A230 ratio were slightly lower. These results may be related to the presence of reagents which absorb at 230 nm.

Table 3.5. Concentration of DNA of the bacterial community present in the initial time, after 30 and 60 days in the experiment, as determined by Nanodrop spectrophotometry. K stands for controls and R corresponds to each replicate.

Time	Sample Name	Nucleic Acid (ng/uL)	A260/A280	A260/A230
Initial time	T0-R1	63.12	1.895	1.648
	T0-R2	56.914	1.928	0.14
	T0-R3	-2.086	1.225	0.402
30 Days	K-R1	5.479	1.425	0.344
	K-R2	4.182	1.527	0.167
	K-R3	5.814	1.759	0.128
	PET-R1	48.043	1.883	1.62
	PET-R2	4.289	1.913	0.343
	PET-R3	3.77	2.466	0.137
	CPE-R1	23.686	1.753	1.251
	CPE -R2	4.313	1.823	0.135
	CPE -R3	4.65	1.657	0.317
	PET+B -R1	10.743	1.401	0.302
	PET+B -R2	4.207	2.09	0.084
	PET+B -R3	3.091	1.765	0.14
	CPE+B -R1	25.59	1.773	0.93
	CPE+B -R2	3.779	1.855	0.1
	CPE+B -R3	5.147	1.627	0.083
60 Days	K -R1	13.853	1.356	0.154
	K -R2	14.737	1.321	0.155
	K -R3	13.289	1.22	0.205
	PET -R1	7.738	1.4	0.376
	PET -R2	9.153	1.413	0.242
	PET -R3	9.908	1.378	0.155
	CPE -R1	7.9	1.401	0.306
	CPE -R2	6.893	1.5	0.157
	CPE C -R3	8.241	1.627	0.175
	PET+B -R1	6.354	1.296	0.203
	PET+B -R2	5.801	1.414	0.175
	PET+B -R3	8.11	1.561	0.135
	CPE+B -R1	5.36	1.444	0.133
	CPE+B -R2	7.619	1.358	0.365
	CPE+B -R3	7.099	1.564	0.253

3.4. Change in plastic's surface properties.

The micrographs shown in Figure 3.6 and Figure 3.7 illustrate the general trend of the morphological changes observed in the surface of MP particles after 60 days of composting. Since these results are not quantitative, the most representative picture for each treatment (negative control, MP and MP+B) has been selected, in terms of the presence of fractures, cavities and holes observed, as well as the presence of bacteria. In addition, in order to standardize all comparisons, 10 μm was used as the scale for all treatments.

3.4.1. PET/PET+B

Scanning electron microscopy (SEM) is a tool that allows us to provide a great depth and higher resolution details of surface textures for MPs in this case (Shi et al., 2022). The SEM technology was used to compare the MPs surfaces of PET, PET+B and negative control (K) after 60 days. The MPs in the negative control were exposed to the same time and temperature but without SS or bioaugmented bacteria. High-resolution images are provided in Figure 3.6

After 60 days, adherence of bacterial biofilms was seen on the surface of PET and BPET+B, however neither treatment exhibited any holes, fractures, or cavities. Biofilm has been described as a necessary stage for the colonization of microplastics by microorganisms, and without them, plastic cannot be effectively degraded (Sivan et al., 2006). As expected, the surface of PET films (K) not exposed to bacteria was free of biofilm attachments and had a smooth appearance (Figure 3.6). However, there was no visible distinction between MP particles subjected to the initial bacterial community (PET) and those treated with bioaugmented bacteria (PET+B).

In the study by Fernández de Villalobos et al., (2022), PET MP demonstrated the formation of holes and dispersed bacteria after 45 days of incubation with a marine bacterial community. Denaro et al., (2020) also observed by SEM analysis irregular surfaces and the presence of small cracks and crinkles in PET films exposed to a community of hydrocarbon-degrading bacteria for 45 days. However, the medium in which the experiments of Fernández de Villalobos et al., (2022) and Denaro et al., (2020) were conducted (aqueous environment) and the present study in solid medium, can affect differently the results obtained. In previous studies, the *Bacillus* genera has shown capacity to degrade PET and PE, LDPE and PS (Auta et al., 2017; Tareen et al., 2022; Torena et al., 2021) but always in an aqueous medium. As far as

we know, this is the first experiment to apply bioaugmented bacteria from the genera *Bacillus* to a composting technique from SS. Most of the research examines the potential of isolated bacteria in aqueous medium but does not apply in conditions closer to reality, namely with microbial consortia that carry out this function through symbiotic relationships and real applications like composting in this case.

The images showed that microorganisms adhered on the plastic surfaces by forming biofilm communities are more abundant in the PET+B. The spatial distribution of microorganisms on the MP surfaces was not homogeneous, though, since some parts of the surface were clear or smooth. Biofilms developed on the surface of PET treatment look more dehydrated than PET+B since the biofilm presented scratches (Figure 3.6).

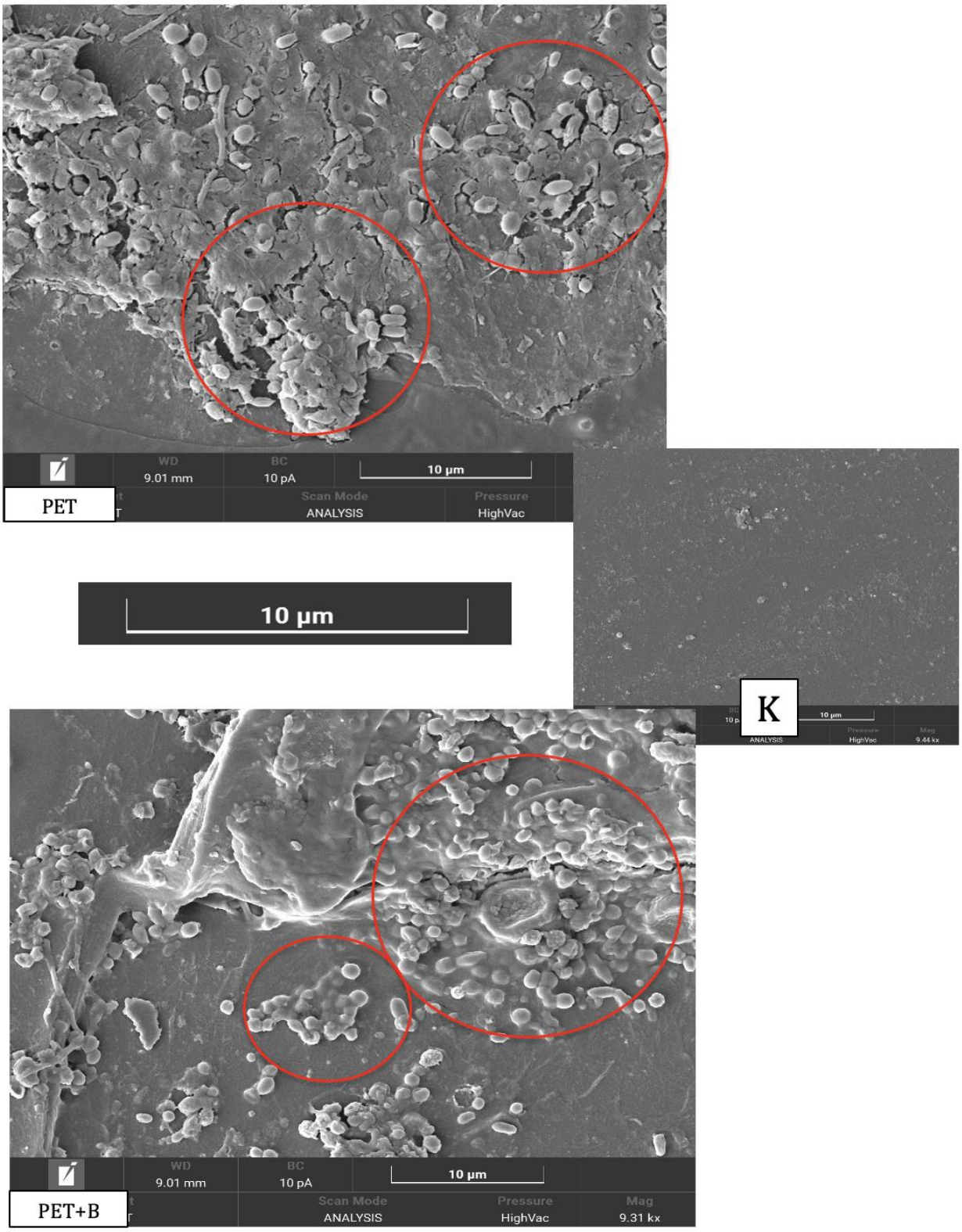

Figure 3.6. SEM micrographs of morphological surface of PET MPs after 60 days of composting compared with treatment without bioaugmentation (labelled as PET), treatment with bioaugmentation (labelled as PET+B) and the control (labelled as K). The red circles indicate the most evident changes of MPs including the *Bacillus* attached in the surface.

3.4.2. CPE/CPE+B

The SEM technology was used to compare the surface of CPE, the CPE+B MP and negative control (K) after 60 days. The negative control MP was exposed to the same time and temperature but without sewage or bioaugmented bacteria. High-resolution images are provided in Figure 3.7.

After 60 days, adhesion of bacterial biofilms was observed on the surface of CPE and CPE+B. There was a visual difference between MPs particles exposed to the bacterial community from the sludge (CPE) and those treated with bioaugmented bacteria (CPE+B). The negative control surface was free of any biofilm attachments and with a smooth surface (K). The treatment with bioaugmented bacteria (CPE+B) presented a huge hole or cavity. This cavity can be related to the activity of enzymes produced by bacteria that use the polymer as a carbon source (Ojha et al., 2017). Also, CPE treatment, showed a cavity but it is small compared to CPE+B. The presence of a biofilm was observed in both treatments but CPE+B presented more rugosity in the surface of MP. The morphological change on the surface of CPE+B treatment has been more affected than CPE, this can be related to the bioaugmentation and the potential of the bacteria to degrade polymers.

It must be mentioned that CPE MP films were obtained from a compostable bag. Considering this, it was not expected to just observe a few holes or cavities, but a clear deterioration (or even complete degradation) of the surface of the particles. Therefore, some questions arise from the production and use of compostable/biodegradable plastic products. When a product is labeled as such, it should be specified under which specific conditions (e.g. in terms of time and temperature) are these products compostable or biodegradable.

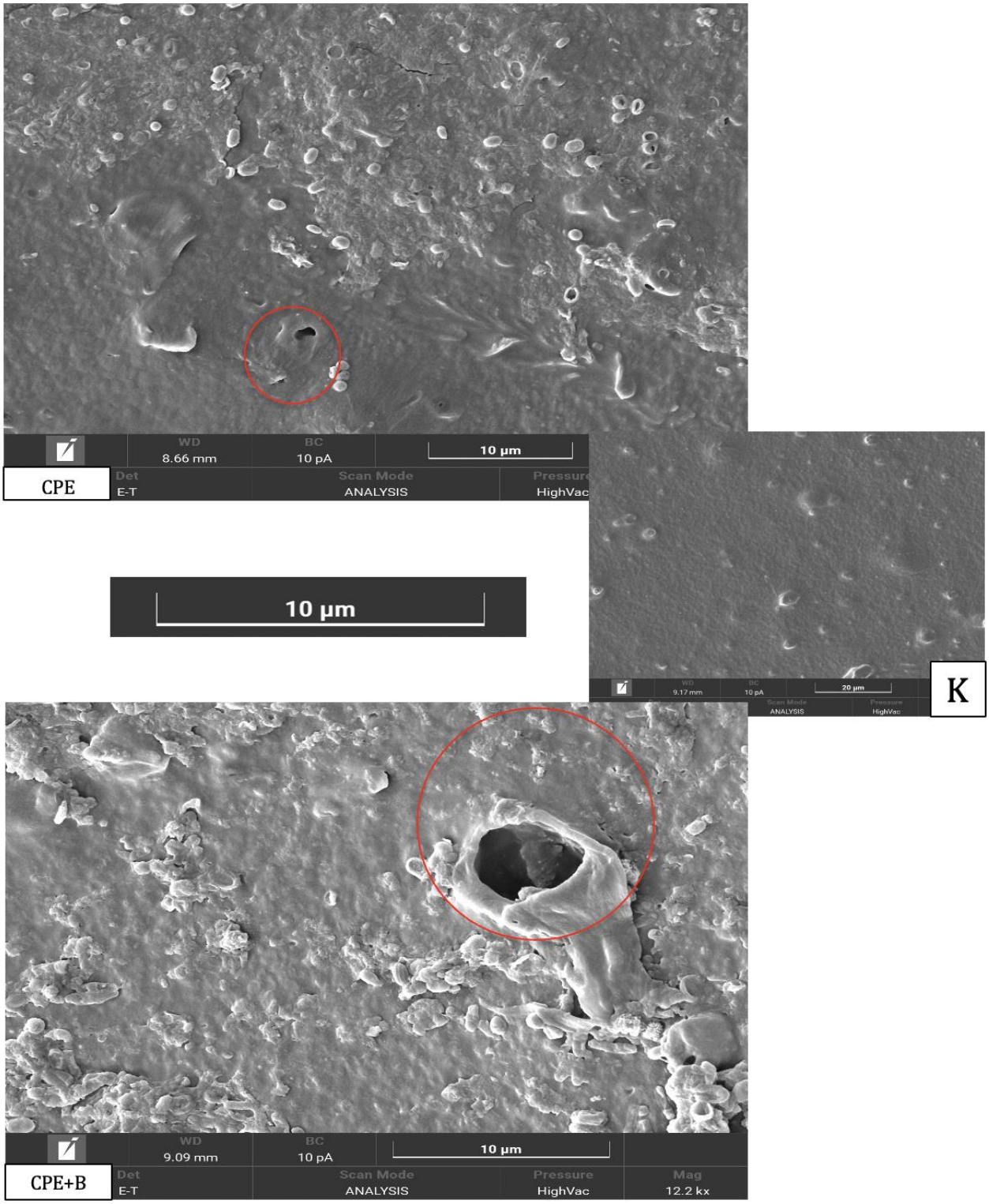

Figure 3.7. SEM micrographs of morphological surface of CPE MPs after 60 days of composting compared with treatment without bioaugmentation (labelled as CEP), treatment with bioaugmentation (labelled as CPE+B) and the control (labelled as K). The red circles indicate the most evident change of MP in the surface.

3.5. MP in sewage sludge in the initial time and after composting (60 days)

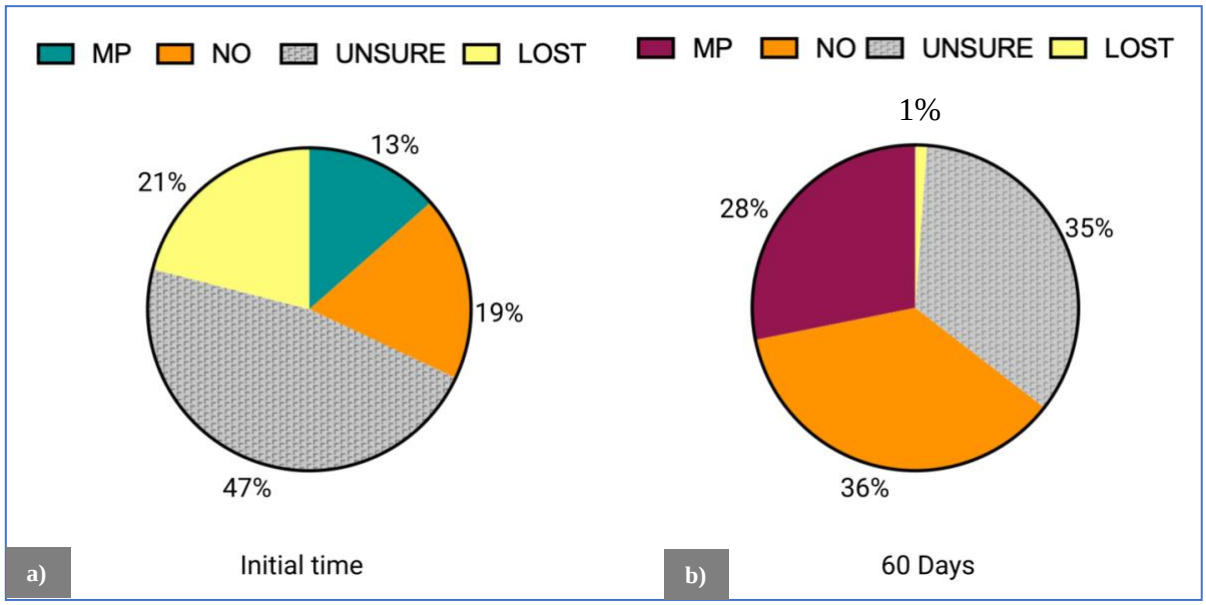

Figure 3.8. Pie-charts of MPs found in the compost at the beginning of the experiment (a), and after 60 days (b). Different colors mean: in green, suspected MP chemically confirmed as such (>40 % match with FTIR library); in orange, suspected MP that were confirmed as not plastics (>40 % match) in the FTIR; in grey, particles that could not be classified as either plastics or not plastics (<40 % match with FTIR library); and in yellow, particles that were lost before the chemical analysis in the FTIR was confirmed.

From all the suspected MPs examined under the microscope from the dehydrated sludge collected at the WWTP, only 13% were verified as such by FTIR (match > 40%). Of the remaining suspected MPs, 19% were not plastics (match > 40%), 47% showed a match < 40% in the FTIR, and were classified as "unsure", and 21% were lost (Figure 3.8 a). For the suspected MPs found in the samples after 60 days of composting, 28% were classified as plastics, 36% not plastics, 35% unsure and 1% of the particles were lost (Figure 3.8 b). The concentration of MPs found in the samples after 60 days of composting was 27 MPs g^{-1}, much higher than the concentration of 4 MP by g^{-1} found in the dehydrated sludge (before starting the compost experiment). The results reflect an increase on MPs after 60 days. The possible reason is because many particles get lost in the initial time. The filters from the initial time (T0) were still covered with remaining of organic matter. This prevented the adequate identification of the particles, getting matches of the spectrum of the particles with the FTIR library below 40%. In addition, measuring fibers covered with organic matter can make them invisible to the FTIR apparatus, therefore, resulted in many particles losses. On the other hand, the initial time had the sample exposed to H_2O_2 for a longer time. According to Maw et al. (2022), who evaluated

5 methods to treat samples with high OM, such as SS (two with H_2O_2 and three Fenton's reaction), the exposure of the MPs to this chemical at a high temperature (50 °C), may breakdown MPs in 24 h. Other studies apply the Fenton's reagent, that uses $FeSO_4.7H_2O$ to catalyse the reaction, to accelerate organic matter degradation (Lavoy & Crossman, 2021).

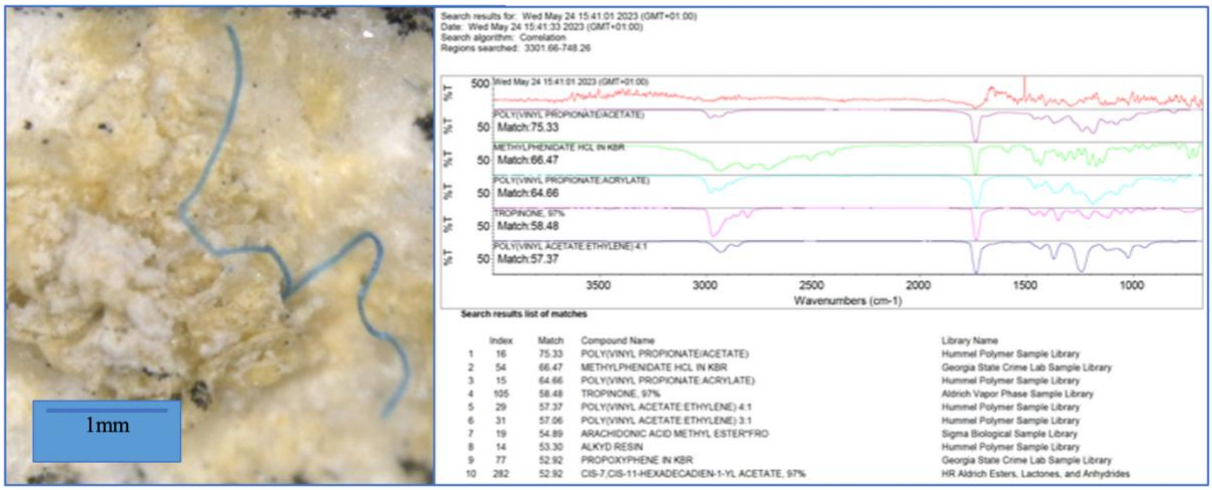

Figure 3.9. Example of a particle verified as plastic through FTIR, showing a good match (75%) with polyvinyl propionate/ polyvinyl acetate. The fiber was found after 60 days of composting.

The results obtained from the current experiment (27 MP by g^{-1}) after 60 days agreed within the range provided by Corradini et al. (2019) which had been investigated the contamination of soils by MPs exposed to consecutive sludge applications and found between 18 and 41 particles g^{-1}, with a median of 34 particles g^{-1} in SS. Furthermore, the findings of Chen et al. (2020), who reported a decline of 4.5% in MPs content after an experiment of/a composting process of 56 days at 70°C of temperature contrasted with the present experiment where the final time showed an increase of 27% in the final concentration. In England, another research has identified MPs through the entire sludge treatment stream with concentrations ranging from 37.7 to 97.2 particles/g of treated sewage sludge (dw) (Harley-Nyang et al., 2022). A study conducted in Ireland characterized MPs in sludge samples from 7 WWTPs and found that abundances ranged from 4.2 to 15.4 particles g^{-1} (dw) (Mahon et al., 2017).

The most prevalent size group for initial time is from 1000 to 2000 µm, accounting for 26% of the particles, and followed by the groups 400-600 µm (23%) and 200-400 µm (15%). After 60 days of composting, most prevalent particles were within the size range 200-400, with 29% followed by 400-600 19%, 1000-2000 18% (Figure 3.10). The results according to their size suggest the composting influenced fragmentation because they increase in number and decrease in size, which means they got fragmented after 60 days. However, since the number of lost particles during the initial time was around 21% and at 60 days just 1% got lost, it is not possible

to assure that the composting enhanced the fragmentation of MPs. Also, at 60 days there were other types of polymers which did not exist at the initial time, therefore, the type of polymer between the initial time and after 60 days does not correlate (Figure 3.11).

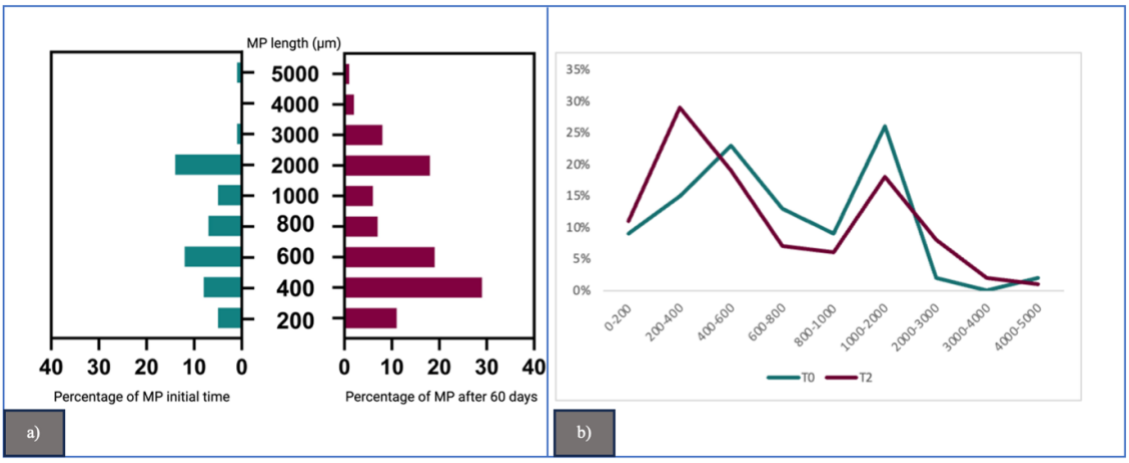

Figure 3.10. Suspected MPs during initial time and after 60 days classified by size. MPs found in initial time (green) vs after 60 days (red). a) the x label is percentage of MP particles within a given range size (µm), the y label is the range. b) the x label is the range and y label is percentage of MP particles.

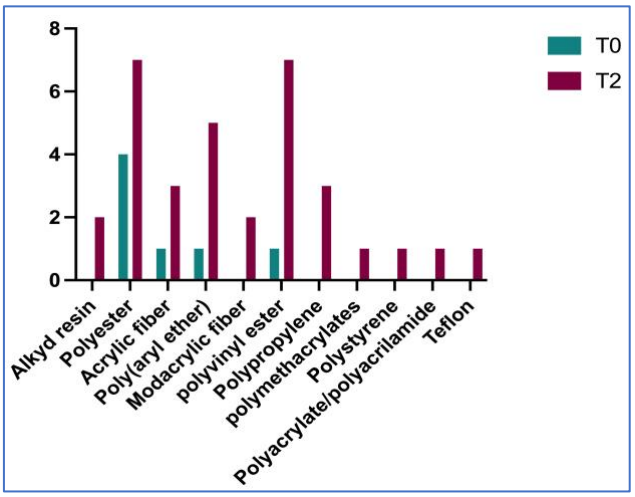

Figure 3.11. Suspected MPs during initial time and after 60 days classified by size. MPs found in initial time (green) vs after 60 days (red). a) the x label is type of polymer the y label is the amount of particles.

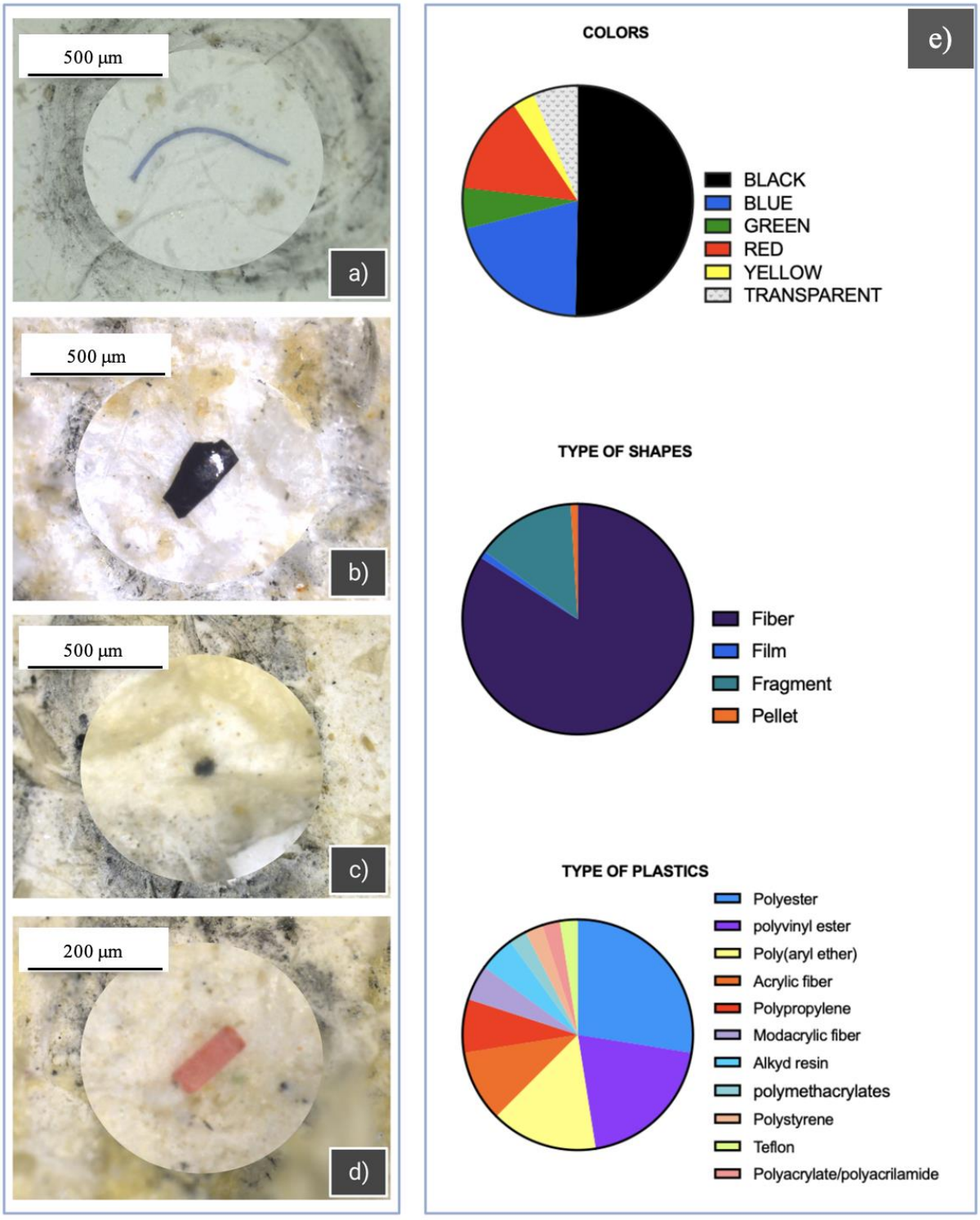

Figure 3.12. Classification of MP found by color, shape and type of polymer. Figures a-d show some examples of the MP particles found through the samples: a) blue fiber, b) black fragment, c) black pellet, d) red film. e) shows classification by color, type of shape and type of plastic

The most common shape present in MPs were fibers (84%), followed by fragments (14%). Films and pellets represent just 1% each (Figure 3.12e). These findings were expected, since fibers are difficult to remove in WWTP and tend to accumulate over time in the SS (Zubris & Richards, 2005). These results agreed with many investigations (Chen et al., 2020; Corradini et al., 2019; Lares et al., 2018; Li et al., 2018). Li et al., (2018) found 82% of fibers in 79 SS samples in China. Chen et al., (2020) that performed hyperthermophilic composting and conventional thermophilic composting − the technique that was applied in this experiment; found 78% of fibers, followed by fragments (7.0%), flakes (6.3%), among others. Furthermore, Corradini et al. (2019) which had investigated the microplastic contamination of soils exposed to consecutive sludge applications also found fibers as a predominant shape in 7 sludge samples (90%) took from soils in Chile.

Most of the MPs were black, representing 50% of the particles, blue represented 21%, red represented 14%, transparent represented 6%, green represented 6% and yellow represented just 3% ((Figure 3.12e). These results contrast with others studies like those shown by Chen et al. (2020), who found mostly white (65.1%), but also orange (26.9%), red (3.2%), black (3.0%), and green (1.3%) MP particles after 56 days in hyperthermophilic composting from SS. Li et al. (2018) also found, mainly white MPs (59.6%) in SS .

The predominant type of polymer determined by FTIR was polyester, representing 28% of the MP particles, followed by polyvinyl ester (20%,) poly(aryl ether) (15%), acrylic fiber (10%), polypropylene (7.5%), modacrylic fiber and alkyd resin (5%) each, polymethacrylates, polystyrene, polyacrylate/polyacrylamide and Teflon (3%) each ((Figure 3.12e). This is in contrast with results reported by Chen et al. (2020), where the most prevalent plastic was polypropylene (34%), followed by PE 33.8%. This type of polymers found in the Chen et al. (2020) study has not been found in this experiment. Lares et al., (2018) had similar results to Chen et al., (2020) since the most abundant polymer reported was PE, that accounted for ca. 64% of all the particles reported. In the study of Li et al. (2018), most of the MP found in SS belonged to polyolefin, acrylic fibers, PE and polyamide. These results are closer to those reported here. Polyester, acrylic fibers and polyamides (e.g., nylon) may have their origin on clothes, that release fibers when subjected to the washing machine (Browne et al., 2011).

3.6. Limitations of the study and future work

In this experiment, we tried to mimic a composting process to evaluate the potential biodegradation that MP particles may undergo before land application. For this, we used dehydrated SS (the final product from the WWTP, before land application), and dry leaves as a bulking agent, to improve the process. This process was selected among others that are applied to soil samples before land application as fertilizers because is cheap and possible to develop at a *lab scale*, However, some challenges were found during the experiment. The composting sample couldn't be exposed to air openly because it was settled in the stove at 50 degrees and slightly covered to avoid other microorganisms. During the experiment, it was decided to manipulate the samples as little as possible, to not contaminate the samples with other microorganisms not initially present in the SS (apart from the intentional addition of *Bacillus* in the bioaugmented treatment). However, we realized that mixing the samples during the experiment, to provide aeration, could have provided better results in terms of enhancing OM remineralization, and, eventually, MPs biodegradation.

Also, to avoid contamination, the temperature inside the flasks was not measured through the experiment. This prevented knowing when the activity of the bacterial population was at its highest point in order to have a better understanding of the compost process in the presence of MPs.

The humidity is a good factor for the organism to grow and biodegrade plastic. At 60 days the samples looked like they lost moisture. This could affect the biodegradation of MPs in the experiment since humidity helps bacteria to attach to MP particles (Lin et al., 2022). For future experiments, water or MSM could be added to the samples every two weeks, in order to maintain the moisture level between 50 to 60% according to the literature (Lin et al., 2022).
It was hard to retrieve spiked MPs from the compost samples (after 30 and 60 days), for FTIR and SEM analysis, because of the shape of the flasks used, and the huge amount of organic matter present in the samples. Biomass tends to cover the MPs, which makes it hard to find, extract, and analyze the MPs. In the future, it would be better to use MPs of bright color, and the flask should be wide to make it easier to get the particles out and mix the sample to get more oxygenation.

For MPs analysis, the supersaturated NaCl solution used to extract the MPs has some limitations to recover relatively dense polymers such as PET (1.32e1.41 g ml) or PVC (1.14e1.56 g ml) (Shim et al., 2016), since they are denser than the solution, and therefore tend to settle down (Li et al., 2018). Still, most of the polymers recovered were polyester fibers, that

have a density similar to PET. Therefore, overall, the methodology was successful on determining different types of plastics.

The high organic matter content in SS is a challenge in the analysis of MPs, since the breakdown of the organic matter may take a long time, depending on the reagent used, the time of exposition, and the temperature reached (Maw et al., 2022). It must be considered that temperatures > 60ºC can alter plastic properties, and thus samples were always kept below that temperature.

For OM digestion, a solution of H_2O_2 (30%) was used. Even though the Fenton reaction, has been proved quite effective and fast (~1 h according to Hurley et al., 2018) to remove most organic compounds from complex environmental substrates (e.g. Hurley et al., 2018; Masura et al., 2015; Tagg et al., 2017), we preferred to avoid its use for safety purposes, since the reaction is very exothermic, and can be "messy" if not handled properly, potentially resulting in the partial loss of sample.

Another drawback comes from the analysis of fibers themselves, which were the most frequent shape observed among the MP found in the sludge. Fibers tend to be quite thin, and the FTIR was not sensitive enough to detect the chemical composition of fibers from such thin objects, with a potential interference from the filters they laid on. It would be preferable, for future research, to identify the chemical composition of the fibers by enhancing the sensitivity of the FTIR apparatus, or using an alternate method such as Raman spectroscopy, that theoretically allows for the identification of particles down to 1 µm (our FTIR instrument theoretically also allows to identify particles as small as 6 µm, but our experience proves that a good identification is only possible for particles bigger than 100 µm).

4. Conclusions

The statistics showed some significant difference in the OM between the PET and PET+B treatments, where PET showed higher values. Also, for the same parameter, the control showed higher OM than CPE. For the C:N ratio, a significant decrease with time was observed. The results regarding the parameters like pH, OM% and C:N ratio were not drastically affected by 40 MP which represent 0.06% in CPE and 0.09% in PET in the sample. As suggested per the results shown, this amount of MPs had no appreciable effect on 25 g of composting. These findings open a gate to understand at what point the mass of MPs can affect the composting process. However, it does not mean that 40 MP cannot affect the process performance or microorganism. Additional tests and studies concerning the toxicological effects of MPs into mesocosm experiment are essential to understand what can be considered safe.

The CPE treatment had significant changes on the functional groups after composting. The footprint region between ~1710-16 cm^{-1} and ~1541-49cm^{-1}, as well as ~1046-10 $cm^{-1}$and ~870-76 cm^{-1} showed the greatest change. After 30 days, the peak ~1641-53 cm^{-1} displayed a difference between CPE+B and CPE. This peak rise can be linked to the production of carboxyl groups and polymer biodegradation.

For PET the most remarkable alteration of peak was in the footprint region from ~1630-52 cm^{-1}, to ~1530-42 cm^{-1} where PET+B treatment showed a higher absorbance than PET. The peak ~1630-52 cm^{-1} could be interpreted as the oxidation of the polymer. Peaks at ~2916-2 cm^{-1}, ~2849-56 cm^{-1}, ~1709-17 cm^{-1}, and ~1234-48 cm^{-1}, which are typical PET bonds, change after 60 days and PET+B treatment peak was greater than PET and the control. Additionally, the peak 1709-17 cm^{-1} PET was greater than the control. The ~1234-48 cm^{-1} peak was greater for the control (K) than for PET+B and PET. The addition or absence of functional groups that is reflected through peaks has been linked to microbial activity (Torena et al., 2021)

PET, BPET+B, CPE and CPE+B showed bacterial biofilms after 60 days, however, no morphological changes were observed between PET and BPET+B treatments. MP particles subjected to the initial bacterial community (CPE) differed from those treated with bioaugmented bacteria (CPE+B). Interestingly, CPE+B MP presented cavities and rough surface, probably linked with bacterial enzymatic activities that used plastic polymer as a carbon source (Ojha et al., 2017).

The concentration of MPs in the dehydrated sludge after 60 days was 27 MP g^{-1}, compared to 4 MP g^{-1}at the beginning (before starting the compost experiment). Polyester and polyvinyl

were the most abundant polymers. The most common form was fibers, and black was the most common color. The most prevalent size group for the initial time is from 1000 to 2000 μm, accounting for 26% of the particles, and followed by the group 400-600 μm (23%). At the final time the most prevalent is 200-400 μm with 29% followed by 400-600 μm (19%). After 60 days the number of MPs in the sample increased but also in size, therefore, it cannot be assumed they have been fragmented during this time increasing in number but decreasing in size. Many suspected MPs were lost during the analysis for the initial time in the experiment and these losses make difficult to give a real comparison between the initial time and after 60 days.

After 60 days it can be concluded that 40 MPs did not affect the composting process. There was a significant difference between peaks that indicate chemical changes for both MPs (PET and CPE) therefore, biodegradation happened within the process even if it was slow. The degradation of a plastic cannot be simulated in 60 days when the normal process takes hundreds of years. The compostable bag just showed cavities but was not degraded as we expected although was it labeled as compostable. The MPs found in the SS cannot be compared through time because there were many MP losses in the initial time due to the high OM. It is essential to do an update of the SS legislation and have it include emerging pollutants like MPs.

Numerous variables can influence degradation, including the type of plastic (molecular weight), the type of bacteria (enzyme capacity), and the environmental conditions, like temperature, pH and UV radiation (Oliveira et al., 2020). Therefore, even if numerous researchers agree that biodegradation might occur, many questions still must be answered.

5. Bibliography

Amobonye, A., Bhagwat, P., Raveendran, S., Singh, S., & Pillai, S. (2021). Environmental Impacts of Microplastics and Nanoplastics: A Current Overview. *Frontiers in Microbiology*, *12*, 768297. https://doi.org/10.3389/fmicb.2021.768297

Ashter, S. A. (2016). 10—New Developments. In S. A. Ashter (Ed.), *Introduction to Bioplastics Engineering* (pp. 251–274). William Andrew Publishing. https://doi.org/10.1016/B978-0-323-39396-6.00010-5

Auta, H. S., Emenike, C. U., & Fauziah, S. H. (2017). Screening of Bacillus strains isolated from mangrove ecosystems in Peninsular Malaysia for microplastic degradation. *Environmental Pollution*, *231*, 1552–1559. https://doi.org/10.1016/j.envpol.2017.09.043

Babel, S., & Dork, H. (2021). Identification of Micro-plastic Contamination in Drinking Water Treatment Plants in Phnom Penh, Cambodia. *Journal of Engineering and Technological Sciences*, *53*(3), 210307. https://doi.org/10.5614/j.eng.technol.sci.2021.53.3.7

Bardoquillo, E. I. M., Firman, J. M. B., Montecastro, D. B., & Basilio, A. M. (2023). Chemical recycling of waste polyethylene terephthalate (PET) bottles via recovery and polymerization of terephthalic acid (TPA) and ethylene glycol (EG). *Materials Today: Proceedings*, S2214785323020564. https://doi.org/10.1016/j.matpr.2023.04.160

Barus, B. S., Chen, K., Cai, M., Li, R., Chen, H., Li, C., Wang, J., & Cheng, S.-Y. (2021). Heavy Metal Adsorption and Release on Polystyrene Particles at Various Salinities. *Frontiers in Marine Science*, *8*. https://www.frontiersin.org/articles/10.3389/fmars.2021.671802

Bengtsson, S., de Blois, M., Wilén, B.-M., & Gustavsson, D. (2019). A comparison of aerobic granular sludge with conventional and compact biological treatment technologies. *Environmental Technology*, *40*(21), 2769–2778. https://doi.org/10.1080/09593330.2018.1452985

Bianchini, A., Bonfiglioli, L., Pellegrini, M., & Saccani, C. (2016). Sewage sludge management in Europe: A critical analysis of data quality. *International Journal of Environment and Waste Management*, *18*, 226. https://doi.org/10.1504/IJEWM.2016.10001645

Boots, B., Russell, C. W., & Green, D. S. (2019). Effects of Microplastics in Soil Ecosystems: Above and Below Ground. *Environmental Science & Technology*, *53*(19), 11496–11506. https://doi.org/10.1021/acs.est.9b03304

Bosker, T., Bouwman, L. J., Brun, N. R., Behrens, P., & Vijver, M. G. (2019). Microplastics accumulate on pores in seed capsule and delay germination and root growth of the terrestrial vascular plant Lepidium sativum. *Chemosphere*, *226*, 774–781. https://doi.org/10.1016/j.chemosphere.2019.03.163

Boucher, J., & Friot, D. (2017). *Primary microplastics in the oceans: A global evaluation of sources*. IUCN International Union for Conservation of Nature. https://doi.org/10.2305/IUCN.CH.2017.01.en

Brandon, J., Goldstein, M., & Ohman, M. D. (2016). Long-term aging and degradation of microplastic particles: Comparing in situ oceanic and experimental weathering patterns. *Marine Pollution Bulletin*, *110*(1), 299–308. https://doi.org/10.1016/j.marpolbul.2016.06.048

Browne, M. A., Niven, S. J., Galloway, T. S., Rowland, S. J., & Thompson, R. C. (2013). Microplastic Moves Pollutants and Additives to Worms, Reducing Functions Linked to Health and Biodiversity. *Current Biology*, *23*(23), 2388–2392. https://doi.org/10.1016/j.cub.2013.10.012

Carr, S. A., Liu, J., & Tesoro, A. G. (2016). Transport and fate of microplastic particles in wastewater treatment plants. *Water Research*, *91*, 174–182. https://doi.org/10.1016/j.watres.2016.01.002

Carvalheira, M., Marreiros, B. C., & Reis, M. A. M. (2022). Chapter 13—Acids (VFAs) and bioplastic (PHA) recovery. In A. An, V. Tyagi, M. Kumar, & Z. Cetecioglu (Eds.), *Clean Energy and Resource Recovery* (pp. 245–254). Elsevier. https://doi.org/10.1016/B978-0-323-90178-9.00016-0

Chen, Z., Zhao, W., Xing, R., Xie, S., Yang, X., Cui, P., Lü, J., Liao, H., Yu, Z., Wang, S., & Zhou, S. (2020). Enhanced in situ biodegradation of microplastics in sewage sludge using hyperthermophilic composting technology. *Journal of Hazardous Materials*, *384*, 121271. https://doi.org/10.1016/j.jhazmat.2019.121271

Coates, J. (2006). Interpretation of Infrared Spectra, A Practical Approach. In R. A. Meyers (Ed.), *Encyclopedia of Analytical Chemistry* (p. a5606). John Wiley & Sons, Ltd. https://doi.org/10.1002/9780470027318.a5606

Cole, M., Lindeque, P., Halsband, C., & Galloway, T. S. (2011). Microplastics as contaminants in the marine environment: A review. *Marine Pollution Bulletin*, *62*(12), 2588–2597. https://doi.org/10.1016/j.marpolbul.2011.09.025

Corradini, F., Meza, P., Eguiluz, R., Casado, F., Huerta-Lwanga, E., & Geissen, V. (2019). Evidence of microplastic accumulation in agricultural soils from sewage sludge disposal. *The Science of the Total Environment*, *671*, 411–420. https://doi.org/10.1016/j.scitotenv.2019.03.368

Council Directive 86/278/EEC, CONSIL, 181 OJ L (1986). http://data.europa.eu/eli/dir/1986/278/oj/eng

Crawford, C. B., & Quinn, B. (2017). Physiochemical properties and degradation. In *Microplastic Pollutants* (pp. 57–100). Elsevier. https://doi.org/10.1016/B978-0-12-809406-8.00004-9

Cydzik-Kwiatkowska, A., Milojevic, N., & Jachimowicz, P. (2022). The fate of microplastic in sludge management systems. *Science of The Total Environment*, *848*, 157466. https://doi.org/10.1016/j.scitotenv.2022.157466

De Frond, H., Cowger, W., Renick, V., Brander, S., Primpke, S., Sukumaran, S., Elkhatib, D., Barnett, S., Navas-Moreno, M., Rickabaugh, K., Vollnhals, F., O'Donnell, B., Lusher, A., Lee, E., Lao, W., Amarpuri, G., Sarau, G., & Christiansen, S. (2023). What determines accuracy of chemical identification when using microspectroscopy for the analysis of microplastics? *Chemosphere*, *313*, 137300. https://doi.org/10.1016/j.chemosphere.2022.137300

de Souza Machado, A. A., Lau, C. W., Kloas, W., Bergmann, J., Bachelier, J. B., Faltin, E., Becker, R., Görlich, A. S., & Rillig, M. C. (2019). Microplastics Can Change Soil Properties and Affect Plant Performance. *Environmental Science & Technology*, *53*(10), 6044–6052. https://doi.org/10.1021/acs.est.9b01339

Denaro, R., Aulenta, F., Crisafi, F., Di Pippo, F., Cruz Viggi, C., Matturro, B., Tomei, P., Smedile, F., Martinelli, A., Di Lisio, V., Venezia, C., & Rossetti, S. (2020). Marine hydrocarbon-degrading bacteria breakdown poly(ethylene terephthalate) (PET). *Science of The Total Environment*, *749*, 141608. https://doi.org/10.1016/j.scitotenv.2020.141608

Ding, Y., Abeykoon, C., & Perera, Y. S. (2022). The effects of extrusion parameters and blend composition on the mechanical, rheological and thermal properties of LDPE/PS/PMMA ternary polymer blends. *Advances in Industrial and Manufacturing Engineering*, *4*, 100067. https://doi.org/10.1016/j.aime.2021.100067

Domini, M., Bertanza, G., Vahidzadeh, R., & Pedrazzani, R. (2022). Sewage Sludge Quality and Management for Circular Economy Opportunities in Lombardy. *Applied Sciences*, *12*(20), Article 20. https://doi.org/10.3390/app122010391

Du, S., Zhu, R., Cai, Y., Xu, N., Yap, P.-S., Zhang, Y., He, Y., & Zhang, Y. (2021). Environmental fate and impacts of microplastics in aquatic ecosystems: A review. *RSC Advances*, *11*(26), 15762–15784. https://doi.org/10.1039/D1RA00880C

ECHA. (2021). *Microplastics—ECHA*. Microplastics. https://echa.europa.eu/hot-topics/microplastics

EEA, E. E. A. (2022). *Microplastics from textiles: Towards a circular economy for textiles in Europe — European Environment Agency* [Briefing]. https://www.eea.europa.eu/publications/microplastics-from-textiles-towards-a

Eerkes-Medrano, D., & Thompson, R. (2018). Occurrence, Fate, and Effect of Microplastics in Freshwater Systems. In *Microplastic Contamination in Aquatic Environments* (pp. 95–132). Elsevier. https://doi.org/10.1016/B978-0-12-813747-5.00004-7

Eriksen, M., Lebreton, L. C. M., Carson, H. S., Thiel, M., Moore, C. J., Borerro, J. C., Galgani, F., Ryan, P. G., & Reisser, J. (2014). Plastic Pollution in the World's Oceans: More than 5 Trillion Plastic Pieces Weighing over 250,000 Tons Afloat at Sea. *PLoS ONE*, *9*(12), e111913. https://doi.org/10.1371/journal.pone.0111913

Eriksson, E., Christensen, N., Ejbye Schmidt, J., & Ledin, A. (2008). Potential priority pollutants in sewage sludge. *Desalination*, *226*(1–3), 371–388. https://doi.org/10.1016/j.desal.2007.03.019

Erostat. (2023). *Statistics | Eurostat*. https://ec.europa.eu/eurostat/databrowser/view/ten00030/default/table?lang=en

EUBIO. (2022a). Bioplastics. *European Bioplastics e.V.* https://www.european-bioplastics.org/bioplastics/

EUBIO. (2022b). Market. *European Bioplastics e.V.* https://www.european-bioplastics.org/market/

EUBIO, I. (2018). *Bioplastics market data 2018*. https://www.european-bioplastics.org/wp-content/uploads/2016/02/Report_Bioplastics-Market-Data_2018.pdf

EurEau. (2021). *Europe's Water in Figures An Overview of the European Drinking water and Waste Water Sectors* (2021 Edition). The European Federation of National Associations of Water Services. https://www.eureau.org/resources/publications/eureau-publications/5824-europe-s-water-in-figures-2021/file

Farrell, P., & Nelson, K. (2013). Trophic level transfer of microplastic: Mytilus edulis (L.) to Carcinus maenas (L.). *Environmental Pollution*, *177*, 1–3. https://doi.org/10.1016/j.envpol.2013.01.046

Fernández de Villalobos, N., Costa, M. C., & Marín-Beltrán, I. (2022). A community of marine bacteria with potential to biodegrade petroleum-based and biobased microplastics. *Marine Pollution Bulletin*, *185*, 114251. https://doi.org/10.1016/j.marpolbul.2022.114251

Fotopoulou, K. N., & Karapanagioti, H. K. (2015). Surface properties of beached plastics. *Environmental Science and Pollution Research*, *22*(14), 11022–11032. https://doi.org/10.1007/s11356-015-4332-y

GESAMP. (2019). *Guidelines for the monitoring and assessment of plastic litter in the ocean*.

Gewert, B., Plassmann, M. M., & MacLeod, M. (2015). Pathways for degradation of plastic polymers floating in the marine environment. *Environmental Science: Processes & Impacts*, *17*(9), 1513–1521. https://doi.org/10.1039/C5EM00207A

Geyer, R., Jambeck, J. R., & Law, K. L. (2017). Production, use, and fate of all plastics ever made. *Science Advances*, *3*(7), e1700782. https://doi.org/10.1126/sciadv.1700782

Gumbi, A. S., Abdulsalam, M. S., Suleiman, A. B., Egbe, N., Umar, Z., Shitu, A. M., Gumbi, A. S., & Yahuza, S. M. (2019). *ISOLATION AND CHARACTERIZATION OF PSEUDOMONAS AERUGINOSA AND BREVIBACILLUS SPECIES AND THEIR POTENTIAL TO BIODEGRADE POLYETHYLENE MATERIAL*. *14*(4).

Hadad, D., Geresh, S., & Sivan, A. (2005). Biodegradation of polyethylene by the thermophilic bacterium Brevibacillus borstelensis. *Journal of Applied Microbiology*, *98*(5), 1093–1100. https://doi.org/10.1111/j.1365-2672.2005.02553.x

Harley-Nyang, D., Memon, F. A., Jones, N., & Galloway, T. (2022). Investigation and analysis of microplastics in sewage sludge and biosolids: A case study from one wastewater treatment works in the UK. *Science of The Total Environment*, *823*, 153735. https://doi.org/10.1016/j.scitotenv.2022.153735

Helmberger, M. S., Tiemann, L. K., & Grieshop, M. J. (2020). Towards an ecology of soil microplastics. *Functional Ecology*, *34*(3), 550–560. https://doi.org/10.1111/1365-2435.13495

Hudcová, H., Vymazal, J., & Rozkošný, M. (2019). Present restrictions of sewage sludge application in agriculture within the European Union. *Soil and Water Research*, *14*(2), 104–120. https://doi.org/10.17221/36/2018-SWR

Iqbal, S., Xu, J., Allen, S. D., Khan, S., Nadir, S., Arif, M. S., & Yasmeen, T. (2020). Unraveling consequences of soil micro- and nano-plastic pollution on soil-plant system: Implications for nitrogen (N) cycling and soil microbial activity. *Chemosphere*, *260*, 127578. https://doi.org/10.1016/j.chemosphere.2020.127578

Jung, M. R., Horgen, F. D., Orski, S. V., Rodriguez C., V., Beers, K. L., Balazs, G. H., Jones, T. T., Work, T. M., Brignac, K. C., Royer, S.-J., Hyrenbach, K. D., Jensen, B. A., & Lynch, J. M. (2018). Validation of ATR FT-IR to identify polymers of plastic marine debris, including those ingested by marine organisms. *Marine Pollution Bulletin*, *127*, 704–716. https://doi.org/10.1016/j.marpolbul.2017.12.061

Kumar, R., Verma, A., Shome, A., Sinha, R., Sinha, S., Jha, P. K., Kumar, R., Kumar, P., Shubham, Das, S., Sharma, P., & Vara Prasad, P. V. (2021). Impacts of Plastic Pollution on Ecosystem Services, Sustainable Development Goals, and Need to Focus on Circular Economy and Policy Interventions. *Sustainability*, *13*(17), Article 17. https://doi.org/10.3390/su13179963

Lares, M., Ncibi, M. C., Sillanpää, M., & Sillanpää, M. (2018). Occurrence, identification and removal of microplastic particles and fibers in conventional activated sludge process and advanced MBR technology. *Water Research*, *133*, 236–246. https://doi.org/10.1016/j.watres.2018.01.049

Lavoy, M., & Crossman, J. (2021). A novel method for organic matter removal from samples containing microplastics. *Environmental Pollution*, *286*, 117357. https://doi.org/10.1016/j.envpol.2021.117357

Lebreton, L. C. M., van der Zwet, J., Damsteeg, J.-W., Slat, B., Andrady, A., & Reisser, J. (2017). River plastic emissions to the world's oceans. *Nature Communications*, *8*(1), 15611. https://doi.org/10.1038/ncomms15611

Li, X., Chen, L., Mei, Q., Dong, B., Dai, X., Ding, G., & Zeng, E. Y. (2018). Microplastics in sewage sludge from the wastewater treatment plants in China. *Water Research*, *142*, 75–85. https://doi.org/10.1016/j.watres.2018.05.034

Li, X., Ke, Z., & Dong, J. (2011). PCDDs and PCDFs in sewage sludges from two wastewater treatment plants in Beijing, China. *Chemosphere*, *82*(5), 635–638. https://doi.org/10.1016/j.chemosphere.2010.11.039

Lin, C., Cheruiyot, N. K., Bui, X.-T., & Ngo, H. H. (2022). Composting and its application in bioremediation of organic contaminants. *Bioengineered*, *13*(1), 1073–1089. https://doi.org/10.1080/21655979.2021.2017624

Lozano, Y. M., & Rillig, M. C. (2020). Effects of Microplastic Fibers and Drought on Plant Communities. *Environmental Science & Technology*, *54*(10), 6166–6173. https://doi.org/10.1021/acs.est.0c01051

Ma, C., Chen, X., Zheng, G., Liu, N., Zhao, J., & Zhang, H. (2022). Exploring the influence mechanisms of polystyrene-microplastics on sewage sludge composting. *Bioresource Technology*, *362*, 127798. https://doi.org/10.1016/j.biortech.2022.127798

Magnusson, K., & Norén, F. (2014). *Screening of microplastic particles in and down-stream a wastewater treatment plant*.

Mahon, A. M., O'Connell, B., Healy, M. G., O'Connor, I., Officer, R., Nash, R., & Morrison, L. (2017). Microplastics in Sewage Sludge: Effects of Treatment. *Environmental Science & Technology*, *51*(2), 810–818. https://doi.org/10.1021/acs.est.6b04048

Maw, M. M., Boontanon, N., Fujii, S., & Boontanon, S. K. (2022). Rapid and efficient removal of organic matter from sewage sludge for extraction of microplastics. *Science of The Total Environment*, *853*, 158642. https://doi.org/10.1016/j.scitotenv.2022.158642

Measuring the Impacts of Microplastics. (n.d.). Eunomia. Retrieved February 8, 2023, from https://www.eunomia.co.uk/case_study/measuring-impacts-of-microplastics/

Mecozzi, M., & Nisini, L. (2019). The differentiation of biodegradable and non-biodegradable polyethylene terephthalate (PET) samples by FTIR spectroscopy: A potential support for the structural differentiation of PET in environmental analysis. *Infrared Physics & Technology*, *101*, 119–126. https://doi.org/10.1016/j.infrared.2019.06.008

Mouafo Tamnou, E. B., Tamsa Arfao, A., Nougang, M. E., Metsopkeng, C. S., Noah Ewoti, O. V., Moungang, L. M., Nana, P. A., Atem Takang-Etta, L.-R., Perrière, F., Sime-Ngando, T., & Nola, M. (2021). Biodegradation of polyethylene by the bacterium Pseudomonas aeruginosa in acidic aquatic microcosm and effect of the environmental temperature. *Environmental Challenges*, *3*, 100056. https://doi.org/10.1016/j.envc.2021.100056

Murphy, F., Ewins, C., Carbonnier, F., & Quinn, B. (2016). Wastewater Treatment Works (WwTW) as a Source of Microplastics in the Aquatic Environment. *Environmental Science & Technology*, *50*(11), 5800–5808. https://doi.org/10.1021/acs.est.5b05416

Neo, E. R. K., Low, J. S. C., Goodship, V., & Debattista, K. (2023). Deep learning for chemometric analysis of plastic spectral data from infrared and Raman databases. *Resources, Conservation and Recycling*, *188*, 106718. https://doi.org/10.1016/j.resconrec.2022.106718

Ngonyani, A. M. (2022). *MARINE BACTERIA AND THEIR ROLE IN POLYETHYLENE TEREPHTHALATE BIODETERIORATION AND BIOFRAGMENTATION*.

Ojha, N., Pradhan, N., Singh, S., Barla, A., Shrivastava, A., Khatua, P., Rai, V., & Bose, S. (2017). Evaluation of HDPE and LDPE degradation by fungus, implemented by statistical optimization. *Scientific Reports*, *7*(1), 39515. https://doi.org/10.1038/srep39515

Oliveira, J., Belchior, A., da Silva, V. D., Rotter, A., Petrovski, Ž., Almeida, P. L., Lourenço, N. D., & Gaudêncio, S. P. (2020). Marine Environmental Plastic Pollution: Mitigation by Microorganism Degradation and Recycling Valorization. *Frontiers in Marine Science*, *7*, 567126. https://doi.org/10.3389/fmars.2020.567126

Pannetier, P., Cachot, J., Clérandeau, C., Faure, F., Van Arkel, K., de Alencastro, L. F., Levasseur, C., Sciacca, F., Bourgeois, J.-P., & Morin, B. (2019). Toxicity assessment of pollutants sorbed on environmental sample microplastics collected on beaches: Part I-adverse effects on fish cell line. *Environmental Pollution*, *248*, 1088–1097. https://doi.org/10.1016/j.envpol.2018.12.091

Peacock, A. (2000). *Handbook of Polyethylene: Structures: Properties, and Applications*. CRC Press.

Plastic Europe. (2022). *Plastics – the Facts 2022*. file:///Users/adrianagonzalez/Downloads/PE-PLASTICS-THE-FACTS_FINAL_DIGITAL-1.pdf

Rajandas, H., Parimannan, S., Sathasivam, K., Ravichandran, M., & Su Yin, L. (2012). A novel FTIR-ATR spectroscopy based technique for the estimation of low-density polyethylene biodegradation. *Polymer Testing*, *31*(8), 1094–1099. https://doi.org/10.1016/j.polymertesting.2012.07.015

Reddy, A. S., & Nair, A. T. (2022). The fate of microplastics in wastewater treatment plants: An overview of source and remediation technologies. *Environmental Technology & Innovation*, *28*, 102815. https://doi.org/10.1016/j.eti.2022.102815

Rochman, C. M., Hoh, E., Kurobe, T., & Teh, S. J. (2013). Ingested plastic transfers hazardous chemicals to fish and induces hepatic stress. *Scientific Reports*, *3*(1), 3263. https://doi.org/10.1038/srep03263

SAPEA, S. A. for P. by E. A. (2020). *Biodegradability of plastics in the open environment*. Science Advice for Policy by European Academies (SAPEA). https://doi.org/10.26356/biodegradabilityplastics

Seleiman, M. F., Santanen, A., & Mäkelä, P. S. A. (2020). Recycling sludge on cropland as fertilizer – Advantages and risks. *Resources, Conservation and Recycling*, *155*, 104647. https://doi.org/10.1016/j.resconrec.2019.104647

Sheik, S., Chandrashekar, K. R., Swaroop, K., & Somashekarappa, H. M. (2015). Biodegradation of gamma irradiated low density polyethylene and polypropylene by endophytic fungi. *International Biodeterioration & Biodegradation*, *105*, 21–29. https://doi.org/10.1016/j.ibiod.2015.08.006

Shi, B., Patel, M., Yu, D., Yan, J., Li, Z., Petriw, D., Pruyn, T., Smyth, K., Passeport, E., Miller, R. J. D., & Howe, J. Y. (2022). Automatic quantification and classification of microplastics in scanning electron micrographs via deep learning. *Science of The Total Environment*, *825*, 153903. https://doi.org/10.1016/j.scitotenv.2022.153903

Shim, W. J., Hong, S. H., & Eo, S. E. (2017). Identification methods in microplastic analysis: A review. *Analytical Methods*, *9*(9), 1384–1391. https://doi.org/10.1039/C6AY02558G

Shim, W. J., Song, Y. K., Hong, S. H., & Jang, M. (2016). Identification and quantification of microplastics using Nile Red staining. *Marine Pollution Bulletin*, *113*(1–2), 469–476. https://doi.org/10.1016/j.marpolbul.2016.10.049

Simon, M., van Alst, N., & Vollertsen, J. (2018). Quantification of microplastic mass and removal rates at wastewater treatment plants applying Focal Plane Array (FPA)-based Fourier Transform Infrared (FT-IR) imaging. *Water Research*, *142*, 1–9. https://doi.org/10.1016/j.watres.2018.05.019

Sivan, A., Szanto, M., & Pavlov, V. (2006). Biofilm development of the polyethylene-degrading bacterium Rhodococcus ruber. *Applied Microbiology and Biotechnology*, *72*(2), 346–352. https://doi.org/10.1007/s00253-005-0259-4

Skariyachan, S., Patil, A. A., Shankar, A., Manjunath, M., Bachappanavar, N., & Kiran, S. (2018). Enhanced polymer degradation of polyethylene and polypropylene by novel thermophilic consortia of Brevibacillus sps. And Aneurinibacillus sp. Screened from waste management landfills and sewage treatment plants. *Polymer Degradation and Stability*, *149*, 52–68. https://doi.org/10.1016/j.polymdegradstab.2018.01.018

Syranidou, E., Karkanorachaki, K., Amorotti, F., Avgeropoulos, A., Kolvenbach, B., Zhou, N.-Y., Fava, F., Corvini, P. F.-X., & Kalogerakis, N. (2019). Biodegradation of mixture of plastic films by tailored marine consortia. *Journal of Hazardous Materials*, *375*, 33–42. https://doi.org/10.1016/j.jhazmat.2019.04.078

Szczurek, A., Tran, T. N. L., Kubacki, J., Gąsiorek, A., Startek, K., Mazur-Nowacka, A., Dell'Anna, R., Armellini, C., Varas, S., Carlotto, A., Chiasera, A., Łukowiak, A., Krzak, J., & Ferrari, M. (2023). Polyethylene terephthalate (PET) optical properties

deterioration induced by temperature and protective effect of organically modified SiO2–TiO2 coating. *Materials Chemistry and Physics*, 128016. https://doi.org/10.1016/j.matchemphys.2023.128016

Talvitie, J., Mikola, A., Koistinen, A., & Setälä, O. (2017). Solutions to microplastic pollution – Removal of microplastics from wastewater effluent with advanced wastewater treatment technologies. *Water Research*, *123*, 401–407. https://doi.org/10.1016/j.watres.2017.07.005

Tareen, A., Saeed, S., Iqbal, A., Batool, R., & Jamil, N. (2022). Biodeterioration of Microplastics: A Promising Step towards Plastics Waste Management. *Polymers*, *14*(11), 2275. https://doi.org/10.3390/polym14112275

Torena, P., Alvarez-Cuenca, M., & Reza, M. (2021). Biodegradation of polyethylene terephthalate microplastics by bacterial communities from activated sludge. *The Canadian Journal of Chemical Engineering*, *99*(S1). https://doi.org/10.1002/cjce.24015

Uçaroğlu, S., & Alkan, U. (2016). Composting of wastewater treatment sludge with different bulking agents. *Journal of the Air & Waste Management Association*, *66*(3), 288–295. https://doi.org/10.1080/10962247.2015.1131205

Van den Auwelant, C. (2022). *Tracking microplastic accumulation in sediments of coastal marine vegetated habitats*. Universidade do Algarve.

Vimala, P. P., & Mathew, L. (2016). Biodegradation of Polyethylene Using Bacillus Subtilis. *Procedia Technology*, *24*, 232–239. https://doi.org/10.1016/j.protcy.2016.05.031

Wang, F., Wang, X., & Song, N. (2021). Polyethylene microplastics increase cadmium uptake in lettuce (Lactuca sativa L.) by altering the soil microenvironment. *Science of The Total Environment*, *784*, 147133. https://doi.org/10.1016/j.scitotenv.2021.147133

Wickham, H., François, R., Henry, L., Müller, K., Vaughan, D., Software, P., & PBC. (2023). *dplyr: A Grammar of Data Manipulation* (1.1.2) [Computer software]. https://cran.r-project.org/web/packages/dplyr/index.html

Wright, S. L., Rowe, D., Thompson, R. C., & Galloway, T. S. (2013). Microplastic ingestion decreases energy reserves in marine worms. *Current Biology*, *23*(23), R1031–R1033. https://doi.org/10.1016/j.cub.2013.10.068

Xing, R., Chen, Z., Sun, H., Liao, H., Qin, S., Liu, W., Zhang, Y., Chen, Z., & Zhou, S. (2022). Free radicals accelerate in situ ageing of microplastics during sludge composting. *Journal of Hazardous Materials*, *429*, 128405. https://doi.org/10.1016/j.jhazmat.2022.128405

Yamada-Onodera, K., Mukumoto, H., Katsuyaya, Y., Saiganji, A., & Tani, Y. (2001). Degradation of polyethylene by a fungus, Penicillium simplicissimum YK. *Polymer Degradation and Stability*, *72*(2), 323–327. https://doi.org/10.1016/S0141-3910(01)00027-1

Yao, Z., Seong, H. J., & Jang, Y.-S. (2022). Degradation of low density polyethylene by Bacillus species. *Applied Biological Chemistry*, *65*(1), 84. https://doi.org/10.1186/s13765-022-00753-3

Zaharioiu, A. M., Bucura, F., Ionete, R. E., Marin, F., Constantinescu, M., & Oancea, S. (2021). Opportunities regarding the use of technologies of energy recovery from sewage sludge. *SN Applied Sciences*, *3*(9), 775. https://doi.org/10.1007/s42452-021-04758-3

Zubris, K. A. V., & Richards, B. K. (2005). Synthetic fibers as an indicator of land application of sludge. *Environmental Pollution*, *138*(2), 201–211. https://doi.org/10.1016/j.envpol.2005.04.013

6.

Annex A: Parameters for Composting experiment

TIME	REPLICATE	pH	OM %	C/N Ratio
T0	T0-R1	5.85	86.38	12.11
	T0-R2	5.74	85.87	13.91
	T0-R3	5.79	82.88	11.18
T1	1 K-R1	8.07	85.35	9.3
	2 K-R2	8.11	87.18	9.26
	3 K-R3	7.68	81.29	9.72
	4P-R1	7.81	82.94	9.88
	5P-R2	7.96	83.73	9.22
	6P-R3	7.86	82.02	9.32
	7C-R1	7.78	81.62	8.87
	8C-R2	8.14	85.26	9.59
	9C-R3	8.03	80.8	9.14
	10P+B-R1	7.5	82.78	8.15
	11P+B-R2	7.45	85.39	8.65
	12P+B-R3	7.4	81.64	9.18
	13C+B-R1	7.75	81.09	8.6
	14C+B-R2	7.68	81.54	8.62
	15C+B-R3	7.66	83.37	8.89
T2	16 K -R1	7.29	88.3	8.8
	17 K -R2	7.23	89.74	8.39
	18 K-R3	7.27	90.52	8.24
	19 P-R1	7.31	89.9	9.38
	20 P-R2	7.35	91.1	8.76
	21 P-R3	7.22	87.38	8.7
	22 C -R1	6.99	82.11	8.85
	23 C-R2	6.9	76.74	9.38
	24 C -R3	7.4	90.16	8.2
	25 P+B-R1	7.01	89.39	8.29
	26 P+B-R2	6.92	82.37	9.1
	27 P+B-R3	6.88	83.91	7.94
	28 C+B-R1	6.55	81.88	9.26
	29 C+B-R2	6.84	82.12	8.7
	30 C+B-R3	6.78	81.64	8.21

K= control R1= replicate 1 R2= replicate 2 R3= replicate 3	P=PET C=CPE P+B=PET + Bioaugmented Bacillus C+B=CPE+ Bioaugmented Bacillus

Annex B: Peaks of CPE MPs after 30 and 60 days

Sampling time	Sample name	#Part	2915 - 2918	2848 - 2851	1710 - 1716	1641 - 1653	1541 - 1549	1458 - 1471	1046 - 1070	870 - 876	717 - 723
T0	CPE	Part 1	0.202	0.181	0.000	0.044	0.000	0.135	0.000	0.089	0.116
		Part 2	0.211	0.192	0.000	0.155	0.000	0.155	0.000	0.098	0.141
		Part 3	0.167	0.151	0.000	0.035	0.000	0.127	0.000	0.063	0.102
		Average	0.193	0.175	0.000	0.078	0.000	0.139	0.000	0.083	0.120
T1	K-CPE	Part 1	0.112	0.105	0.000	0.000	0.006	0.081	0.002	0.046	0.069
		Part 2	0.089	0.083	0.000	0.000	0.000	0.068	0.024	0.020	0.049
		Part 3	0.091	0.087	0.000	0.000	0.000	0.069	0.020	0.030	0.052
		Average	0.101	0.094	0.000	0.000	0.000	0.075	0.013	0.033	0.059
	7CPE-R1	Part 1	0.091	0.084	0.000	0.000	0.000	0.073	0.010	0.017	0.069
		Part 2	0.092	0.085	0.000	0.000	0.000	0.077	0.014	0.022	0.063
		Part 3	0.116	0.106	0.000	0.000	0.000	0.087	0.014	0.030	0.081
		Average	0.100	0.092	0.000	0.000	0.000	0.079	0.013	0.023	0.071
	8CPE-R2	Part 1	0.116	0.106	0.000	0.000	0.000	0.087	0.014	0.030	0.081
		Part 2	0.075	0.069	0.000	0.000	0.000	0.053	0.000	0.000	0.051
		Part 3	0.101	0.094	0.000	0.000	0.000	0.078	0.010	0.028	0.074
		Average	0.097	0.090	0.000	0.000	0.000	0.073	0.012	0.029	0.068
	9CPE-R3	Part 1	0.072	0.066	0.000	0.000	0.000	0.063	0.000	0.008	0.057
		Part 2	0.104	0.094	0.000	0.000	0.000	0.093	0.036	0.049	0.072
		Part 3	0.121	0.110	0.000	0.000	0.000	0.101	0.034	0.060	0.096
		Average	0.099	0.090	0.000	0.000	0.000	0.086	0.035	0.039	0.075
	13CPE+B-R1	Part 1	0.183	0.162	0.018	0.000	0.028	0.115	0.066	0.089	0.122
		Part 2	0.134	0.118	0.000	0.000	0.000	0.086	0.000	0.049	0.078

		Part 3	0.177	0.159	0.047	0.071	0.062	0.131	0.000	0.109	0.144
		Average	0.165	0.146	0.032	0.000	0.045	0.111	0.000	0.082	0.115
	14CPE+B -R2	Part 1	0.141	0.128	0.022	0.045	0.036	0.105	0.000	0.072	0.101
		Part 2	0.169	0.152	0.023	0.037	0.032	0.119	0.000	0.080	0.129
		Part 3	0.182	0.162	0.028	0.042	0.038	0.131	0.000	0.110	0.138
		Average	0.164	0.147	0.024	0.041	0.035	0.118	0.000	0.087	0.123
	15CPE+B -R3	Part 1	0.172	0.154	0.032	0.047	0.042	0.119	0.000	0.093	0.132
		Part 2	0.081	0.073	0.000	0.017	0.006	0.065	0.000	0.022	0.056
		Part 3	0.078	0.069	0.000	0.000	0.000	0.061	0.000	0.003	0.056
		Average	0.110	0.099	0.000	0.032	0.024	0.082	0.000	0.039	0.082
T2	**K-CPE**	Part 1	0.170	0.151	0.063	0.069	0.084	0.138	0.000	0.057	0.096
		Part 2	0.175	0.158	0.085	0.088	0.103	0.160	0.000	0.075	0.105
		Part 3	0.178	0.160	0.099	0.097	0.112	0.166	0.000	0.083	0.112
		Average	0.174	0.156	0.082	0.085	0.100	0.155	0.000	0.072	0.104
	22 CPE-R1	Part 1	0.189	0.169	0.000	0.000	0.000	0.000	0.138	0.067	0.094
		Part 2	0.190	0.170	0.000	0.000	0.000	0.143	0.072	0.078	0.189
		Part 3	0.162	0.148	0.000	0.100	0.092	0.146	0.090	0.087	0.116
		Average	0.180	0.162	0.000	0.000	0.000	0.145	0.100	0.077	0.133
	23 CPE-R2	Part 1	0.170	0.153	0.000	0.088	0.000	0.139	0.077	0.082	0.112
		Part 2	0.166	0.149	0.000	0.086	0.000	0.147	0.082	0.102	0.113
		Part 3	0.153	0.136	0.000	0.049	0.000	0.119	0.048	0.061	0.088
		Average	0.163	0.146	0.000	0.074	0.000	0.135	0.069	0.082	0.104
	24 CPE-R3	Part 1	0.189	0.169	0.000	0.078	0.000	0.154	0.074	0.089	0.120
		Part 2	0.192	0.173	0.000	0.079	0.000	0.161	0.073	0.092	0.119
		Part 3	0.175	0.155	0.000	0.054	0.000	0.136	0.000	0.060	0.090
		Average	0.185	0.166	0.000	0.071	0.000	0.150	0.074	0.080	0.110
	28CPE+B	Part 1	0.151	0.137	0.068	0.119	0.116	0.139	0.085	0.061	0.105

		Part 2	0.167	0.150	0.069	0.093	0.093	0.135	0.000	0.072	0.100
		Part 3	0.137	0.125	0.052	0.083	0.082	0.130	0.000	0.052	0.098
		Average	0.152	0.137	0.063	0.098	0.097	0.135	0.000	0.061	0.101
	29 CPE+B-R2	Part 1	0.152	0.138	0.049	0.079	0.083	0.135	0.059	0.066	0.098
		Part 2	0.160	0.142	0.029	0.045	0.052	0.118	0.000	0.044	0.080
		Part 3	0.167	0.147	0.000	0.044	0.054	0.118	0.034	0.041	0.160
		Average	0.160	0.142	0.039	0.056	0.063	0.124	0.046	0.050	0.113
	30 CPE+B-R3	Part 1	0.187	0.167	0.062	0.079	0.090	0.148	0.061	0.071	0.102
		Part 2	0.191	0.170	0.064	0.089	0.097	0.155	0.077	0.094	0.119
		Part 3	0.171	0.151	0.047	0.074	0.080	0.135	0.048	0.055	0.044
		Average	0.183	0.163	0.058	0.081	0.089	0.146	0.062	0.073	0.088

Annex C: Peaks of PET MPs after 30 and 60 days

Sampling time	Name	#Part	2916 - 2927	2849 - 2856	1709 - 1717	1630 - 1652	1547 - 1558	1530 - 1542	1452 - 1467	1406 - 1409	1335 - 1342	1234 - 1248	1082 - 1098	1016 - 1020	870 - 874	717 - 730
T0	**PET**	Part 1	0.202	0.181	0.000	0.000	0.000	0.000	0.135	0.000	0.000	0.000	0.039	0.000	0.089	0.116
		Part 2	0.068	0.000	0.134	0.000	0.000	0.000	0.000	0.088	0.095	0.173	0.170	0.134	0.119	0.220
		Part 3	0.000	0.000	0.100	0.000	0.000	0.000	0.000	0.061	0.060	0.136	0.137	0.104	0.083	0.190
		Average	0.135	0.000	0.117	0.000	0.000	0.000	0.000	0.074	0.077	0.155	0.115	0.119	0.097	0.175
T1	KPET	Part 1	0.121	0.104	0.155	0.084	0.069	0.068	0.094	0.119	0.095	0.200	0.324	0.191	0.153	0.286
		Part 2	0.045	0.033	0.016	0.004	0.000	0.000	0.018	0.032	0.008	0.046	0.147	0.074	0.037	0.145
		Part 3	0.105	0.088	0.104	0.066	0.054	0.054	0.078	0.097	0.074	0.147	0.264	0.155	0.121	0.227
		Average	0.090	0.075	0.092	0.051	0.041	0.041	0.063	0.082	0.059	0.131	0.245	0.140	0.104	0.219
	4 PET-R1	Part 1	0.104	0.088	0.163	0.000	0.000	0.000	0.087	0.097	0.098	0.211	0.215	0.161	0.123	0.275
		Part 2	0.074	0.075	0.082	0.000	0.000	0.000	0.066	0.066	0.064	0.112	0.118	0.097	0.078	0.150
		Part 3	0.000	0.061	0.000	0.000	0.000	0.000	0.000	0.000	0.000	0.000	0.000	0.000	0.000	0.000
		Average	0.089	0.075	0.122	0.000	0.000	0.000	0.077	0.082	0.081	0.162	0.167	0.129	0.100	0.213
	5 PET-R2	Part 1	0.000	0.000	0.089	0.000	0.000	0.000	0.000	0.000	0.077	0.135	0.147	0.114	0.085	0.203
		Part 2	0.000	0.000	0.046	0.040	0.000	0.000	0.000	0.034	0.033	0.080	0.097	0.084	0.053	0.146
		Part 3	0.000	0.000	0.000	0.000	0.000	0.000	0.000	0.000	0.000	0.000	0.000	0.000	0.000	0.000
		Average	0.000	0.000	0.068	0.000	0.000	0.000	0.000	0.000	0.055	0.107	0.122	0.099	0.069	0.175
	6 PET-R3	Part 1	0.033	0.027	0.077	0.000	0.000	0.000	0.034	0.050	0.046	0.118	0.130	0.100	0.062	0.205
		Part 2	0.024	0.018	0.083	0.000	0.000	0.000	0.031	0.045	0.040	0.123	0.130	0.093	0.055	0.202
		Part 3	0.000	0.000	0.000	0.000	0.000	0.000	0.000	0.000	0.000	0.000	0.000	0.000	0.000	0.000
		Average	0.028	0.023	0.080	0.000	0.000	0.000	0.033	0.047	0.043	0.121	0.130	0.097	0.058	0.204
	10P	Part 1	0.050	0.000	0.065	0.148	0.124	0.119	0.000	0.099	0.086	0.134	0.129	0.108	0.087	0.187

		Part 2	0.029	0.024	0.018	0.105	0.087	0.080	0.046	0.058	0.000	0.072	0.070	0.057	0.036	0.132
		Part 3	0.045	0.038	0.000	0.138	0.116	0.108	0.066	0.082	0.000	0.094	0.096	0.083	0.061	0.018
		Average	0.041	0.031	0.041	0.130	0.109	0.102	0.056	0.079	0.000	0.100	0.099	0.082	0.061	0.112
	11 PET+B-R2	Part 1	0.045	0.038	0.000	0.138	0.116	0.108	0.066	0.082	0.000	0.094	0.096	0.083	0.061	0.151
		Part 2	0.072	0.062	0.107	0.069	0.049	0.048	0.064	0.077	0.074	0.161	0.166	0.123	0.100	0.232
		Part 3	0.076	0.000	0.169	0.094	0.071	0.069	0.000	0.108	0.104	0.239	0.233	0.171	0.149	0.303
		Average	0.064	0.050	0.138	0.100	0.079	0.075	0.065	0.089	0.089	0.165	0.165	0.126	0.103	0.229
	12 PET+B-R3	Part 1	0.303	0.109	0.125	0.000	0.062	0.061	0.091	0.092	0.092	0.163	0.161	0.138	0.124	0.222
		Part 2	0.121	0.104	0.143	0.076	0.060	0.060	0.087	0.093	0.093	0.187	0.188	0.153	0.136	0.222
		Part 3	0.129	0.108	0.091	0.068	0.060	0.059	0.083	0.081	0.079	0.135	0.000	0.159	0.130	0.216
		Average	0.184	0.107	0.120	0.072	0.061	0.060	0.087	0.089	0.088	0.162	0.175	0.150	0.130	0.220
T2	KPET	Part 1	0.000	0.000	0.140	0.111	0.110	0.117	0.101	0.099	0.103	0.153	0.154	0.129	0.107	0.182
		Part 2	0.000	0.000	0.188	0.130	0.127	0.136	0.121	0.123	0.130	0.215	0.209	0.164	0.137	0.242
		Part 3	0.000	0.000	0.156	0.115	0.122	0.131	0.112	0.111	0.115	0.178	0.175	0.143	0.117	0.210
		Average	0.000	0.000	0.161	0.119	0.120	0.128	0.111	0.111	0.116	0.182	0.179	0.145	0.120	0.211
	19 PET-R1	Part 1	0.000	0.000	0.035	0.000	0.000	0.000	0.000	0.036	0.037	0.050	0.057	0.056	0.048	0.076
		Part 2	0.103	0.084	0.106	0.036	0.034	0.000	0.071	0.070	0.070	0.139	0.143	0.119	0.085	0.212
		Part 3	0.000	0.000	0.106	0.000	0.000	0.000	0.000	0.000	0.000	0.140	0.139	0.103	0.000	0.183
		Average	0.000	0.000	0.082	0.000	0.000	0.000	0.000	0.053	0.053	0.110	0.113	0.093	0.066	0.157
	20 PET-R2	Part 1	0.120	0.097	0.096	0.000	0.000	0.058	0.074	0.069	0.066	0.126	0.137	0.119	0.082	0.209
		Part 2	0.120	0.096	0.000	0.045	0.000	0.000	0.062	0.000	0.000	0.052	0.000	0.078	0.052	0.132
		Part 3	0.177	0.149	0.108	0.110	0.000	0.101	0.120	0.102	0.000	0.132	0.000	0.149	0.116	0.196
		Average	0.139	0.114	0.000	0.077	0.000	0.000	0.085	0.085	0.000	0.103	0.000	0.115	0.083	0.179
	21 PET-R3	Part 1	0.130	0.107	0.095	0.000	0.000	0.078	0.090	0.077	0.077	0.124	0.138	0.126	0.096	0.204
		Part 2	0.162	0.134	0.000	0.094	0.000	0.092	0.108	0.000	0.084	0.098	0.000	0.121	0.097	0.130
		Part 3	0.066	0.053	0.000	0.048	0.045	0.055	0.048	0.000	0.036	0.000	0.000	0.000	0.000	0.041
		Average	0.119	0.098	0.000	0.071	0.000	0.075	0.082	0.000	0.066	0.111	0.000	0.124	0.096	0.125

	25 PET+B-R1	Part 1	0.112	0.098	0.000	0.143	0.000	0.134	0.124	0.115	0.109	0.143	0.000	0.151	0.097	0.173
		Part 2	0.125	0.111	0.107	0.132	0.000	0.129	0.126	0.000	0.108	0.133	0.000	0.138	0.090	0.152
		Part 3	0.107	0.093	0.100	0.130	0.000	0.123	0.114	0.000	0.101	0.136	0.151	0.140	0.090	0.169
		Average	0.115	0.101	0.104	0.135	0.000	0.129	0.121	0.000	0.106	0.137	0.000	0.143	0.092	0.165
	26 PET+B-R2	Part 1	0.070	0.061	0.084	0.086	0.000	0.085	0.081	0.075	0.074	0.094	0.093	0.087	0.063	0.104
		Part 2	0.167	0.148	0.119	0.137	0.127	0.135	0.145	0.000	0.120	0.130	0.000	0.000	0.110	0.148
		Part 3	0.097	0.084	0.092	0.104	0.000	0.101	0.098	0.090	0.087	0.114	0.123	0.119	0.081	0.147
		Average	0.111	0.098	0.099	0.109	0.000	0.107	0.108	0.082	0.094	0.113	0.108	0.103	0.084	0.133
	27 PET+B-R3	Part 1	0.122	0.106	0.096	0.109	0.101	0.108	0.111	0.000	0.093	0.107	0.000	0.109	0.079	0.126
		Part 2	0.195	0.171	0.155	0.185	0.000	0.173	0.165	0.151	0.146	0.168	0.178	0.172	0.146	0.192
		Part 3	0.100	0.088	0.100	0.105	0.100	0.106	0.105	0.091	0.089	0.111	0.112	0.104	0.075	0.135
		Average	0.139	0.122	0.117	0.133	0.100	0.129	0.127	0.121	0.109	0.129	0.145	0.128	0.100	0.151

Annex C: Suspected MPs in the initial time and after 60 days. (K) control, (T0) initial time, (T2) after 60 days

Time	Sample ID	Plastic number ID	Colour	Size (µm)	Shape	FTIR - REFLECTION	Match reflection (%)	Plastic (YES / NO)
K	K	1	Red		Fiber	URETHANE ALKYD, LINSEED OIL RICH	41	YES
		2	Green		Pellet	URETHANE ALKYD, LINSEED OIL RICH	43	YES
T0	T0.R3.1-1S	7	Green	1142.30	Fragment	ANDRADITE	43	NO
		3	Blue	93.05	Fragment	COPROPORPHYRIN I DIHYDROCHLORIDE	43	NO
		10	Black	792.09	Fiber	POLYESTER	42	YES
		1	Black	404.40	Fiber	POLYESTER	39	UNSURE
		11	Black	1379.42	Fiber	COPOLYMER ETHYLENE-TETRAFLUOROETHYLENE	37	UNSURE
		2	Black	549.33	Fiber	POLYURETHANE ADHESIVE	36	UNSURE
		4	Blue	438.65	Fiber	LOST	0	LOST
		5	Blue	421.00	Fiber	LOST	0	LOST
		6	Black	708.24	Fiber	LOST	0	LOST
		8	Blue	1209.76	Fiber	LOST	0	LOST
		9	Black	319.88	Fiber	LOST	0	LOST
	T0.R3.2-1S	6	Blue	273.64	Fiber	ACRYLIC	64	YES
		1	Red	1793.22	Fiber	POLYESTER	54	YES
		2	Black	756.78	Fiber	POLYESTER	45	YES
		5	Blue	949.57	Fiber	POLYESTER	38	UNSURE
		3	Black	279.45	Fiber	POLY(ARYLETHER)	34	UNSURE
		4	Blue	480.18	Fiber	1-HEPTANESULFONIC ACID	31	UNSURE
		7	Green	100.27	Fiber	L-A-PHOSPHATIDYLINOSITOL	30	UNSURE
	T0.R3.3-1S	5	Black	1403.13	Fiber	AMSPEC ANTIMONY OXIDE	47	NO
		3	Black	759.80	Fiber	POLYESTER	39	UNSURE
		10	Green	848.14	Fragment	POLY(ARYLETHER)	38	UNSURE
		12	Red	360.87	Fragment	POLYETHERURETHANE	37	UNSURE
		9	Blue	360.51	Fiber	L-ALPHA-ACETYLMETHADOL HLC IN KBR	37	UNSURE
		8	Black	1871.60	Fiber	2-ACETOXY-N-(DIPHENYLMETHYLENE)GLYCINE ETHYL ESTHER	35	UNSURE

		2	Black	196.74	Fiber	ISOPRORONE	32	UNSURE
T0		6	Blue	470.32	Fiber	POLYETHERURETHANE	32	UNSURE
		7	Black	483.87	Fiber	11-KETOETIOCHOLANONE	28	UNSURE
		1	Black	4395.06	Fiber	ALKYD REYESN	26	UNSURE
		4	Black	1360.05	Fiber	N-PROPYL OLEATE	22	UNSURE
		11	Black	1013.54	Fiber	LOST	0	LOST
	T0.R3.4-1S	9	Black	878.49	Fiber	POLYESTER	50	YES
		5	Yellow	240.97	Fragment	TOURMALINE	40	NO
		11	Green	240.90	Fiber	POLY(ARYLETHER)	40	YES
		8	Blue	638.18	Fiber	POLY(ETHYLENE:VYNIL CHLORIDE)	39	UNSURE
		1	Black	1040.48	Fiber	POLY(ARYLETHER)	35	UNSURE
		7	Black	650.91	Fiber	POLY(ARYLETHER)	33	UNSURE
		6	Black	180.24	Fiber	POLYVINYL CHLORIDE	33	UNSURE
		10	Blue	270.58	Fragment	POLYVINYL ALCOOHOL	31	UNSURE
		2	Black	1140.22	Fiber	LOST	0	LOST
		3	Black	1736.31	Fiber	LOST	0	LOST
		4	Red	797.04	Fiber	LOST	0	LOST
	T0.R3.3-2S	1	Black	418.23	Fiber	2,4,6-COLLIDINE, 99%	52	NO
		7	Transparent	991.53	Fiber	HEXAFLUOROTITANE (IV); POTASYESUM	68	NO
		5	Blue	836.08	Fiber	CHLOROFORM	59	NO
		6	Transparent	519.49	Fiber	HEXAFLUOROTITANE (IV); POTASYESUM	58	NO
		8	Transparent	1853.41	Fiber	CARBON DIOXIDE	52	NO
		4	Blue	1071.67	Fiber	1,3-DIARACHIDIN	42	NO
		12	Blue	543.75	Fiber	4-(TRIFLUOROMETHOXY)BENZENESULFONYL CHLORIDE, 98%	42	NO
		11	Transparent	79.67	Film	VINYLIDENECYANIDE + VINYL ACETATE	41	YES
		3	Blue	521.34	Fiber	POLY(STRYRENE:ACRYLONITRILE:MMA)	36	UNSURE
		9	Transparent	2224.48	Fiber	1-BROMOADAMANTANE	27	UNSURE
		2	Transparent	1883.73	Fiber	LOST	0	LOST
		10	Transparent	402.16	Fiber	LOST	0	LOST
T2	T2-R1.1	8	Blue	2223.43	Fiber	MODACRYLIQUE	59	YES
		4	Black	938.38	Fiber	POLY(ARYLETHER)	42	YES
		5	Black	332.62	Film	POLYVINYL ALCOOHOL	41	YES
		1	Black	1547.47	Fiber	POLY(ARYLETHER)	41	YES
		6	Black	537.01	Fiber	POLY(ARYLETHER)	41	YES
		10	Yellow	138.82	Fragment	1,3-DIARACHIDIN	40	UNSURE
		11	Black	445.16	Fiber	POLY(ARYLETHER)	39	UNSURE

		3	Transparent	3293.68	Fiber	POLY(ARYLETHER)	38	UNSURE
	T2-R1.1	9	Black	2213.91	Fiber	POLY(ARYLETHER)	37	UNSURE
		7	Red	1044.66	Fiber	POLYETHYLENE	36	UNSURE
		2	Black	2315.62	Fiber	POLYETHYLENE	34	UNSURE
	T2-R1.2	2	Blue	1760.87	Fiber	POLY(ARYLETHER)	46	YES
		7	Black	302.58	Fiber	POLY(ARYLETHER)	41	YES
		6	Red	831.16	Fiber	ETHER REAGENT	40	UNSURE
		4	Black	278.53	Fiber	POLY(ARYLETHER)	40	UNSURE
		1	Trans/red	2500.63	Fiber	POLYVINYL ALCOOHOL	38	UNSURE
		3	Blue	600.32	Fiber	QUININE SULFATE	37	UNSURE
		5	Trans/yellow	2375.77	Fiber	POLYSTYRENE - STYROFLEX	35	UNSURE
	T2-R1.3	4	Orange	88.42	Fragment	URETHANE ALKYD, LINSEED OIL RICH	48	YES
		7	Black	562.76	Fiber	URETHANE ALKYD, LINSEED OIL RICH	47	YES
		6	Black	720.30	Fiber	MONOELAIDIN	41	NO
		10	Red	1146.69	Fiber	POLY(ETHYLENE:VYNIL CHLORIDE)	38	UNSURE
		5	Black	267.96	Fiber	NYLON	35	UNSURE
		8	Red	428.53	Fiber	POLYESTER NON RESORBABLE LIGATURE	34	UNSURE
		9	Black	224.80	Fiber	BENZONITRILE	34	UNSURE
		1	Blue	818.53	Fiber	POLY(BUTADIENE)	33	UNSURE
		11	Black	708.71	Fiber	PENYL SULFONE	32	UNSURE
		3	Black	421.28	Fiber	4-METHYLBENZENETHIOL	31	UNSURE
		2	Blue		Pellet	APOMORPHINE HCL IN KBR	30	UNSURE
	T2-R1.4	9	Black	729.96	Fiber	POLY(VINYL PROPIONATE/ACETATE)	63	YES
		14	Blue	166.37	Fiber	CELLULOSE	60	NO
		10	Black	403.87	Fiber	CELLULOSE	59	NO
		12	Black	265.45	Fragment	POLYESTER	55	YES
		4	Black	391.91	Fiber	ALUNITE	53	NO
		11	Yellow	129.38	Fiber	CELLULOSE	52	NO
		7	Black	301.12	Fiber	ILLITE/SMECTITE	51	NO
		13	Black	415.16	Fiber	POLYESTER	50	YES
		8	Black	499.32	Fiber	CELLULOSE	46	NO
		5	Green	125.95	Fragment	ETHYL CAPRYLATE	43	NO
		2	Green	109.19	Fragment	SORBITAN MONOSTEARATE	43	NO
		6	Black	408.74	Fiber	POLYETHYLENE	39	UNSURE
		3	Black	393.89	Fiber	CELLULOSE	35	UNSURE
		1	Blue	1279.18	Fiber	VISCOSE RAYON	31	UNSURE
T2	T2-	2	Blue	204.60	Fiber	PP SHET	61	YES

		4	Red	1429.53	Fiber	MODACRYLIQUE	48	YES
		5	Green	228.20	Fragment	ANTHRACENE	48	NO
		3	Black	299.91	Fragment	CELLULOSE	43	NO
		1	Black	406.81	Fiber	FUROSEMIDE	30	UNSURE
	T2-R2.2	3	Black	640.03	Fiber	POLY(METHACRYLATE)	80	YES
		4	Brow	302.52	Fragment	DICYCLOPENTADIENE	70	NO
		2	Black	563.84	Fiber	POLY(VINYL PROPIONATE/ACETATE)	54	YES
		1	Black	989.78	Fiber	(1S)-(-)-CAMPHOR P-TOSYLHYDRAZONE	37	UNSURE
	T2-R2.3	4	Black	205.59	Fiber	POLY(VINYL PROPIONATE/ACETATE)	81	YES
		3	Blue	176.51	Fragment	POLYPROPYLENE	62	YES
		1	Red	235.51	Fragment	POLYPROPYLENE	51	YES
		2	Blue	203.73	Fiber	POLYESTER RESINE	46	YES
		5	Black	1201.28	Fiber	POLY(METHACRYLATE)	40	YES
		6	Black	305.08	Fragment	LEVORPHANOL HCL IN KBR	31	UNSURE
	T2-R2.4	4	Green	1159.15	Fiber	ACRYLIQUE	69	YES
		6	Red	2110.05	Fiber	ACRYLIQUE	66	YES
		10	Black	2417.99	Fiber	(1S)-(-)-VERBERONE	62	NO
		8	Black	1268.36	Fiber	POLYESTER RESINE	59	YES
		5	Black		Fiber	PERCHLOROPENTACYCLODECANE	54	NO
		7	Red	1760.58	Fiber	POLYESTER RESINE	53	YES
		9	Red	427.89	Fiber	ACRYLIQUE	53	YES
		1	Red	88.43	Fiber	ETHINAZONE	52	NO
		2	Black	475.79	Fiber	POLYESTERISOCYANATE	45	YES
		11	Red	312.05	Fiber	2-(CHLOROMETHYL)ANTHRAQUINONE	41	NO
		3	Black	637.49	Fiber	BARBIAL FREE ACID CRYSTALLINE	33	UNSURE
	T2-R3.1	2	Black	1323.24	Fiber	PHOSPHORUS OXYCHLORIDE	64	NO
		9	Black	576.48	Fiber	CHLOROFORM	61	NO
		3	Black	1895.79	Fiber	PHOSPHORUS OXYCHLORIDE	60	NO
		1	Red	249.28	Fiber	ISOPROPYLNAPHTHALENE	55	NO
		5	Blue	254.94	Fragment	DIETHYL ETHYLMALONATE	47	NO
		8	Blue	450.46	Fiber	(BICYCLO(2.2.2)HEPTA-2,5-DIENE)CHLORHODIUM(I) DIMER	45	NO
		4	Blue	101.91	Fragment	4-4PR-DICHLOROBENZOPHENONE	28	UNSURE
		7	Brow	510.96	Fragment	1, 4-DIPHENYLBUTADIYNE	27	UNSURE
		6	Brow	821.27	Fragment	PREDNISONE IN KBR	26	UNSURE
	T2-	2	Blue	1677.34	Fiber	POLY(VINYL PROPIONATE/ACETATE)	75	YES

		4	Black	185.35	Fiber	POLY(VINYL PROPIONATE/ACETATE)	51	YES
		7	Transparent	367.28	Fiber	ETHER REAGENT	48	NO
		8	Black	397.71	Fiber	POLY(STRYRENE:ACRYLONITRILE: MMA)	46	YES
		5	Black	1675.49	Fiber	2,4,6-COLLIDINE, 99%	40	NO
		1	Red	1175.15	Fiber	MESCALINE HCL IN KBR	38	UNSURE
		9	Transparent	3168.81	Fiber	SACARIM SODIUM	34	UNSURE
		3	Black	513.22	Fiber	BISMUTITE	33	UNSURE
		6	Red	545.69	Fiber	LOST	0	LOST
	T2-R3.3	3	Black	159.45	Fiber	CELLULOSE	64	NO
		4	Blue	1462.75	Fiber	POLY(ETHYLACRYLATE:ST: ACRYLAMIDE)	60	YES
		5	Black	354.17	Fiber	CELLULOSE	54	NO
		1	Blue	351.24	Fiber	CELLULOSE	34	UNSURE
		2	Yellow	440.64	Fragment	BENZYL SULFOXIDE	27	UNSURE
	T2-R3.4	7	Black	325.70	Fiber	BROMOFORM	66	NO
		14	Blue	1304.96	Fiber	POLYESTER	59	YES
		6	Red	549.42	Fiber	1,4-DIPHENYLBUTADIYNE	59	NO
		13	Red	1265.06	Fiber	POLY(VINYL PROPIONATE/ACETATE)	57	YES
		5	Black	4210.10	Fiber	BENZONITRILE	51	NO
		9	Black	1519.77	Fiber	BROMOFORM	50	NO
		12	Black	821.84	Fiber	VALERALDEHYDE	45	NO
		2	Black	272.14	Fiber	ALUNITE	43	NO
		1	Black	246.27	Fiber	VALERALDEHYDE	42	NO
		11	Red	2687.37	Fiber	COPOLYMER ETHYLENE-TETRAFLUOROETHYLENE	41	YES
		8	Black	202.06	Fiber	BENZONITRILE	41	NO
		4	Black	714.93	Fiber	POLY(METHYLPHENSILOXANE)	35	UNSURE
		3	Blue	276.37	Fiber	2-IODOPROPANE	31	UNSURE
		10	Green	381.71	Fiber	COPOLYMER ETHYLENE-TETRAFLUOROETHYLENE	29	UNSURE